COO-3158-36

Need ERDA-427

A TIME-OF-FLIGHT ATOM-PROBE FIELD-ION MICROSCOPE FOR THE STUDY OF DEFECTS IN METALS

by

Thomas M. Hall, Alfred Wagner, Arnold S. Berger and David N. Seidman

MASTER

June 1975
Cornell University
Ithaca, New York 14853

Report #2357
Issued by
The Materials Science Center

DISCLAIMER

A TIME-OF-FLIGHT ATOM-PROBE FIELD-ION MICROSCOPE FOR THE STUDY OF DEFECTS IN METALS*

by

Thomas M. Hall, Alfred Wagner, Arnold S. Berger‡ and David N. Seidman

Cornell University, Bard Hall,
Department of Materials Science and Engineering and the
Materials Science Center, Ithaca, New York 14853

ABSTRACT

An ultra-high vacuum time-of-flight (TOF) atom-probe field ion microscope (FIM) specifically designed for the study of defects in metals is described. The variable magnification FIM image is viewed with the aid of an internal image intensification system based on a channel electron-multiplier array. The specimen is held in a liquid-helium-cooled goniometer stage, and the specimen is exchanged by means of a high-vacuum ($<10^{-6}$torr) specimen exchange device. This stage allows the specimen to be maintained at a tip temperature anywhere in the range from 13 to 450K. Specimens can also be irradiated in-situ with any low-energy (<1keV) gas ion employing a specially constructed ion gun. The pulse-field evaporated ions are detected by a Chevron ion-detector located 2.22m from the FIM specimen. The TOF of the ions are measured by a specially constructed eight-channel digital timer with a resolution of $\pm$10nsec. The entire process of applying the evaporation pulse to the specimen, measuring the dc and pulse voltages, and analyzing the TOF data is controlled by a NOVA 1220 computer. The computer is also interfaced to a Tektronix graphics terminal which displays the data in the form of a histogram of the number of events versus the mass-to-charge ratio. An extensive set of computer programs to test and operate the atom-probe FIM have been developed. With this automated system we can presently record and analyze 10 TOF sec^{-1}. In the performance tests reported here the instrument has resolved the seven stable isotopes of molybdenum, the five stable isotopes of tungsten, and the two stable isotopes of rhenium in a tungsten-25at.% rhenium alloy.

---

* Research supported by the Energy Research and Development Administration. Additional support was received from the National Science Foundation through the use of the technical facilities of the Materials Science Center at Cornell University.

‡ Now at: Argonne National Laboratory, The Materials Science Division, Argonne, Illinois 60439.

Table of Contents

1. INTRODUCTION

The time-of-flight (TOF) atom-probe field-ion microscope (FIM) makes it possible to measure the mass-to-charge ratio (m/n) of an individual atom pulse-field evaporated from the surface of an FIM specimen. This instrument was first described by Müller, Panitz and McLane[1] and subsequently developed by Müller and co-workers[2] as an extension of the FIM.[3] Several other working TOF atom probe FIM's have been reported.[4] Thus, it is now possible to combine the microstructural information obtainable by the pulse-field evaporation[5] of successive atomic layers with a simultaneous chemical analysis (on an atom-by-atom basis) of the bulk of an FIM specimen. This unique feature of the TOF atom-probe FIM makes it ideally suited for the study of the interaction of solute atoms (both substitutional and interstitial) with lattice defects (point, line and planar). Brenner and co-workers[6,7,8] and also Turner and Southon and co-workers[9,10] have successfully applied the TOF atom-probe FIM to a number of materials science problems. Their work clearly demonstrates the potential of this instrument for studying a wide range of materials science problems.

1.1 Physical principles of the TOF atom-probe FIM

A highly schematic diagram illustrating the main features of a TOF atom-probe FIM is shown in Fig. 1. The FIM specimen is, typically, a wire about 0.01cm in diameter and about 1 to 1.5cm in length. Before it is inserted into the FIM, it is etched or electropolished to a very fine point that may have an initial radius of curvature (r_T) of only 50 to 100A. The specimen is maintained at a positive potential with respect to a grounded imaging screen. Since the specimen has a very small r_T, one can easily obtain a local electric field of $\sim$4.5 to 5VA^{-1} with the application of only a few thousand volts (typically in the range 5 to 20kV) to the tip. As a result of this high local field the imaging gas atoms (typically helium or neon) are field ionized[11] over individual protruding atoms, after each gas atom has been accommodated thermally to the temperature of the FIM specimen.

The positively charged helium (or neon) ion which is created by the field ionization process is then accelerated along an electric field line to the internal image intensification system where its energy is converted into visible light. The visual image that one observes corresponds to a point projection of the atoms on the surface of the FIM tip.

When the local electric field on the tip is increased by applying a short high voltage pulse (25nsec duration and a few kilovolts in magnitude) atoms are desorbed (sublimed) in the form of charged ions by the process of field evaporation. A certain number of the pulse field evaporated atoms will have trajectories which take them through a small probe hole (3mm in diameter) in the imaging screen. These pulse field evaporated atoms travel down a flight tube to a high gain ($\sim 10^6$) ion detector which is located approximately 2m from the FIM specimen. The ion detector produces a small voltage pulse whenever it is struck by a pulse field evaporated ion. The time interval between the application of the field evaporation pulse and the voltage pulse produced by the ion detector is measured by a digital timer.[12] The value of (m/n) of the pulse field evaporated ion is then deduced by equating the potential energy of the ion to its kinetic energy from the equation

$$neV_T = \frac{1}{2} mv^2,$$

where n is the charge state of ion, e is the electronic charge, V_T is the effective <u>total</u> voltage (the sum of the steady-state imaging and pulse voltages) applied to the specimen, m is the mass of the ion, and v is the terminal velocity of the ion. The quantity v is given by (d/t) where d is the flight distance and t is the flight time, under the assumptions that the terminal velocity is obtained in a time $\ll t$ and a distance $\ll d$. These assumptions are valid for a value of $d \gtrsim 1m$, since the ions reach their terminal velocity within a few tip radii ($\sim$300 to 1000A). The ratio (m/n) is then readily shown to be given by

$$\frac{m}{n} = 2eV_T t^2/d^2.$$

The above relationship is basically the one used to determine the value of m/n for each pulse field evaporated ion. In section 3.4 it will be shown that this relationship must be modified slightly to determine m/n to a high degree of accuracy.

1.2 Special features of the Cornell TOF atom-probe FIM.

The Cornell TOF atom-probe FIM has a number of unique features which make it ideally suited for the study of materials science problems. The entire FIM is contained in a stainless-steel ultra-high vacuum (UHV) system to prevent the contamination of the metal or alloy specimen being examined. The FIM specimen is mounted on a helium-cooled goniometer stage (consisting of a liquid-helium cooled cryostat plus a two-axis of tilt goniometer stage) so that any portion of the surface of the tip can be projected over the probe-hole for mass analysis. The goniometer stage is cooled by liquid helium to improve the quality of the FIM image and also to allow the investigator to change the diffusivity of point defects such as self-interstitial atoms (SIA's). The FIM specimen is inserted into the microscope via a high-vacuum specimen exchange device which makes it possible to change specimens without having to bring the entire FIM up to atmospheric pressure. The specimen can also be irradiated in-situ with any low energy (<1keV) gas ion (He^+, Ne^+, Ar^+, or Xe^+) as well as H^+. The FIM image is viewed on the phosphor screen of an internal image intensification system consisting of a channel-electron-multiplier array (CEMA) and a phosphor screen. The entire internal image intensification system can be moved relative to the FIM specimen to vary the magnification by an areal factor of 64.

The pulse-field evaporated ions are detected by two CEMA's arranged in the Chevron configuration[13]. The TOF of up to eight different species produced by a single field evaporation pulse are measured by a digital timer[11] with a $\pm$10nsec resolution. Since accurate and rapid measurement of the TOF of the pulse

field evaporated ions is an essential aspect of quantitative atom-probe field-ion microscopy, the entire process of applying and measuring the pulse-field evaporation voltage to the FIM specimen, measuring the dc voltage and analyzing the TOF data has been automated. To accomplish this the specimen high-voltage system and the digital timer are interfaced to a Nova 1220 computer which analyzes the TOF and stores the data on magnetic tape. The computer is also interfaced to a Tektronix 4010 graphics display terminal which plots a histogram of the number of events versus m/n on a cathode-ray tube. With this automated system it is presently possible to analyze and record 10 TOF events per second.†

The principal purpose of this paper is to describe the features of the atom-probe FIM that we have designed and built. We have included some discussion of the reasons for several of our design decisions as well as the results of performance tests and preliminary experiments. Because of the complexity of the overall atom-probe system we have chosen to divide the paper up into three main sections. The first section is concerned primarily with the FIM portion of the TOF atom-probe FIM such as the internal image intensification system, goniometer stage, the specimen exchange device, the gas ion-gun, and the vacuum system. The second section is concerned primarily with the TOF mass spectrometer portion of the atom-probe FIM such as the specimen voltage supplies, the digital timer, and the Chevron ion-detector. The computer system which controls the operation of the TOF atom-probe FIM is discussed in a third section.

---

† An effort is being made to increase this rate.

2. FIELD-ION MICROSCOPE SYSTEM

This section contains a description of those portions of the TOF atom-probe FIM that are primarily concerned with obtaining a visible image of the FIM specimen.

2.1 Internal image intensification system and focusing lens.

Figure 2 is a diagram of the TOF atom-probe FIM showing details of the internal image intensification system, viewing mirror and Chevron ion detector. Note that the tip of the FIM specimen faces a Gallileo 75mm diameter channel-electron-multiplier array (CEMA). The internal image intensification system consists of the CEMA plus a phosphor coated glass screen. The screen was made by first coating a glass disk with a transparent and conducting layer of tin oxide; then laying the disk flat in a petri-dish containing a suspension of Sylvania P14 phosphor powder in a dilute solution of potassium silicate. The mixture of phosphor and potassium silicate was first agitated and then the phosphor was allowed to precipitate onto the glass plate. The excess water was drained with a syringe and then the screen was baked at 180°C for 3 hr.[14] This process yields a uniform screen which does not flake or peel under normal handling conditions.

The probe tube and lens arrangement shown in Fig. 2 was the result of numerous trial-and-error attempts at obtaining a configuration that would efficiently collect the pulse-field-evaporated ions and focus them onto the Chevron ion detector. As indicated in Fig. 2 the internal image intensification system has a 3mm hole through its center. To electrostatically shield the ion beam from the back of the CEMA and the front of the screen, which are maintained at 1kV and 3kV respectively, a grounded probe tube was inserted into this hole. The probe tube consists of a stainless steel tube whose walls were thinned to $\sim$25μm by electropolishing. The grounded stainless-steel tube is electrically insulated from the CEMA and the front of the glass screen by a glass tube with $\sim$50μm thick walls. This insulating tube

was thinned from stock glass tubing using hydrofluoric acid. The outer diameter was decreased by dipping the tube in the acid and the inner diameter was increased by squirting the acid through the tube until the desired size was obtained. A 50μm diameter stainless steel wire was spot-welded to the back of the probe tube and clamped under tension so that the probe tube could not move. The back side of the glass screen was given a separate coating of tin oxide which is electrically isolated from the phosphor screen and which is maintained at ground potential. This grounded coating ensures that the ion beam is electrostatically shielded from the CEMA and screen potentials and prevents any possible electrostatic charging of the glass.

Immediately behind the image intensification system (see Fig. 2) is a focusing lens in the form of a stainless steel bushing passing through a glass plate coated on both sides with tin oxide. A beryllium-copper coil spring and a small washer spot-welded onto the side of the bushing away from the specimen serve to keep the bushing in a fixed position. This lens is maintained at a voltage which is proportional to the dc voltage on the specimen. (See Section 3.1 for a description of the voltage control system.) The constant of proportionality required to focus the ions onto the Chevron ion detector at the end of the flight tube varies between 0.30 and 0.54 as the distance from the specimen to the image intensification system varies between 100mm and 12mm.

Alignment of the probe hole and the focusing lens were found to be quite critical if the focusing lens was not to distort the ion beam. The focusing lens was aligned by sighting through it and adjusting its position until no eccentricity was visible. This procedure resulted in the formation of an image ∿1mm in diameter on the Chevron ion detector at the downstream end of the flight tube.

Behind the focusing lens is a front-surfaced glass mirror, placed at an angle of 45° (see Fig. 2) with respect to the flight path, containing a 10mm diameter hole through its center. This mirror allows the image of the specimen, which is produced by the image intensification system, to be viewed without obstructing the flight path. The hole through the mirror is lined with a grounded stainless steel metal sleeve which is essential in order to prevent charged particles from accumulating on the exposed glass surfaces.

The entire assembly consisting of the image intensification system, focusing lens, and viewing mirror is attached to two UHV metal bellows arranged so that the distance from the tip of the specimen to the front surface of the image intensification system is continuously variable. When the probe hole is moved in close to the specimen a large area of the specimen's surface is projected over the probe hole; conversely when the image intensification system is translated away from the specimen only a few atoms are projected over the probe hole. Since the tip-to-image intensification system distance can be varied from ∿12 to 100mm there is a lineal magnification change of ∿8x and an areal magnification change of ∿64x.

2.2 Helium-cooled goniometer stage

A liquid-helium-cooled goniometer stage has been constructed which has the following features: (1) The specimen can be cooled to cryogenic temperatures to improve the quality and resolution of the FIM image and also to change the diffusivity of point defects such as self-interstitial atoms; (2) the specimen is rotatable about two orthogonal axes which intersect at the tip of the specimen so that a selected region of the specimen can be projected over the probe hole for chemical analysis; and (3) the goniometer stage is translatable in three mutually orthogonal directions (x, y and z) to facilitate the alignment of the tip with respect to both the probe hole and the low-energy gas ion-gun described in Section 2.4.

A cutaway view of the helium-cooled goniometer stage is shown in Fig. 3. The FIM specimen is mounted in a copper specimen holder that is removed when one specimen is exchanged for another. This copper specimen holder is threaded into a copper plate which is bolted onto the back of the upper sapphire electrical insulator. On the top of this sapphire insulator is a copper plate into which are clamped 25 strands of 0.3mm diameter pure gold wire. The upper end of this inner cooling braid is clamped to the lower end of the cold finger.

The cold finger, which is similar to one described by Seidman et al.[15], is shown in Fig. 4. The design incorporates what are essentially two heat exchangers. At the bottom of the cold finger is a hollow copper rod with a bored hole that serves as a liquid helium reservoir. The walls of this rod are extended upward 50mm around the outer vacuum jacket of the liquid helium transfer tube. The cold exhaust gas from the boiling liquid helium is forced between the vacuum jacket and the copper tube and consequently cools the copper bottom of the cold finger. This feature was found to be crucial in the initial cool down when most of the liquid helium boils before reaching the end of the cold finger and all cooling is performed by the cold helium gas.

Approximately 150mm from the bottom of the cold finger is a second copper tube, ∿100mm long, surrounding the vacuum jacket of the transfer tube. This tube serves as a heat exchanger for cooling the radiation shields which surround the cold finger. The lower end of the radiation shield is connected by a flexible gold braid to the radiation shield surrounding the goniometer stage.

The upper sapphire electrical insulator of the goniometer stage is thermally isolated from the lower part of the cryostat by a 12mm diameter stainless steel tube with a 50μm wall as shown in Fig. 3. Beneath this is the lower sapphire electrical insulator (similar to the upper sapphire insulator) which is intended to support an optional high-voltage pulse ring. This ring, which is not shown in the figure, may be pulsed negative with respect to the specimen tip if desired.[6]

In assembling the cryostat 50μm thick gold gaskets were inserted between all clamped heat conducting surfaces, such as the copper clamp plate on top of the upper sapphire electrical insulator.

To test the cooling ability of the helium cooled goniometer stage an additional platinum-resistance thermometer (PRT) was temporarilly mounted on the top of the upper sapphire block in the cryostat (see Fig. 3). In addition, iron-constantan thermocouples were attached to the copper specimen holder and the outer radiation shield. The results of these tests showed that the specimen is cooled to 18K within ∿20 min. and to 13K within 1 hour. The thermal gradient across the gold braid was between 7 and 12K and within the accuracy of the measurements the specimen[15] was at the same temperature as the bottom end of the braid. The outer radiation shield was found to cool more slowly than the inner specimen support, but reached 100K within approximately an hour. The excellent performance of the goniometer stage is attributable to the small size of the cryostat, the radiation shields, and the dimensions and shape of the liquid helium cold-finger.

The goniometer supporting the cryostat was adapted from plans kindly and generously supplied by Dr. S.S. Brenner of U.S. Steel Corporation. This goniometer provides the rotation about two orthogonal axes while maintaining UHV conditions by the use of two linear-motion stainless steel UHV bellows seals. As shown in Fig. 3, the entire cryostat is supported on an arm at the end of a hollow rotating tube. This tube-arm assembly is rotated about a horizontal axis by a bell crank coupled to the inside of one of the bellows seals. The outside of this bellows seal is moved in and out by a crank and lead screw threaded through a fixed plate.

Motion about the vertical axis is provided for by a bearing at the lower end of the support arm. The lower cryostat support shaft, which passes through this bearing, is turned by a crank that is linked to the inner sliding shaft that passes through the outer rotating tube. This shaft is coupled to the inside of a

second bellows assembly. The portion of the goniometer† external to the FIM is mounted on three machinist's slides and is connected to the vacuum system through a bellows seal so that it can be translated in three mutually orthogonal directions to facilitate alignment.

The goniometer stage has been found to provide precise and reproducible rotation of the specimen and allows us to project any portion of the specimen's surface over the probe hole in the internal image intensification system. Due to the compact design of the goniometer stage the lateral position of the tip varies by less than 1mm when the tip is rotated through its full arc. The x, y and z motion, provided by the three external orthogonal machinist's slides, is found to be useful for initial alignment of the TOF atom-probe FIM and for making small corrections to the alignment during an experimental run.

2.3 Low-energy gas ion gun

A simple low-energy gas ion-gun[16] has been constructed to enable us to irradiate FIM specimens in-situ. A schematic diagram of the ion gun is shown in Fig. 5. A gas such as hydrogen, helium, neon, or xenon is bled into the ion gun through a Varian leak valve to a pressure of 10^{-4} to 10^{-5}torr. The gas atoms are ionized by electrons which are thermionically emitted from a resistively-heated tungsten filament maintained at -30 to -40Vdc (see Figs. 5 and 6). The cylindrically shaped plasma chamber is located in the center of a solenoid which produces a magnetic field of a few hundred gauss. The ions are extracted from the plasma chamber with the aid of a conically-shaped extraction lens that operates at -200Vdc and then the ions are focused with a cylindrically-shaped lens that is operated at -700Vdc. The gas ions are then deaccelerated and simultaneously focused onto the FIM specimen which in this illustrative example is maintained

---

† See Fig. 3 in Brenner and McKinney's article.[6]

at -300Vdc. The potential diagram as a function of distance is shown in Fig. 6.

The low-energy ions will be used to produce a sea of self-interstitial atoms (SIA's) by the focused replacement collision sequence mechanism (RCS).[17] As a result of the RCS events the immobile vacancies remain at the irradiated surface and the SIA's are injected into the bulk of the FIM specimen. It is the only presently known mechanism capable of producing isolated self-interstitial atoms. The ion-gun can also be used to implant gas atoms such as hydrogen in the tip of the FIM specimen.

2.4 Ultra-high vacuum system

The use of an ultra-high vacuum system minimizes the interaction of residual gas atoms with the FIM specimen in two important ways. First, it reduces the number of peaks observed in the m/n spectra because the absolute number of metal atom-gas atom complexes is decreased. Second, it reduces the concentration of artifact contrast effects which are produced as a result of impurity gas atom-surface atom interactions (e.g., artifact vacancies[18] and SIA's[19]). This second point is important for our research, since it is intended to study the interaction of both substitutional and interstitial atoms with point defects. With the above information in mind a UHV atom-probe FIM was constructed.

A schematic diagram of the vacuum system is shown in Fig. 7. The stainless steel main chamber is connected directly to a Varian 916-0014 titanium sublimation pump (TSP) and subsequently through a 4 inch diameter right-angle valve to a Varian 912-7000 $140\ell sec^{-1}$ Vac-ion pump. The vacuum chamber is rough pumped by two Varian sorption pumps. The use of the TSP, ion pump and sorption pumps maintain ultraclean conditions and avoids contamination with pump oil. The sorption pumps are connected through the specimen exchange port so that they can be used either for rough pumping the main chamber or for rough pumping the specimen exchange air lock to be described in more detail in the following section. A small TSP and a Varian $20\ell sec^{-1}$ triode ion pump are also connected

to the specimen-exchange air lock. In addition a 2 inch diameter Consolidated Vacuum Corporation diffusion pump, filled with DC705, trapped with a Granville-Phillips liquid-nitrogen cold-trap, and backed by an Alcatel Z2007 direct drive pump, is connected to the main chamber by a 1½ inch diameter UHV valve. The oil diffusion pump is used to pump the main chamber when the atom-probe FIM contains an imaging gas (either helium or neon), since the ion pumps and TSP's cannot be used for this purpose. At all other times the diffusion pumps are valved off to prevent possible backstreaming of oil into the vacuum system.

The internal image intensification system containing the probe-tube and the 45° viewing mirror are mounted on a moveable section which is connected to the fixed portions of the vacuum system by two 60190-5 bellows seals manufactured by the Metal Bellows Corporation.

The flight tube is isolated from the main chamber by an UHV straight-through valve and it has its separate vacuum system consisting of a sorption pump and a liquid-nitrogen trapped oil-diffusion pump. This arrangement allows a vacuum to be maintained in the ion detector section even when the main chamber is not under vacuum and also provides the possibility of differentially pumping the flight tube to reduce the partial pressure of helium imaging gas in the flight tube.

As shown in Fig. 7 most of the vacuum equipment is inside the electrically heated bake-out oven (indicated by the dotted line) so that adsorbed gases can be baked off the inner surfaces of the atom-probe FIM to lower the ultimate pressure obtained. The sorption pumps, oil-diffusion pumps, and cold traps not inside the bake-out oven are all baked using separate heating mantles.

The entire vacuum system was initially carefully cleaned with tri-chlorethylene and ethanol using an ultrasonic cleaner for the smaller pieces and mechanical scrubbing to the larger components. Ultimate pressures of 4×10^{-10} torr are obtained after baking to 150°C for several hours, while under typical operating conditions the pressure is 1×10^{-9} torr. The pressure above the cold trap on the

main chamber diffusion pump is less than 5×10^{-10} torr. Thus, the performance of the atom-probe FIM vacuum system is satisfactory for studying defect-impurity atom interactions.

2.5 Specimen-exchange device

A novel specimen exchange device was incorporated into the design of the goniometer stage to allow the FIM specimen to be replaced without breaking the vacuum in the main chamber. The essential features of this device are shown in Fig. 8. The copper specimen holder is attached to the end of a 1m long, 9.5mm diameter specimen-exchange rod with a bayonet-type clip. The copper specimen holder is surrounded by a retractable protection shield which serves as an alignment guide when screwing the specimen holder into the goniometer stage. The specimen exchange rod passes through a Vacuum Research Corporation S 102 Wilson type sliding motion feedthrough that is sealed with two viton gaskets which are lubricated with Apezon L vacuum grease. The specimen exchange rod passes through a Varian UHV straight-through valve which seals the main chamber until the air lock has been evacuated. The air lock is rough pumped using the two Varian Vacsorb pumps in sequence, and is then evacuated further by the small TSP and the Varian $20\ell sec^{-1}$ triode pump. The specimen exchange device eliminates the long pump-down period that is required if the main chamber is brought back to atmospheric pressure. The pressure in the air lock is reduced to 10^{-6} torr before the exchange takes place and the pressure in the main chamber remains below 10^{-7} torr during the exchange and drops to 3×10^{-9} torr within 15 min. after the exchange. In conclusion use of the specimen exchange device has reduced the time required for specimen replacement to less than 1 hr.

3. TIME-OF-FLIGHT MASS SPECTROMETER

This section contains a description of those parts of the TOF atom-probe FIM that are primarily concerned with determining the (m/n) ratios of the pulse-field evaporated metal ions. We will first describe the general features of the TOF mass spectrometer and then will describe some details of the most important subsystems; namely, the specimen voltage system, the chevron ion detector, and the digital timer. The calibration procedure for the TOF atom-probe FIM is also discussed. The computerized control system is described only to the extent necessary for understanding the operation of the mass spectrometer, since a detailed description of the computer system is given in Section 4.

Figure 9 shows a block diagram of the TOF mass spectrometer. The FIM specimen is connected to a high voltage dc power supply and is maintained at a positive voltage sufficient to field ionize the helium or neon imaging gas atoms, and thus produce an image of the FIM specimen, but at a voltage below that required to field evaporate the metal atoms. A high voltage pulse, triggered by the computer, is added to the constant dc voltage and momentarily raises the voltage on the specimen to a value sufficient to pulse field evaporate a few atoms. The controls of the dc and pulse high voltage power supplies as well as the power supply for the electrostatic lens are mechanically ganged together as shown in Fig. 9, so that the pulse and lens voltages are maintained at a fixed fraction of the dc voltage. The advantages of having the pulse voltage track the dc voltage are discussed in Section 3.4 on calibration of the TOF mass spectrometer. The outputs of the high voltage power supplies are measured by the analog-to-digital (A/D) converter and input to the computer whenever a TOF measurement is made. A small fraction of the high voltage pulse is picked off and fed to a discriminator which starts the digital timer and also triggers a gate generator. The voltage pulse produced when an ion reaches the Chevron ion detector is amplified, delayed 500nsec, and then fed to the stop discriminator. The stop discriminator is gated

by the gate generator which is typically set to open 600nsec after the start pulse. Delaying the stop pulses and gating the stop discriminator ensures that any interference from the high voltage pulse will not improperly trigger the stop discriminator and that only true events will be detected. A total of eight consecutive stop signals can be analyzed and thus eight ion species can be identified. The TOF data is stored in binary-coded-decimal (BCD) format within the timer until the computer is ready to read the TOF data. The computer calculates m/n using the TOF and voltage data from the equation

$$\frac{m}{n} = 2e\,(V_{dc} + \alpha\, V_{pulse}) \quad \frac{(t-t_o)^2}{d^2} \quad ,$$

where α is the pulse factor, t is the measured TOF, and t_o is the total delay time. The nature of the quantities α, t_o, and d, which are called the calibration parameters, is discussed in more detail in Section 3.4.

After the m/n ratios are computed they are stored in the computer memory in the form of a histogram which is the number of events versus (m/n). In addition, the raw data consisting of the TOF and the voltages are stored on a magnetic cassette tape so that the results of the run can be reanalyzed in the future. The computer is interfaced to a Tektronix 4010 graphics display terminal and a Tektronix 4610 hard copy unit, so that the histogram of (m/n) can be displayed graphically and a permanent record can be obtained in less than a minute. In the following subsections the specimen voltage system, the Chevron ion detector, and the digital timer will be described in detail. Since the large number of interacting systems in the TOF atom-probe FIM are principally under the control of the computer during operation, we have made it our policy to thoroughly test the performance of each portion of the TOF atom-probe FIM, so that we can have absolute confidence in the data accumulated during experimental runs. We have included some of the results of these performance tests in the following discussion.

3.1 Specimen voltage system

This section contains a description of the dc and pulse high-voltage power supplies, the high-voltage pulser, and the high-voltage measuring-system. Design of this system was found to be critical to the overall performance of the TOF mass spectrometer. As shown in Fig. 9 the FIM specimen is connected through a 100MΩ pulse-blocking resistor to a Spellman RHR 30PN30* high voltage positive power supply. A 20nsec long high voltage pulse with a rise time of <1nsec produced by a Cayuga Associates CA-101 mercury-relay charging line pulser is coupled to the FIM specimen through a 4.7nF,30kV capacitor. A Spellman RHR 10PN100 high-voltage dc power supply is used to provide the high voltage to the pulser. The output of the charging-line pulser is approximately half of the supply voltage.

As shown in Fig. 10 the controls of the high voltage dc and pulse power supplies as well as the lens power supply are coupled together so that the pulse and lens voltages are always a constant fraction of the dc voltage. The 5kΩ ten-turn potentiometer in the dc power supply control circuit and the 10kΩ ten-turn potentiometers in the pulse and lens power supply control circuits are mechanically gauged together so that they track within 0.05%. The two 1kΩ potentiometers in the pulse and lens supply circuits control the pulse and lens fraction, respectively. The 2.5kΩ resistor in the dc supply circuit and the 500Ω resistor in the lens supply circuit are included to limit the range of these two supplies to 20kV maximum. The 100Ω resistor in the common return line of the dc supply circuit was introduced to allow the zero points of the pulse and dc supplies to be adjusted for optimum linearity. Typically the pulse voltage is maintained at 4 to 20% of V_{dc} and the lens is maintained at 30 - 50% of V_{dc}. Below

---

* This has recently been replaced by a CPS 110R power supply.

approximately 4% of V_{dc} the charging line pulser behaves erratically and the continuous dc-field-evaporation rate becomes comparable to the pulse-field-evaporation rate. Above 20% of V_{dc} the increased spread in the energy of the field-evaporated ions degrades the mass resolution of the spectrometer.

The values of V_{dc} and V_{pulse} are measured employing an Analogic 5800 series, 13 bit, 16 channel A/D converter which consists of a multiplexer module with 16 differential inputs, a sample and hold module, and a 13 bit A/D converter module. The input channel is computer selected and analog inputs of $0 \pm 10V$ are converted in $\sim$100μsec to a 13 bit binary number. The first bit represents the sign and the remaining 12 bits represent the magnitude, hence the resolution is 1 part in 4096.

The outputs of the high voltage power supplies are reduced by precision voltage dividers to bring these voltages within the 10V maximum range of the A/D converter. The dc voltage divider (shown in Fig. 11) contains two voltage division stages. The first stage, which consists of one-hundred-sixteen 0.825MΩ half-watt metal film resistors[20] in series with a single 0.825MΩ resistor of the same type, is encapsulated in Dow Corning Sylgard 184 resin to prevent high voltage breakdown. The second stage consists of two 1.5MΩ half-watt metal film resistors in series with 0.233MΩ. Since the first stage was constructed from 117 identical resistors, variations of resistance with either voltage or temperature do not affect the voltage division ratio of this stage. The use of identical resistors in the second stage was found to be unnecessary. Electrical noise was reduced below the resolution of the A/D converter by connecting both the power supply chassis ground and the A/D converter analog ground to a grounded water pipe. The pulse voltage divider consists of fifty 1.5MΩ half-watt metal film resistors in series with a 0.075MΩ metal film resistor. This simpler arrangement was found to be adequate for the pulse voltage measurement because the pulse voltage is typically $\lesssim$2kV. The high input impedances ($\gtrsim$75MΩ) of the voltage dividers minimizes heating and the use of metal film resistors contributes to the stability of the dividers.

The high-voltage power-supplies, the voltage dividers, and the A/D converter were tested by monitoring the measured voltage on the computer and comparing it with the known voltage obtained using a high-precision Hewlett-Packard 3439A

digital volt meter. These tests indicated that the voltages are known to within 5 volts which corresponds to one bit in the A/D converter. In addition, the stability of the power supplies† was tested by programming the computer to detect any changes in the output voltages. These tests indicated that the voltages are stable to within 5 volts over periods of several hours.

The shape of the high-voltage pulse was measured employing a Tektronix 7904 oscilliscope with a 7S11 sampling plug-in unit and an S-2 sampling head. Both a P6056 10x passive probe (with an input impedance of 500Ω and a rise time of 0.10nsec) and a P6057 100x passive probe (with an input impedance of 5kΩ and a rise time of 0.25nsec) were connected to the point at which the specimen is normally attached.

Typical pulse shapes are shown in Fig. 12. Figure 12(a) is a sketch of the overall pulse shape showing the large initial peak which is probably caused by reflections from the unterminated specimen. Figures 10(b), (c), and (d) represent actual oscilliscope traces of the top of the initial peak. Figure 10(b) was recorded with the 10x probe connected directly to the specimen holder. Figure 10(c) was recorded with the 100x probe connected directly to the specimen while Fig. 10(d) was recorded with the probe connected to the specimen by a 2 cm wire. The rise time of the leading edge is observed to be nearly equal to the inherent rise time of the probe and sampling head (0.35nsec) indicating that the pulse rise time is $\lesssim$0.2nsec. Although the maximum height of the first peak was found to be sensitive to the position of the probe, the overall features of the pulse shape remained the same as can be seen from a comparison of Figs. 12(b), (c) and (d).

3.2 Chevron ion detector

In the TOF atom-probe FIM the pulse-field evaporated ions are detected at

---

† Some long term stability problems were encountered with the Spellman 30kV power supply, which has recently been replaced by a CPS 100R power supply.

the downstream end of the flight tube by a fast electron multiplier. A large number of electron multipliers such as the curved channel electron multiplier,[21] Johnston detector,[22] magnetic strip detector[21,23] and channel-electron multiplier-array (CEMA)[13] have been used in atom-probe FIM's. We have chosen to use CEMA's (in the Chevron configuration) because they have particle detection characteristics which are as good as (or better than) any other detector and they also produce a visible ion image which is extremely useful for the alignment and focusing of the TOF spectrometer.

Two 25mm diameter CEMA's are used in the Chevron configuration(see Fig. 9). The 37.5μm diameter channels in the first CEMA are at an angle of 5° with respect to the normal to the front surface of the CEMA to prevent secondary ion feedback through both CEMA's. The value of the voltage applied to each of the two CEMA's can be varied. This was done because it has been shown that by making the voltage on the first CEMA 60% of the total voltage across both CEMA's that the number of after-pulses produced by positive ions being accelerated back through the channels is radically reduced.[21]

Behind the two CEMA's is a 25mm diameter phosphor screen which was prepared in the same way as the viewing screen described in Section 2.1. This viewing screen is capacitively coupled to a Lecroy Research System (LRS) 133B dual amplifier which is operated at a gain of 25. The output of the amplifier is delayed 500nsec (by ∿150m of RG 58 cable) and then triggers one channel of an LRS 161 discriminator which stops the digital timer.

Two types of tests were performed on the Chevron ion detector to determine the frequency of spurious pulses. The first test was a measurement of the background count rate and the second test was a measurement of the frequency of artifact pulses following the true pulse. The Chevron ion detector must be well characterized with respect to spurious pulses if small concentrations (e.g., in the 10^{-5}at.fr. or lower range) of impurity atoms are to be reliably measured.

Background counts from the Chevron ion detector are produced both by spontaneous emission within the CEMA's and by ionization of residual gases at the FIM tip. With the tip voltage off, a total voltage across both CEMA's of 1850V, and with 50% of the voltage across the front CEMA the dark current due to spontaneous emission was found to be 1 count sec^{-1}. Alternatively with the specimen voltage on, at a background pressure of $4x10^{-10}$torr, the count rate rises to $\sim$10 count sec^{-1}. These counts are attributed to field ionization of the residual gases in the FIM. For example, when the FIM is back-filled with helium to $4x10^{-6}$ torr the ion count rate is $\sim 10^5$ count sec^{-1}. Thus at a pressure of $4x10^{-10}$torr a background count rate of $\sim$10 count sec^{-1} would be expected in agreement with the observations. Since the digital timer has a maximum range of 100μsec the time window of the TOF mass spectrometer is open for $\approx 10^{-4}$sec. Thus, a background count rate of 10sec^{-1} will lead to a background of $1:10^3$ over the whole spectrum of m/n from 0 to 200 amu and a background of $1:2x10^5$ per amu. Hence, impurity atoms in the 10appm range can be detected if more than 1 or 2 ions are observed.

Artifact pulses following the true pulse are caused by ringing in the detector circuits and by after-pulses produced when secondary ions are back scattered through the channels of the CEMA's. To test for ringing the output of the detector was observed on a Tektronix 7904 oscilliscope with a 7A11 plug-in unit. Some ringing was observed, but it decayed within 50nsec. Thus, it was possible to eliminate any effects of ringing by increasing the width of the discriminator output pulse to $\geq$50nsec.

To test for after-pulses the digital timer was employed. The output of the discriminator connected to the Chevron ion detector was fed to both the start and stop inputs of the digital timer. Thus, the digital timer would start on the first random pulse received and would stop either on another random pulse or on an after-pulse if either were occurring. At a pressure of 10^{-7}torr helium gas in the FIM the count rate was 1400 count sec^{-1}. Since the timer was set to record all

events occurring within 10μsec after an event, one would expect 0.014 random counts for each true count. The observed fraction was 0.018 ± 0.002 which indicates that the frequency of afterpulses is ≈0.004 ± 0.002.

To examine the effect of the gas pressure on the occurence of afterpulses the gas pressure was raised to 2×10^{-6} torr helium, but the beam was deflected slightly so that the total count rate was constant at 1400 sec^{-1}. The observed fraction of random pulses was 0.016 ± 0.002 which indicates that the fraction of afterpulses is ≈0.002 ± 0.002. Thus increasing the gas pressure did not increase the occurence of after-pulses, and we can conclude that under normal operating conditions the occurence of afterpulses is negligible.

3.3 Digital timer

The digital timer which measures the TOF of the pulse-field evaporated ions is the key electronic instrument in the TOF mass spectrometer. There are basically three types of timers that could have been used with the atom-probe FIM.

The most commonly used timer is a fast oscilliscope[24] or a storage oscilliscope.[6] The oscilliscope has the advantages that it is simple and relatively inexpensive and is capable of a high precision over a limited time range. For example, using the delayed sweep a short time interval can be expanded to obtain a time resolution of ± 1nsec over a 100nsec range which might correspond for typical conditions to ± 0.03amu over a 3amu range. The disadvantages of the oscilliscope are twofold. First, each event must be analyzed individually by examining photographs of the oscilliscope traces. Second, although the oscilliscope is very precise over short intervals the absolute accuracy over longer intervals is not as good because of the nonlinearity of the sweep delaying circuit. Moreover, since only part of the m/n spectrum can be examined at one time, events outside that region are never detected.

The second timing instrument that could be used is a time-to-amplitude converter (TAC).[25] In this instrument a constant current source starts charging a capacitor when the START pulse is received and stops charging it when a STOP pulse is received. Thus, the voltage across the capacitor is proportional to the time interval between the start and stop signals. The TAC has the advantage that the measured times can be digitized and therefore automatically analyzed. In terms of time resolution it has the same advantages and disadvantages as the oscilliscope. It can provide a high resolution over a limited time interval (±50psec over 50nsec range), but over longer time intervals the accuracy is limited by a non-linearity of ∿0.1%.

The third timing instrument, and the one which we have chosen to use with our computer-operated atom-probe FIM, is the digital timer.[12] In operation, a high precision oscillator produces clock pulses with a precisely known period. Digital circuits count the number of clock pulses occurring between the start and stop signals whose time interval is to be measured. The advantages of the digital timer are that the output is directly compatible with a computer and that the accuracy over long time intervals is excellent. The principal disadvantage is that the resolution is limited to ± 1 clock period. Since digital counters with a bandwidth much above 100MHz are difficult to construct, time resolution is usually limited to ± 10nsec.

The digital timer that we have constructed[12] can measure the TOF of up to eight consecutive ions and can also measure a TOF as large as 99.99μsec with an accuracy of ± 0.01μsec. A greatly simplified schematic diagram of this instrument is shown in Fig. 13. The START signal, derived from the high voltage pulse applied to the specimen is fed to the AND gate input of CLOCK-IN on the START SYNCHRONIZER FLIP-FLOP. The other input of this AND gate is supplied with CLOCK pulses from the 100 MHz oscillator. The TRUE OUTPUT opens the CLOCK AND GATE thus allowing CLOCK pulses to pass through to the eight counters. Using this

arrangement, a START signal causes the OUTPUT of the START FLIP-FLOP to switch to the TRUE or +1 state synchronously with the CLOCK thus ensuring that the amplitude and width of the first CLOCK to the eight counters is identical to all subsequent clock pulses, so that all eight counters will detect the first CLOCK pulse.

The STOP signal is synchronized in a similar way so that the OUTPUT of the STOP SYNCHRONIZER FLIP-FLOP switches to the TRUE state synchronously with the CLOCK. The OUTPUT signal is delayed by .02μsec and fed into the RESET input of the STOP SYNCHRONIZER FLIP-FLOP which causes the OUTPUT to switch FALSE. Thus, a STOP signal causes a pulse of approxiamtely .02μsec duration which is synchronous with the CLOCK, to be produced at the OUTPUT of the STOP SYNCHRONIZER FLIP-FLOP. This STOP OUTPUT pulse is fed to CLOCK-IN of the STOP-LOGIC FLIP-FLOP CHAIN.

The STOP-LOGIC FLIP-FLOPS, which have the property that the OUTPUT is switched to the value present at DATA-IN whenever a pulse is applied to CLOCK-IN, are interconnected so that each FLIP-FLOP is triggered in sequence when a STOP signal is received. This is accomplished by connecting DATA-IN of each FLIP-FLOP to the OUTPUT of the preceeding FLIP-FLOP. Thus, when the first stop signal is received, only the first FLIP-FLOP will change state, since its DATA-IN input is always equal to 0 or FALSE. None of the succeeding FLIP-FLOPS will be triggered, however, since their DATA-IN inputs are connected to the OUTPUTS, all of which are initially TRUE. When the second STOP signal is received the second FLIP-FLOP will be triggered since the OUTPUT of the first FLIP-FLOP is now FALSE. Since the OUTPUTS of each of the STOP-LOGIC FLIP-FLOPS is connected to one of the inputs of each of the eight STOP AND GATES of the corresponding COUNTER-CHAIN, the counters are stopped in sequence as the STOP signals are received. Since the STOP-LOGIC FLIP-FLOPS change state in synchronization with the CLOCK, the STOP AND GATES are closed sychronously with the CLOCK. Thus, the last CLOCK pulse to each of the COUNTER-CHAINS is identical to all preceeding CLOCK pulses. The TOF

are read into the computer and following this a RESET pulse is sent out which returns all of the FLIP-FLOPS to the untriggered state, and also resets all the COUNTERS to zero in preparation for the next measurement.

The digital timer was tested by injecting pulses with known relative delays into the start and stop inputs. The computer was programmed to read in the measured times and test them for any variation. The results of this test were that the timer performed $>10^6$ simulated measurements without an error, indicating that the times measured during experiments can be treated with confidence. The synchronization of the starting and stopping of the counting chains with the 100 MHz CLOCK was found to be essential to realize the theoretical time resolution of ±10nsec. Test conducted with asynchronous START and STOP signals indicated errors in time measurements as large as ±70nsec in up to 5% of the cases.

3.4 Calibration of the TOF atom-probe FIM

As stated previously, the m/n values are computed from the measured TOF, V_{dc}, and V_{pulse} using the equation[27]

$$\frac{m}{n} = 2e\,(V_{dc} + \alpha\, V_{pulse})\,\frac{(t-t_o)^2}{d^2},$$

where m/n is in amu, V_{dc} and V_{pulse} are in Volts, t and t_o are in μsec, d is in mm and α is the dimensionless pulse-factor. For this choice of units the constant 2e is equal to 193.0. The value of V_{pulse} is taken to be one-half of the dc voltage applied to the charging-line pulser. The quantity α is required because the peak pulse voltage reaching the tip is not equal to V_{pulse}. This discrepancy is caused by inaccuracy in the charging line pulser, impedance variations along the pulse line, and reflections at the unterminated specimen. The quantity t_o is required because of the 500nsec delay time which was intentionally inserted between the amplifier and the stop discriminator and because of other smaller time shifts occurring in the electronic apparatus. The length d denotes the flight path determined by calibrating the instrument for known m/n ratios. This flight length, d, is used, rather than the physical length of the flight tube, since they are not necessarily equivalent distances. For example, the actual ion trajectory is affected by the focusing lens, the earth's magnetic field, and stray electrical and magnetic fields. In general, the TOF atom-probe FIM must be calibrated using ions with known values of (m/n), before unknown (m/n)'s can be identified. Since there has been some uncertainty in the past concerning the best method of calibration, we will describe in detail the two methods that we have used.

The first method tried was similar to the first of two methods described by Panitz, McLane, and Müller.[27] It involves a systematic determination of the calibration parameters α, t_o, and d using the TOF of two species of ions with known m/n. The value of t_o is determined first. If $(m/n)_1$ and $(m/n)_2$ are the known (m/n) ratios and t_1 and t_2 are the corresponding observed TOF of the two species, the quantity t_o is readily shown to be

$$t_o = \left\{ t_2 \left[\frac{(m/n)_1}{(m/n)_2} \right]^{1/2} - t_1 \right\} \Bigg/ \left\{ \left[\frac{(m/n)_1}{(m/n)_2} \right]^{1/2} - 1 \right\} .$$

Thus, for example, for $(m/n)_1$=62amu ($^{186}W^{+3}$) and $(m/n)_2$=4amu (He^+) the values of t_1 and t_2 are observed to be t_1=14.17μsec and t_2=4.02μsec. Hence, we obtain t_o=0.56μsec. The determination of t_o is most sensitive to the measured TOF of the lighter ion since this is weighted by the factor $[(m/n)_1/(m/n)_2]^{1/2}$ which is 3.9 for the example given here. To obtain the pulse factor, TOF measurements are made with two different sets of pulse and dc voltages. If t_1 is the TOF for a given isotope when the pulse and dc voltages are $(V_{pulse})_1$ and $(V_{dc})_1$ respectively, while t_2 is the TOF for the same isotope when the voltages are $(V_{pulse})_2$ and $(V_{dc})_2$, the quantity α can be shown to be given by

$$\alpha = \frac{(V_{dc})_2 (t_2-t_o)^2 - (V_{dc})_1 (t_1-t_o)^2}{(V_{pulse})_1 (t_1-t_o)^2 - (V_{pulse})_2 (t_2-t_o)^2} .$$

For typical experimental conditions we found α=1.5±0.5. Since α and t_o are now known we can obtain d simply by solving the equation for m/n to obtain

$$d = (t-t_o) \sqrt{193.0 \times (V_{dc} + \alpha V_{pulse}) \cdot (n/m)} .$$

Thus, for example if V_{dc}=8,000V, V_{pulse}=400V, t=14.18μsec and m/n=62amu (W^{+3}), we obtain d=2228mm. As mentioned this method is similar to the one described by Panitz, McLane, and Müller.[27] The principal difference is the order in which the parameters are obtained. Their method has the advantage that the pulse factor α can be obtained without varying the voltage. The method described here has the advantage that t_o is essentially determined by the position of the He^+ peak, and is therefore accurately known. Both methods suffer from the fact that in practice it is difficult to determine the pulse factor α with sufficient precision to prevent broadening individual peaks in the m/n spectra. To eliminate the problem of determining α we have developed a new method of calibrating our TOF atom-probe FIM. Ths basis of our precedure is to make V_{pulse} a constant

fraction of V_{dc}

$$V_{pulse} = f\, V_{dc},$$

where f is a constant. This is accomplished by mechanically coupling the potentiometers controlling the dc and pulse power supplies. The equation for m/n is now rewritten as

$$\frac{m}{n} = \frac{2e(1+\alpha f)V_{dc}(t-t_o)^2}{d^2} .$$

The lumped parameter $(1+\alpha f)/d^2$ is considered to be simply one adjustable parameter. This reduces the problem of calibration to finding only two parameters, t_o and the effective length (d_{eff}), where d_{eff} is given by

$$d_{eff} = d/(1+\alpha f)^{1/2},$$

so that the equation for m/n reduces to

$$\frac{m}{n} = \frac{2e}{d_{eff}^2} V_{dc}\ (t-t_o)^2.$$

At present the linearity of V_{pulse} with V_{dc} is only ±1%*, therefore (V_{pulse}/V_{dc}) = f±0.01f. In view of this variation of f with voltage, both V_{dc} and V_{pulse} were measured independently and the data were analyzed using the general equation for (m/n). With the tracking power supplies for V_{dc} and V_{pulse}, the calibration procedure is quite straightforward; employing reasonable first estimates of α, t_o, and d to compute (m/n) a histogram (number of events versus m/n) is constructed. In a typical case for tungsten the ions He^+ and W^{+3} are used to calibrate the (m/n) scale. The position of the He^+ peak is very sensitive to the value of t_o, hence t_o is varied until the He^+ peak lies at exactly 4amu. Similarly, d is varied until the observed isotope peaks of W^{+3} lie at the correct mass-to-charge ratios. This process is iterated until a self consistent set of

---

* This has been reduced by at least a factor of 10 by replacing the Spellman power supply with the CPS power supply (see page 16).

t_o and d values is obtained. The calibration always converged rapidly and not more than two iterative approximations have been found necessary.

A computer simulation* was performed to test the sensitivity of the spectrum to the choice of α in view of the measured variation of f with voltage. These calculations indicated that for f=0.05±0.0005, a 100% error in α (e.g., α varying from 1.00 to 2.00) lead to a broadening in (m/n) of <0.03amu at 60amu with V_{dc} ranging from $4x10^3$ to $16x10^3$V. This uncertainty in (m/n) is much smaller than the uncertainty introduced by the time measurement (i.e., $2\Delta t/t$ where Δt=±10nsec for our atom-probe FIM). The principal advantages of keeping V_{pulse} a constant fraction of V_{dc} are: (1) the value of α chosen has a negligible effect on the shape of the peaks in the observed spectra; (2) the shapes of the observed spectral peaks do not depend on an exact determination of the calibration parameters α, t_o, and d (although the absolute positions do depend on an exact determination); and (3) possible changes in α with goniometer position or specimen-to-image intensification system distance have a negligible effect on the observed spectra.

4. COMPUTER SYSTEM

This section describes the computer system which has been interfaced to the TOF atom-probe FIM. The system is under complete software control and, in the course of an experiment, it rapidly collects, stores and analyzes the mass spectrometer data and also presents results in both graphical and numerical form.

The system hardware consists of: (1) a Nova 1220 minicomputer; (2) three cassette tape transports; (3) a teletype; (4) a graphics display terminal; (5) an A/D converter for measuring the dc and pulse voltage on the specimen; and

---

* See Section 4.

(6) the atom-probe interface which connects the digital timer and high-voltage pulser the computer. The vast majority of the software material consists of the program which controls the operation of the TOF atom-probe FIM. The four primary functions of this program during an experiment are as follows:

(1) Take data - Pulse the tip, read the TOF's from the digital timer, and read V_{dc} and V_{pulse} from the A/D Converter.

(2) Store data on cassette - The TOF's, V_{dc} and V_{pulse}, and the number of pulses necessary to field evaporate the atoms detected are stored on cassette tapes.

(3) Analyze data - Calculate the (m/n) ratios and store the histogram in the core memory.

(4) Present results - Plot the histograms in the form of the number of events versus m/n, and tabulate the histogram in numerical form.

Section 4.1 contains a description of all hardware except the TOF atom-probe FIM interface which is described in Section 4.2. Section 4.3 contains a discussion of the programming languages used and a description of the program used to operate the TOF atom-probe FIM. The auxilliary programs we have developed for use in conjunction with the atom-probe are described in Section 4.4.

4.1 The Nova 1220 computer and peripherals

In its most elementary form a typical computer consists of: (1) a central processor which is the computational and control element of a computer; (2) an information storage device, (e.g., core memory); (3) a front panel which contains a series of switches and lights through which one can exchange information with the central processor and core memory; (4) a power supply; and (5) a chassis housing all of the above components. The combination of a chassis, power supply and front panel constitutes the computer main frame. The central processor and memory are contained on circuit boards inserted into this main frame. The typical computer system also contains several peripheral components; notably an auxilary storage medium which supplements core memory, such as a disk memory or a magnetic

tape, and standard input-output (I/O) devices which supplement the front panel such as a teletype, a line printer, and a graphics display terminal. In addition, computer systems linked to experiments contain non-standard I/O devices. Thus, for example, from the point-of-view of the computer, the digital timer and the high-voltage pulser used with the TOF atom-probe FIM appear as non-standard I/O devices. Each auxilliary storage device and each I/O device requires an interface. The interface is contained on a circuit board housed in the computer main frame and serves as the electronic link through which the device may communicate with the computer. We now present a description of the Nova 1220 computer and peripherals. The computer TOF atom-probe FIM interface will be discussed in Section 4.2. The central element in this computer system is the Nova 1220 computer. The computer consists of a four-accumulator central processor, 32K (i.e., 32, 768), sixteen bit words of core memory, and the computer main frame. Accumulators are static 16 bit storage devices in the central processor through which all data that enters or leaves the computer must pass. The central processor and memory occupy four of the ten circuit board slots in the Nova 1220 main frame. The memory capacity of the computer is sufficient to store the BASIC language interpreter occupying 12K of core and a BASIC program of roughly 2000 statements and 1000 variables.

Three cassette tape transports serve as high speed auxilliary storage devices. The three transports are housed in one chassis and share a common interface, requiring one circuit board slot in the computer main frame. The cassette tapes serve as a high density medium for the storage of programs and data; thus greatly reducing the use of paper tape. Each cassette tape can store $\sim$50,000 16 bit words. With the present software, this corresponds to the storage of the TOF, V_{dc} and V_{pulse} for 10^4 atoms. An entire tape can be read in less than two minutes.

The standard I/O devices are: (1) an ASR 33 teletype; (2) a Tektronix 4010 graphics display terminal and 4610 hardcopy unit; and (3) an Analogic 5800 series analog-to-digital (A/D) converter. The teletype, terminal, and hardcopy unit share

a common interface which occupies one circuit board slot in the computer main frame. The teletype is generally used only for reading and punching paper tapes. All alphanumeric and graphics I/O is handled by the 4010 terminal. Permanent copies of the information displayed on the terminal are made by the 4610 hardcopy unit.

The Analogic 5800 series A/D converter is used to measure the dc and pulse voltages applied to the specimen. The interface for the A/D converter occupies one circuit board slot in the computer main frame. Further details concerning the A/D converter voltage measurement system can be found in Section 3.1. With the exception of the 4010 graphics display terminal and 4610 hardcopy unit, all equipment was supplied as a functioning system by the Data General Corporation. The terminal and hardcopy unit, purchased directly from Tektronix, were found to be both hardware and software compatible with the Data General Corporation system.

4.2 TOF atom-probe FIM interface

Since the computer system hardware described in Section 4.1 cannot communicate with either the digital timer or high voltage pulser additional hardware is required to make communication possible. This section contains a description of the TOF atom-probe FIM interface, whose function is to provide the link through which information may pass between the computer and the TOF atom-probe FIM.

The interface allows the computer to perform the following four functions: (1) trigger the high voltage pulser; (2) select any one of the eight timing chains in the digital timer; (3) read in the TOF from the previously selected timing chain; and (4) reset the digital timer in preparation for another TOF measurement. In addition, the interface signals the computer when the pulser is ready to produce another high voltage pulse. The interface was constructed on a Data General Corp. model 4040 general purpose interface board and occupies one circuit board slot in the main frame. Approximately one-half of the interface board contains the manufacturer's circuits while the other half is reserved for user electronics. We have constructed this board to allow the parallel input of a 16 bit number, the parallel

output of a three-bit number and the output of two independent control pulses. A block diagram of the interface circuit is shown in Fig. 14. The interface functions, and corresponding assembly language program instructions are shown on the left hand side and the instrument functions are shown on the right hand side of the figure. The tip is pulsed whenever a DOCS 0, 44 instruction is encountered in the program. Here the key identifiers are the S, which stands for output a Start pulse and the device code number 44, which directs the Start pulse to the TOF atom-probe FIM interface. This pulse triggers the high-voltage pulser, sets the BUSY-DONE flip-flop on the interface into the BUSY state, and triggers a monostable multivibrator. After a delay equal to the cycle time of the high voltage pulser ($\sim$10msec) the monostable multivibrator resets the BUSY-DONE flip-flop into the DONE state. By monitoring the state of this flip-flop, the computer is able to determine if the high voltage pulser is ready to produce another pulse (i.e., done) or if it is in the process of producing a pulse (i.e., busy).

Since there are only 16 binary inputs to the computer and since there are eight separate TOF counters each of which contains 16 bits of data, a multiplexer is needed to read one counter at a time into the computer. The counters are selected by first loading the number of the desired counter in accumulator 0 and then issuing a DOA 0, 44 (Data Out A, from accumulator 0, to device 44). This causes the three bit number to be output from the interface board to the timer and the multiplexer to connect the appropriate counter onto the 16 data input lines into the TOF atom-probe FIM interface. After the counter has been selected a DIA 1, 44 (Data In A; into accumulator 1; from device 44) loads the 16 bit BCD TOF data into accumulator 1.

After all of the TOF have been read in, the command NIOP 0, 44 (No Input Output Pulse) causes a pulse to be sent out which resets all the flip-flops and counters in the digital timer in preparation for the next measurement.

If any ions were detected the dc and pulse voltages are read in from the

A/D converter in much the same way as the TOF were read in from the digital timer. First the channel is selected by loading the number 2 or 3 into accumulator 0 and executing the command DOAS 0, 21 (Data Out A plus Start from accumulator 0, to device 21; i.e., the A/D converter). This selects either the dc or pulse voltage channel, and initiates an A/D conversion. A DIC 1, 21 command (Data In C, into accumulator 1, from device 21) then loads the 13 bit voltage data into accumulator 1.

4.3 Computer programs to operate the TOF atom-probe FIM

The software that we have developed consists of 4 programs written in BASIC and ASSEMBLY programming languages which: (1) operate the atom probe; (2) prepare a dictionary of (m/n) ratios; (3) generate simulated mass spectrometer data; and (4) diagnose hardware malfunctions. This section begins with a description of the programming languages used and the reasons for their selection, followed by a description of the program used to operate the atom-probe FIM. The three remaining programs will be described in Section 4.4.

A combination of BASIC and ASSEMBLY languages has, so far, been found to be the most flexible and efficient system for operating the TOF atom-probe FIM, since BASIC language programs can be easily changed during operation and ASSEMBLY language subroutines are fast. ASSEMBLY language is the least abstract of all programming languages, since each statement can be directly translated into a single hardware function. Thus, ASSEMBLY language provides the most direct control of the computer functions on the finest possible scale. For example, the instruction LDA 0, 100 causes the contents of core memory location 100 to be Loaded into Accumulator 0. In contrast, the BASIC instruction X=Y expresses a much more abstract idea and would require translation by a computer into many Assembly language statements. However, ASSEMBLY language is extremely tedious so that it has only been used when absolutely necessary. The majority of our ASSEMBLY language subroutines were developed only to implement functions not provided by BASIC. For example, since there are no BASIC statements which allow communication

of the TOF atom-probe FIM with the computer, it was necessary to develop ASSEMBLY language subroutines which would pulse the tip, read in the 4 digit BCD time-of-flight, etc. In addition, four ASSEMBLY language subroutines which create, read, and clear the hsitogram and find the peak containing the maximum number of (m/n) values in the histogram were written to replace equivalent but much slower BASIC program sections. All of these subroutines can be called by BASIC statements. The general form of a Basic call is: (statement number) CALL (subroutine number), (up to 8 arguments). For example, the statement 100 CALL 6, T(1), T(2), T(3), T(4), T(5), T(6), T(7), T(8) causes eight TOF's stored in the digital timer to be transmitted to the computer, translated from BCD to floating point notation and passed to variables T(1) through T(8).

Most BASIC statements have FORTRAN analogs and, in general, the languages are similar in most respects. However, there is a major difference between the languages in that an entire FORTRAN program must be first compiled and then executed, thus involving a two step process; while BASIC programs are compiled and executed simultaneously in one step, one statement at a time. Thus BASIC allows on-line development and modification of programs without requiring time consuming recompilation of the entire program. For example, modification of even a single statement in a FORTRAN program always requires recompilation of the entire program which, for our computer system can take well over 1 hr ; while in BASIC, the same modification would consume only the time required to type it into the computer. Thus, program development and in particular program modification during an experiment was found to be easier in BASIC than in FORTRAN. The major drawback of BASIC is that, since each statement must be re-interpreted (recompiled) each time it is executed, BASIC programs run considerably slower than the equivalent FORTRAN or ASSEMBLY language programs. However, as mentioned previously, the running time can be substantially reduced by suitable replacement of particularly time consuming sections of BASIC programs with functionally equivalent, but faster running, ASSEMBLY

language subroutines.

An extensive computer program to operate the TOF atom-probe FIM called the Atom-Probe-Operating System (APOS) has been written and tested. The program is arranged in a three-level heirarchy as shown in Fig. 15. At the top is the controlling EXECUTIVE program which initializes variables and selects the appropriate function of APOS. Under the EXECUTIVE program are the five main BASIC language subroutines PULSE, GRAPH, READ, CALIBRATION, and DICTIONARY SCANNING. At the lowest level in the heirarchy are the ASSEMBLY language subroutines. A sample computer-operator dialogue is presented in APPENDIX A.

4.4 Auxilliary programs

This section describes three programs which: (1) create an ordered table of (m/n) ratios of selected elements: (2) generate simulated mass spectrometer data; and (3) diagnose hardware malfunctions. Although these programs have contributed to the maintenance of the TOF atom-probe FIM and our interpretation of experimental results we have classified them as auxilliary programs since they are not essential to the operation of the TOF atom-probe FIM. The DICTIONARY GENERATING program was written to prepare an ordered table of m/n ratios for selected combinations of elements. An example of the information provided in the dictionary is given in Appendix A on the dictionary scanning subroutine of APOS. Briefly, the information is the m/n value of the combination, the elements in the combination, the charge state, and the percent natural abundance. The dictionary of m/n values generated has proven to be useful for indicating potential difficulties in attempting to identify unambiguously the peaks observed in the experimental spectra. In preparing the dictionary, the isotopic masses and percent natural abundances of the elements[28] of interest are first stored in the computer. The ranges of charge states desired for each element and the names of the elements which are to be paired with all other elements, (e.g., the gases hydrogen and helium) are obtained and stored. Special cases, such as combinations of three atoms, are typed in individually. The dictionary generating program then calculates the m/n values of all the desired

combinations and writes them as well as the atomic numbers of the elements, the charge state, and the percent natural abundance on a cassette tape in the order they are calculated. After all the combinations have been computed, the entries are arranged in order of increasing m/n values. Since the computer storage is far too small to accomodate all the data at once, a multiple-pass process is required. The program scans the tape once to determine how large a range of (m/n) values can be handled on each pass. It then re-reads the tape, selecting only the first group of m/n values. These are written in order on a second tape and the first (unordered) tape is re-read. For a typical dictionary containing 50 elements there will be approximately 5000 entries, and the ordering process will consist of 5 passes requiring a total time of 0.5h.

An empirical data simulation program called SYNGEN was written to test the effect of the voltage and TOF uncertainty on the (m/n) resolution. The operator selects the total number of events to be simulated, N, the voltage range, the length of the flight tube, the resolution of the dc and pulse voltage measurements, the pulse fraction, and the resolution of the digital timer. In addition an exponential tail of the form exp $(\frac{-m/n}{\rho})$, where ρ is a constant, can be added to each of the peaks. The physical origin of this exponential tail is believed to be due to a spread in the energy of the field evaporated ions and has been termed energy deficits by workers in the field.[29] The program begins by breaking the voltage range into N equal segments. For each event the actual voltage, V_a, is picked at random from within the corresponding segment. This randomizing feature was added to prevent any possibility of systematic errors being introduced by having the voltages for each event equally spaced. The measured voltage, V_m, is computed from the true voltage by first calculating the dc and pulse voltage using the pulse fraction, and then rounding these voltages off to correspond to the resolution of the dc and pulse measurements. The sum of these is taken as V_m. The (m/n) ratio, M_i, of an isotope of the element to be simulated is selected at random and weighted by the known

isotopic concentration. An energy deficit of exponential form is added using the relation

$$M_o = M_i - \rho \ln r$$

where M_o is the observed mass, including energy deficits, and r is a random number between 0 and 1. The actual TOF is calculated from

$$t_a = \sqrt{\frac{M_o d^2}{2e V_a}}$$

and the measured time, t_m, is calculated by rounding this off to within the resolution of the digital timer. The measured mass is then calculated from the measured voltage and measured TOF employing the usual formula

$$M_m = 2e V_m t_m^2 / d^2,$$

and then stored as a histogram. Since ρ is the only unknown parameter when modelling experimental results, it provides a measure of the relative importance of energy deficits on the (m/n) resolution. A forthcoming report on factors affecting resolution will deal with this in greater depth. In addition, the program has proven useful as a guide for predicting the minimum detectable concentration of solute atoms in an alloy; Fig. 16 shows a synthetic histogram for tungsten-25 atomic % rhenium generated by this program. The voltage range was 3600 to 4400V, the flight distance was 2222mm, the dc and pulse resolution was ±2V and ±0.5V respectively, the time resolution was ±10nsec, the total number of events was 2000, and the energy deficit parameter, ρ, was 0.25amu.

This figure can be compared with Fig.25 for an actual W-25at.%Re spectrum taken under equivalent conditions. The agreement between the two is good and indicates both that our rather simple empirical model is adequate for reproducing the shape of observed spectrum and that (except for the energy deficit tail) the actual resolution of the TOF atom probe FIM approaches the theoretical limits of resolution imposed by the measurement of the voltages and the TOF.

In order to insure the reliable operation of the computer system, an extensive diagnostic program which tests all hardware functions is run periodically. The computer system was supplied with a diagnostic program capable of testing the central processor, core memory, the cassette transports and the three standard I/O devices. The scope of this program was extended to allow testing of the TOF atom-probe FIM interface, digital timer and high-voltage pulser.

The high-voltage pulser and associated interface circuits are tested by comparing the total number of high-voltage pulses produced with the number of pulse commands issued by the computer. Since only high voltages pulses which can trigger a discriminator, set about 5% below the peak pulse voltage, are counted the incidence of substandard pulses can be determined. The test is usually run for 1 h, in which time about 10^5 pulses are produced. Thus far no substandard pulses have been detected. There are two tests run on the digital timer and associated interface circuits. In the first test 4 digit numbers are manually entered into each of the eight counting chains in the digital timer, such that none of the counting chains contain the same number. The computer then repeatedly reads the digital timer and compares the number read with the number which was entered. Any error in the selection of the counting chain or in the transmission of the contents of the counting chain to the computer is detected. In the second test pulses with known relative delays are sent to the start and stop inputs of the digital timer. The measured times are read by the computer and tested for variations. In over 10^6 operations, no errors were detected by either of these two tests.

5. SOME EXPERIMENTAL RESULTS

This section contains a description of typical spectra obtained for pure tungsten and molybdenum specimens, and also a spectrum obtained from a tungsten-25% rhenium alloy. These sample spectra show very clearly the mass resolution capabilities of this atom-probe FIM.

5.1 Tungsten (W^{+3} and W^{+4} spectra)

Histograms of the data obtained for tungsten are shown in Figures 17-20. Figure 17 shows the entire mass range from 0 to 100amu. The W^{+3} and W^{+4} peaks located near 60 and 40amu, respectively, are clearly visible. A small peak due to residual helium gas at 4amu can also be seen. Histograms of the W^{+3}, W^{+4} and He peaks are shown on expanded scales in Figures 18, 19 and 20 respectively. Peaks associated with the five naturally occuring isotopes of W (W^{180}, W^{182}, W^{183}, W^{184}, and W^{186}) can be readily distinguished from one another in the W^{+3} spectrum (Fig. 18) which contains 6009 events. The W^{+4} spectrum (Fig. 19) shows only three clearly distinguishable peaks because the mass resolution in the W^{+4} range is less than in the W^{+3} range. This decrease in resolution is attributable principally to the ±10nsec time resolution of the digital timer used to measure the TOF's. The 1240 W^{+4} events represent 17% of the total number of events recorded.

These W spectra were recorded with the atom-probe FIM at a background pressure of 6×10^{-10}torr, at a tip temperature of ~25K, and with the probe-hole in the internal image intensification system over the (551) plane. The value of f was set at 0.05 and the calibration parameters used were $\alpha=2.0$, $t_o=0.56\mu$sec, and d=1600.3mm. A comparison of our experimental W^{+3} isotopic aboundances with the handbook values[28] of these quantities is shown in Table 1. It is seen that the agreement is rather good. The fact that the W^{+4} peaks fall where expected indicates that the mass scale calibrated from the He^{+} and W^{+3} peaks is linear.

5.2 Molybdenum (Mo^{+2} and Mo^{+3})

Histograms of the data obtained for molybdenum are shown in Figs. 21, 22 and 23. Figure 21 shows the entire mass range from 0 to 100amu. The Mo^{+2}, Mo^{+3} and Mo^{+4} peaks at about 50, 33, and 25amu are very clearly seen. In addition, there are peaks at 1amu and 4amu which are associated with the residual hydrogen and helium in the atom-probe FIM. Histograms with expanded scales of the Mo^{+2} spectrum, and the Mo^{+3} spectrum are shown in Figures 22 and 23, respectively. Peaks associated

with the seven naturally occuring isotopes of Mo (Mo^{92}, Mo^{94}, Mo^{95}, Mo^{96}, Mo^{97}, Mo^{98}, Mo^{100}) are clearly distinguishable from one another. These Mo spectra were recorded with the atom-probe FIM at a background pressure of $5x10^{-9}$torr, at a tip temperature of ~60K, and with the probe hole in the image intensification system near the (110) pole. The pulse fraction f was set at 0.025, and the calibration parameters used were α=1.482, t_o=0.56μsec, and d=2213mm. A comparison of our experimental Mo^{+2} isotopic abundances with the handbook values of these quantities is shown in Table 2. It is seen that there is good agreement between the two sets of values. Figure 23 exhibits the Mo^{+3} spectrum recorded simultaneously with the Mo^{+2} spectrum and in Table 3 a comparison between the handbook values of the isotopic abundances and our experimental values is given.

5.3 Tungsten-25at.% Rhenium

A histogram of the data obtained from a specimen of tungsten-25at.% rhenium thermocouple wire is shown in Figs. 24 and 25. The W-Re spectra were recorded at a tip temperature of 25K and with f=0.10. The calibration parameters used were α=1.5, t_o=0.56μsec, and d=2232mm. The $^{185}Re^{+3}$ peak at 61.67amu and the $^{185}Re^{+3}$ peak at 62.33amu are readily seen. The total number of events was 1834 of which approximately 95% had charge state +3 while only 5% had charge state +4; this result is in strong contrast to our observations on pure tungsten where 17% of the events were in the +4 charge state. The composition profiles shown in Figs. 26 and 27 demonstrate that the $^{185}Re^{+3}$ and $^{187}Re^{+3}$ isotopes are uniformly distributed throughout the sample. The relative percentages are 10.7at.% $^{185}Re^{+3}$ and 14.7at.% $^{187}Re^{+3}$ for a total rhenium concentration of 25.4at.% which is in agreement with the nominal concentration. A comparison of our experimental isotopic abundances with the handbook values for a W-25% Re alloy is given in Table 4. The total Re concentration is 28.5at.% This result was obtained counting only those atoms in the ranges shown in Table 4. In contrast, the 25.4at.% Re result obtained from the composition profile is the number of atoms in the ranges 61.6 to 62.0 and 62.3 to 62.6 divided by the total number of atoms in the W-Re^{+3} peak including the tail from 62.6 to 65 amu.

Clearly there is a problem in accounting for the atoms in the tail in a simple way because each peak has its own tail which interferes with the peaks at higher (m/n). To resolve this a third method was used to obtain the relative concentration of rhenium. A relatively simple least-squares procedure was used to fit all seven peaks in the W-Re^{+3} spectrum assuming they are of pure exponential form. The adjustable parameters were the concentration of rhenium and the decay constant of the exponential tail. In addition a third parameter, which compensated for any error in the absolute position of the m/n spectrum, was least-squares adjusted. The results of the fit were 22±2% for the rhenium concentration, 0.31 amu for the decay constant of the exponential tail, and 0.065 amu for the required shift in the m/n scale to obtain the best fit.

6. SUMMARY

An ultra-high vaccuum time-of-flight (TOF) atom-probe field-ion microscope (FIM) specifically designed for the study of defects in metals is described. The description of the instrument is subdivided into the following three main categories: (1) field-ion microscope system; (2) TOF mass spectrometer; and (3) computer system. The paper is now summarized following this categorization.

1. Field-ion microscope system

The FIM is a stainless-steel ultra-high vaccuum ($\lesssim 5 \times 10^{-10}$ torr) system employing an internal-image-intensification system based on a 75mm diameter Gallileo channel-electron-multiplier array (CEMA) with a 3mm diameter probehole. The internal-image-intensification system is immediately followed by a focusing lens which is used to focus the pulse-field evaporated ions onto the ion detector in the TOF spectrometer. The intensified FIM image is viewed with a front-surfaced glass mirror placed at 45° to the flight path; it contains a 10mm diameter hole and is positioned immediately behind the focusing lens. The assembly consisting of the internal-image-intensification system, focusing lens and viewing mirror is attached to two UHV metal bellows (see Fig. 2) so that the distance from the tip of the specimen to the front surface of the internal-image-intensification system is continuously variable. This latter feature provides a lineal magnification change of ∿8X and hence an areal magnification change of ∿64X. The FIM specimen is held in a liquid-helium cooled Brenner-style goniometer stage. The Brenner-style goniometer stage provides rotation about two orthogonal axes which intersect at the tip of the specimen; the goniometer stage is also translatable in three mutually orthogonal directions to facilitate alignment of the tip with respect to the probe hole. The specimen is exchanged by means of a high-vaccuum ($<10^{-6}$ torr) specimen exchange device which allows for the rapid transfer of specimens without having to break the vaccuum in the FIM. The temperature of the FIM tip is continuously variable from 13 to 450K. The FIM tip can also be irradiated in-situ with any low-energy (<1keV) gas ion employing a specially constructed ion-gun.

2. Time-of-flight mass spectrometer

The pulse-field evaporated ions are detected by a Chevron ion-detector located 2.22m from the FIM specimen. The flight tube of the TOF mass spectrometer is isolated from the FIM by an UHV straight-through valve and the flight tube also has its own separate vaccuum system. This arrangement allows a vaccuum to be maintained in the Chevron ion detector section even when the main chamber is not under vaccuum and also provides for differential pumping of the flight tube to reduce the partial pressure of helium gas in it. The controls of the dc and pulse high voltage power supplies as well as the power supply for the focusing lens are mechanically ganged together (see Fig. 9), so that the pulse and focusing lens voltages are maintained at a constant fraction of the dc voltage. The outputs of the high voltage power supplies are measured by an analog-to-digital (A/D) converter and input to a Nova 1220 computer whenever a TOF measurement is made. A small fraction of the high voltage pulse is picked off and fed to a discriminator which starts an eight-channel digital timer and also triggers a gate generator. The voltage pulse produced when an ion reaches the Chevron ion detector is amplified, delayed 500nsec, and then fed to the stop discriminator. The stop discriminator is gated by the gate generator which is typically set to open 600nsec after the start pulse. This latter procedure guarantees that any interference from the high voltage pulse will not improperly trigger the stop discriminator and that only true events will be detected. A total of eight consecutive stop signals can be analyzed and thus eight ion species can be identified. The TOF data is stored in binary-coded-decimal (BCD) format within the timer until the computer is ready to read the TOF data. The computer then calculates the mass-to-charge ratio (m/n) using the TOF data and voltage data. After the m/n ratios are computed they are stored in the computer memory in the form of a histogram of the number of events versus (m/n). In addition, the raw data consisting of the TOF and the voltages are stored on a magnetic cassette tape so that the results of the run can be re-analyzed in the future. The computer is interfaced to a Tektronix 4010

graphics display terminal and a Tektronix 4610 hard copy unit, so that the histogram can be displayed graphically and a permanent record can be obtained in less than a minute.

3. Computer system

The TOF atom-probe FIM is under complete software control and, in the course of an experiment, the system rapidly collects, stores and analyzes the mass spectrometer data and also presents it in both graphical and numerical form. The system hardware consists of: (1) a Nova 1220 minicomputer with 32K of memory; (2) three cassette tape transports; (3) a teletype; (4) a Tektronix 4010 graphics display terminal; (5) a Tektronix 4610 hard copy unit; (6) an A/D converter for measuring the dc and pulse voltages applied to the specimen; and (7) the atom-probe interface which connects the digital timer and high-voltage pulser to the computer. The majority of the software material consists of a program which controls the operation of the TOF atom-probe FIM. The four primary functions of this program during an experiment are as follows: (1) Take data - Pulse the tip, read the TOF's from the digital timer and read the voltages from the A/D converter; (2) Store data on cassette - The TOF's, voltages and number of pulses necessary to field evaporate the atoms detected are stored on cassette tape; (3) Analyze data - Calculate the (m/n) ratios and store the histogram in core memory; and (4) Present results - Plot the histograms in the form of the number of events versus m/n, and tabulate the histogram in numerical form.

The capabilities of this TOF atom-probe FIM are demonstrated in Section 5 where some typical spectra for pure tungsten and molybdenum specimens and also a spectrum obtained from a tungsten-25% rhenium alloy are presented. The peaks associated with the five naturally occurring isotopes of W (W^{180}, W^{182}, W^{183}, W^{184} and W^{186}) are readily distinguished from one another in the W^{+3} spectrum (Fig. 18). The seven naturally occurring isotopes of Mo (Mo^{92}, Mo^{94}, Mo^{95}, Mo^{96}, Mo^{97}, Mo^{98} and Mo^{100}) are clearly separated from one another in the Mo^{+2} and Mo^{+3} spectra (Figs. 22 and 23). The two isotopes of rhenium (Re^{185} and Re^{187}) are clearly separated from the five

isotopes of W in a tungsten-25% rhenium alloy (see Fig. 25). In all cases the isotopi abundances of the different isotopes were in good agreement with the handbook values. In the case of the W-25% Re alloy the TOF atom-probe FIM determination was 25.4at.%. Thus, the present TOF atom-probe FIM appears to have a resolution which is satisfactory for many materials science problems.

ACKNOWLEDGEMENTS

We are indebted to Dr. S.S. Brenner of the U.S. Steel Corporation for the plans of the goniometer stage and for helpful advice and discussions concerning the TOF atom-probe FIM technique. We also thank Prof. R.W. Balluffi for encouragement, Mr. R. Whitmarsh and Mr. J. Hart for technical assistance, and Mr. Anthony Babbaro for machining the liquid helium-cooled goniometer stage.

REFERENCES

1. E.W. Müller, J.A. Panitz, and S.B. McLane, Rev. Sci. Instrum. 39, 83 (1968); E.W. Müller and T.T. Tsong in Field Ion Microscopy (Elsevier, New York, 1969) pp. 130-134, 292-296.

2. E.W. Müller, S.V. Krishnaswamy and S.B. McLane, Surface Sci. 23, 112 (1970); E.W. Müller, S.B. McLane and J.A. Panitz, Surface Sci. 17, 430 (1969); S.V. Krishnaswany, S.B. McLane and E.W. Müller, J. Vac. Sci. Tech. 11, 899 (1974); E.W. Müller and T.T. Tsong, in Prog. in Surf. Sci. 4 (Pergamon Press, New York, 1973) pp. 1-137.

3. E.W. Müller, Z. Physik 131, 136 (1951).

4. S.S. Brenner and J.T. McKinney, Surf. Sci. 23, 88 (1970); P.J. Turner, B.J. Regan, and M.J. Southon, Vacuum 22, 443 (1972); S. Nakamura, Jap. J. Vac. Soc. 7, 228 (1974); J.H. Block, Vac. Tech. 22, 190 (1974); and A.L. Suvorov and V.V. Trebukhovskii Sov. Phys. 15(4), 471 (1973).

5. E.W. Müller, Phys. Rev. 102, 618 (1956).

6. S.S. Brenner and J.T. McKinney, Appl. Phys. Letters 13, 29 (1968); S.S. Brenner and J.T. McKinney Surf. Sci. 23, 88 (1970).

7. S.S. Brenner and S.R. Goodman, Scripta Met. 5, 865 (1971).

8. S.R. Goodman, S.S. Brenner and J.R. Low, Jr., Met. Trans. 4, 2363 (1973); S.R. Goodman, S.S. Brenner and J.R. Low, Jr., Met. Trans. 4, 2371 (1973).

9. P.J. Turner, B.J. Regan and M.J. Southon, Vacuum, 22, 443 (1972); P.J. Turner, B.J. Regan and M.J. Southon, Surface Sci. 35, 336 (1973).

10. A. Youle, P.J. Turner and B. Ralph, J. Microscopy 101, 1 (1973); P.J. Turner and M.J. Papazion, Met. Sci. 7, 81 (1973).

11. E.W. Muller and T.T. Tsong in Field Ion Microscopy (Elsevier, New York 1969) Chapt.

12. A.S. Berger, Rev. Sci. Instrum. 44, 592 (1973).

13. S.S. Brenner and J.T. McKinney, Surf. Sci. 23, 88 (1970); W.B. Colson, J. McPherson and F.T. King, Rev. Sci. Instrum. 44, 1694 (1973).

14. F. Rosebury, Handbook of Electron Tube and Vacuum Techniques (Addison Wesley, New York 1965).

15. D.N. Seidman, R.M. Scanlan, D.L. Styris, and J.W. Bohlen, J. Sci. Instrum. (J. of Phys. E) 2, 473 (1969).

16. A.T. Finkelstein, Rev. Sci. Instrum. 11, 94 (1940); R.C. Bradley, Phys. Rev. 93, 719 (1954); M. Abele and W. Meckbach, Rev. Sci. Instrum. 30, 335 (1959) and P.B. Bowden and D.G. Brandon, J. Sci. Instrum. 40, 213 (1963).

17. M.W. Thompson, Defects and Radiation Damage in Metals (Cambridge Press, London 1969) pp. 188-240.

18. A.S. Berger, D.N. Seidman, and R.W. Balluffi, Acta Met. 21, 123 (1973).

19. D.N. Seidman and K.H. Lie, Acta Met. 20, 1045 (1972); J.T. Robinson, K.L. Wilson, D.N. Seidman, Phil. Mag. 27, 1417 (1973); R.M. Scanlan, D.L. Styris, and D.N. Seidman, Phil. Mag. 23, 1439 (1971).

20. Available from International Resistance Company (IRC).

21. S.S. Brenner and J.T. McKinney, Rev. Sci. Instrum. 43, 1264 (1972).

22. R.J. Lewis and G.D. Smith at 20th Field Emission Symposium, Pennsylvania State University, August, 1973.

23. E.W. Müller, S.V. Krishnaswamy, and S.B. McLane, Rev. Sci. Instrum. 44, 84 (1972).

24. E.W. Müller and S.V. Krishnaswamy, Rev. Sci. Instrum. 45, 1053 (1974).

25. W. Meiling and F. Stary, Nanosecond Pulse Techniques (Gordon and Breach, N.Y.,1968) p. 219.

26. C.A. Johnson, Rev. Sci. Instrum. 41, 1812 (1970); P.J. Turner, B.J. Regan, and M.J. Southon, Surf. Sci. 35, 336 (1973).

27. J.A. Panitz, S.B. McLane, and E.W. Müller, Rev. Sci. Instrum. 40, 1321 (1969).

28. Handbook of Chemistry and Physics (Chemical Rubber Co., 1967).

29. S.V. Krishnaswamy and E.W. Müller, Rev. Sci. Instrum. 45, 1049 (1974).

APPENDIX A

The following description of the functions of APOS will follow the order of a typical operating session. The input and output statements from the computer are in capital letters, and the responses that have been typed in from the keyboard are underlined. Headings labelling the part of the program being used are double underlined. Comments are in lower case letters.

The EXECUTIVE PROGRAM is as follows:

RUN -- starts APOS running in the EXECUTIVE program.

DATE = 21 APRIL 1975 - requests input of date for labelling graphs.

IDENTIFICATION = TUNGSTEN 551 PLANE - identification for labelling graphs.

CLEAR HISTOGRAM? Y response Y for yes clears m/n histogram, N for no does not.

P,R,D,G, OR C? P - selects desired function of APOS as follows:

P - pulse tip and take data

R - read data from cassette tape

D - scan dictionary of (m/n)'s

G - graph data

C - compute calibration parameters

This concludes the functions of the EXECUTIVE program. The response P on the last interrogation passes control to subroutine PULSE.

The PULSE SUBROUTINE is as follows:

HISTOGRAM STORAGE RANGE IS 0 TO 200,

BIN SIZE = .2 AMU OK? N

PICK LENGTH = 90 LENGTH = 100 PICK START = 5

HISTOGRAM STORAGE RANGE IS 0 TO 100,

BIN SIZE = .1 AMU OK? Y

This sequence of requests and responses has changed the histogram storage range from 0-200 to 0-100 and consequently changed the bin size from 0.2 to 0.1 amu. The program has

automatically converted the requested range to a range that will be compatible with the graph labeling procedure. Thus the requested length 90 was changed to the standard length 100 and the starting value 5 was changed to 0.

PRINT ERROR MESSAGES WHEN M/N TOO LARGE? Y

Whenever a calculated m/n is outside the histogram storage range the value m/n will be printed on the CRT.

ALPHA=1.0 LENGTH=2000 TO=56

NEW PARAMETERS? Y -- requests if new values of calibration parameters are desired.

ALPHA=1.5

LENGTH IN M.M.=2228

TO=56

New calibration parameters are: pulse factor α=1.5; flight distance d=2228mm; and total delay time t_o=0.56μsec

CLEAR HIST? N

NO FILES OPEN

OPEN A NEW FILE? Y

TYPE DRIVE AND FILE CT2:1

Since no cassette tape file was open for writing the data, the cassette on tape drive number 2 has been opened at file number 1.

PULSE Y -- Yes response branches to actual pulsing of tip. (N response branches to RETURN TO EXECUTIVE? request, to be discussed below.)

HOW MANY PULSES? 1000

The computer now begins pulsing the tip 1000 times. As the FIM specimen is field evaporated the voltage is slowly raised by the operator to maintain a steady evaporation rate as monitored by the rate meter. After each pulse the computer reads the timer. If the TOF is an acceptable BCD

number and is less than 90.00μsec it is assumed to correspond to a true event and a voltage measurement by the A/D converter is initiated. The value of m/n for each TOF is calculated and the appropriate bin of the histogram is incremented by one. The TOF's are recorded on cassette tape preceeded by the negative of the number of pulses since the last event. If the voltages have changed since the last event they are also recorded on cassette tape preceeded by a zero. Thus, when the tape is read back, a negative number is interpreted as a number of pulses and all positive definite numbers following it are interpreted as TOF's. The two numbers following a zero are interpreted as the dc and pulse voltages. The data are written in blocks of fixed length (186 numbers) so that data can be read back in a consistent way.

130 ATOMS

1 RECORD -- 130 events recorded and 1 cassette tape record filled.

HOW MANY PULSES? 0

RETURN TO EXECUTIVE Y_ - Request for zero pulses passes control out of the pulsing mode to the branching request. A Y response causes return to EXECUTIVE program. An N response would have caused return to the beginning of PULSE subroutine.

CT2:1 IS STILL OPEN FOR WRITING

CLOSE IT? Y

CT2:1 HAS BEEN CLOSED AND CONTAINS 2 RECORDS

The cassette tape file can be left open when returning to the EXECUTIVE program, but has been closed since the data taking has been concluded.

CLEAR HISTOGRAM? N

P, R, D, G, OR C? G - Select the graphing subroutine.

GRAPH SUBROUTINE

STORAGE RANGE 0 TO 100 BIN SIZE = .1 AMU HISTOGRAM PLOTTING RANGE IS 0 TO 100 OK? N PICK LENGTH 4 LENGTH=5 PICK START 59 HISTOGRAM PLOTTING RANGE IS 59 TO 64 OK? Y

The horizontal range to be plotted has been selected to be between 59 and 64 amu. Note that the program automatically restricts the selected range to a standard size within the storage range of the histogram.

MAX = 24 VERT RANGE = 30 OK? N

PICK VERT RANGE = 50

MAX = 24 VERT RANGE = 60 OK? Y

The program automatically picks a vertical range large enough for the maximum of the histogram over the selected m/n range. If the operator has chosen a larger range, it is converted to a standard size by the program.

IDENT = TUNGSTEN 551 PLANE OK? Y

At this point the CRT screen of the graphics terminal is cleared automatically and a histogram similar to those shown in the results section is plotted. The operator then makes a hard copy of the histogram and clears the CRT screen.

RETURN TO EXECUTIVE? Y - An N response would cause a return to the beginning of subroutine GRAPH.

CLEAR HIST Y

P, R, D, G, OR C? R - Read the data from the cassette tape.

READ SUBROUTINE

DRIVE & FILE TO BE READ CT2:1

CT2:1 OPENED FOR READING

FIRST RECORD = 0

LAST RECORD = 5 - The cassette tape on drive 2 has been opened to file 1. Records 0 to 5 will be read and analyzed.

EXCLUDE ANY DATA GROUPS? Y

EXCLUDE DATA IN GROUPS OF SIZE = (TERM. W NO. <> 1 TO 8)
?8
?0 - Any TOF data which came in groups of 8 (i.e., all 8 counters in the digital timer contain true events) will be excluded. The 0 terminates the list because it is outside the range 1 to 8.

EXCLUDE ANY DATA NUMBERS = (1 TO 8)
?7
?0 - All data from the seventh counter chain will be ignored; again 0 terminates the list.

CREATE HIST (H), COMP PROFILE (P) OR BOTH (B)? B

Select whether to create a histogram, composition profile or both.

HISTOGRAM STORAGE RANGE IS 0 TO 100,

BIN SIZE = .1 AMU OK? Y

CLEAR PRESENT HISTOGRAM Y

ALPHA = 1.5 LENGTH = 2228 TO=56

NEW PARAMETERS? N -- The histogram information requested as in subroutine PULSE

COMPO PROFILE INFO

Y AXIS M/N RANGES FROM 10 TO 20 -- The vertical axis of the composition profile will indicate the total number of events with m/n between 10 and 20.

LENGTH OF Y AXIS = 3 (events)

OK? Y

X AXIS M/N RANGES FROM 0 TO 100 -- The horizontal axis of the composition profile will indicate the total number of events with m/n between 0 and 100.

LENGTH OF X AXIS = 200 (events)

OK? Y

IDENT = TUNGSTEN 551 PLANE 10 TO 20 AMU VS 0 TO 100 AMU

OK Y - The computer now begins to read the tape and computes the histogram while simultaneously plotting the composition profile on the CRT. The computer then makes a hard copy of the composition profile and clears the CRT.

EOF AT RECORD 1 DATA 35

CT 2:1 HAS BEEN CLOSED - When the program encounters an end of file (EOF) mark on the tape it notes the record and data numbers and then closes the file.

RETURN TO EXECUTIVE? Y

CLEAR HISTOGRAM? N

P, R, D, G, OR C? C

CALIBRATION SUBROUTINE (See section 3.4)

For the following example we will assume that the tungsten data (hypothetical) was taken at two sets of voltages. The data were then analyzed using the following (incorrect) calibration parameters: t_o=0.50μsec; α=1.2; and d=2200. The $^{4}He^{+}$ peak and the $^{186}W^{+3}$ peak for the two sets of voltages were observed at the following m/n:

	V_{dc}	V_{pulse}	$^{4}He^{+}$	$^{186}W^{+3}$
Case I	8000V	400V	4.19 amu	63.25 amu
Case II	8400V	200V	4.22 amu	63.71 amu

The first step in the calibration procedure is to work backward from the observed m/n values to obtain the equivalent TOF's.

COMPUTE TOF? Y

VDC=8000 VPLSE=400 ALPHA = 1.2 TO = 50 LENGTH = 2200

M/N = 4.19 TOF = 402.008 - (all times in tens of nanoseconds)

M/N = 63.25 TOF = 1417.65

M/N = 0 TOF W NEW PARAMETERS? Y

VDC = 8400 VPLSE = 200 ALPHA = 1.2 TO = 50 LENGTH = 2200

M/N = 4.22 TOF = 399.98

M/N = 63.71 TOF = 1409.85

M/N = 0 TOF W NEW PARAMETERS? N

Input m/n = 0 passes to branch statement allowing recomputation of TOF's with new parameters. Typing N causes program to continue.

COMPUTE TO? Y Compute t_o.

1ST M/N = 4 1ST TOF = 402.008

2ND M/N = 62 2ND TOF = 1417.65

TO = 56.1985

COMPUTE ALPHA? Y

1ST VDC = 8000 VPLSE = 400 TOF = 1417.7

2ND VDC = 8400 VPLSE = 200 TOF = 1409.85 TØ = 56.2

ALPHA = 1.50338

COMPUTE LENGTH? Y

TO = 56.2 ALPHA = 1.5 VDC = 8000 VPLSE = 400

M = 186 N = 3 TOF = 1417.7

LENGTH = 2227.91

COMPUTE LENGTH WITH NEW PARAMETERS? N

This completes the actual calibration. The following computation of m/n serves as a check.

COMPUTE M/N? Y

VDC = 8000 VPLSE = 400 ALPHA = 1.5 TO = 56 LENGTH = 2228

TOF = 402.008 M/N = 4.00311

TOF = 1417.65 M/N = 61.9949

TOF = 0 M/N WITH NEW PARAMETERS? Y

VDC = 8400 V PLSE = 200 ALPHA = 1.5 TO = 56 LENGTH = 2228

TOF = 399.98 4.00233

TOF = 1409.85 61.9994

TOF = 0 M/N WITH NEW PARAMETERS? N

Thus, the new calibration parameters t_o = 0.56μsec α = 1.5, and d = 2228mm give consistent results for the m/n values of $^{4}He^{+}$ and $^{186}W^{+3}$.

RETURN TO EXECUTIVE? Y

CLEAR HISTOGRAM? N

P, R, D, G, OR C? D

DICTIONARY SCANNING SUBROUTINE

TAPE FILE OF M/N DICT CT1:1

M/N RANGE 0 TO 8 - selected m/n range of interest is 0 to 8 amu

ALL ELEMENTS? N

INPUT ELEMENTS, INCLUDE BLANKS, SEPARATE WITH CARRIAGE RETURN, END WITH ZZ

? HE

? N

? ZZ

ELEMENTS ARE HE N

OK? Y Selected elements are helium and nitrogen. All others will be excluded.

M/N	ELEM	N	%	COMMENTS
2	HE-	+2	100	
4	HE-	+1	100	
4	HE-HE	+2	100	
4.7	N-	+3	99.6	
5	N-	+3	.4	
6	N-HE	+3	99.6	
6.3	N-HE	+3	.4	
7	N-	+2	99.6	
7.5	N-	+2	.4	
8	HE-HE	+1	100	

The first column contains the m/n value in amu, the second column contains the name(s) of the elements, the third column contains the charge state and the fourth column contains the percent natural abundance of the combination having that particular (m/n). The last column is for comments.

RETURN TO EXECUTIVE? Y

CLEAR HISTOGRAM Y

P,R,D,G, OR C? _

Table 1: Comparison of our experimental W^{+3} isotopic abundances calculated from Fig.18 and the actual[28] isotopic abundances.

Isotope	AMU Range	Number of Atoms	Experimental %	Actual %
W^{180}	59.8 to 60.2	20±4	0.33±0.07	0.14
W^{182}	60.5 to 60.85	1520.5±39	25.3±0.6	26.41
W^{183}	60.85 to 61.2	1026.5±32	17.1±0.5	14.4
W^{184}	61.2 to 61.8	1789±42	29.9±0.7	30.64
W^{186}	61.8 to 64.0	1644±41	27.4±0.7	28.41
Totals		6009	100	100

Table 2: Comparison of the experimental Mo^{+2} isotopic abundances calculated from Fig. 22 and the actual[28] isotopic abundances.

Isotope	AMU Range	Number of Atoms	Experimental %	Actual %
Mo^{92}	45.8 to 46.6	108	15.5±1.5	15.84
Mo^{94}	46.8 to 47.4	70	10.1±1.2	9.04
Mo^{95}	47.4 to 47.9	100	14.4±1.4	15.72
Mo^{96}	47.9 to 48.4	113	16.2+1.5	16.53
Mo^{97}	48.4 to 48.9	67	9.6±1.2	9.46
Mo^{98}	48.9 to 49.5	158	22.6±1.8	23.78
Mo^{100}	49.7 to 50.5	80	11.5±1.3	9.63
Totals		696	100	100

Table 3: A comparison of our experimental Mo^{+3} isotopic abundances calculated from Fig. 23 and the actual[28] isotopic abundances.

Isotope	AMU Range	Number of Atoms	Experimental %	Actual %
Mo^{92}	30.5 to 31	197	15.1±1.1	15.84
Mo^{94}	31.1 to 31.5	97	7.5±0.8	9.04
Mo^{95}	31.5 to 31.9	219	16.8±1.1	15.72
Mo^{96}	31.9 to 32.2	188	14.4±1.1	16.53
Mo^{97}	32.2 to 32.5	125	9.6±0.9	9.46
Mo^{98}	32.5 to 33.1	324	24.9±1.4	23.78
Mo^{100}	33.1 to 33.7	153	11.7±0.9	9.63
Totals		1303	100	100

Table 4: A comparison of the experimental W-25% Re^{+3} isotopic abundances with actual[28] isotopic abundances.

(a) Tungsten Isotopes

Isotope	AMU Range	Number of Atoms	Experimental %	Actual %
W^{180}	59.9 to 60.4	1	0.1±0.1	0.1
W^{182}	60.4 to 60.9	310	24.7±1.4	26.4
W^{183}	60.9 to 61.3	243	19.3±1.2	14.4
W^{184}	61.3 to 61.6	394	31.4±1.6	30.7
W^{186}	62.0 to 62.3	307	24.5±1.4	28.4
Totals		1255	100.0	100.0

(b) Rhenium Isotopes

Isotope	AMU Range	Number of Atoms	Experimental %	Actual %
Re^{185}	61.6 to 62.0	214	42.8±3.1	37.1
Re^{187}	62.3 to 62.6	286	57.2±3.1	62.9
Totals		500	100.0	100.0

(c) Relative Concentrations

Element	Number of Atoms	Experimental %	Nominal* %
W	1255	71.5±1.6	75.0
Re	500	28.5±1.6	25.0
Totals	1755	100.0	100.0

* Based on nominal concentrations for W-25at.% Re.

FIGURE CAPTIONS

FIG. 1: A highly schematic diagram illustrating the principle of the TOF atom-probe FIM employing a digital timer to measure the TOF.

FIG. 2: The overall arrangement of the TOF atom-probe FIM showing the specimen, the internal image intensification system based on a CEMA, the focusing lens, the ion-gun, the front-surface viewing mirror and the Chevron ion detector based on two CEMA's.

FIG. 3: The liquid-helium cooled goniometer stage which allows the FIM specimen to be rotated about two mutually orthogonal axes.

FIG. 4: A cut-away view of the liquid-helium cold-finger. The FIM specimen is cooled by both the liquid helium and the cold helium gas. The radiation shields are cooled by the helium exhaust gas.

FIG. 5: A low-energy gas ion-gun for irradiating FIM specimens in-situ. A gas such as hydrogen, helium, neon or xenon is ionized in the plasma chamber; extracted with the extraction lens; then focused with the focusing lens onto the FIM specimen. The indicated voltages are for illustrative purposes only, although they are typical values.

FIG. 6: A schematic diagram illustrating the potentials as a function of distance for the ion-gun shown in Fig. 5. The energy with which the ion arrives at the FIM specimen is essentially determined by the voltage on the specimen.

FIG. 7: An overall view of the ultra-high vacuum system employed for the TOF atom-probe FIM. Note that the flight tube has its own independent vacuum system. The dotted line indicates the extent of the bakeout ovens.

FIG. 8: The high-vacuum specimen exchange device which allows a specimen to be changed without breaking the vacuum is the main chamber.

FIG. 9: A block diagram of the TOF mass spectrometer illustrating the operation of the system. The voltage system, the digital timer and the Nova 1220 mini-computer are all shown.

FIG. 10: The voltage system for the TOF atom-probe FIM indicating how the power supplies are ganged so that the supplies provide a constant ratio of pulse to dc voltage.

FIG. 11: A schematic diagram of the voltage dividing networks employed.

FIG. 12: Shape of a 20nsec long high voltage pulse at the specimen. Figure 10 (a) is a sketch of the overall pulse shape showing the large initial peak which is probably caused by reflections from the unterminated specimen. Figures 10 (b), (c), and (d) represent actual oscilloscope traces of the top of the initial peak which were measured with a Tektronix 7904 oscilliscope, 1S11 sampling plug-in, and S-2 sampling head. Figure 10 (b) was recorded with a P6056 10x probe connected to the specimen holder. Figure 10 (c) was recorded with a P6057 100x probe connected directly to the specimen holder while Fig. 10 (d) was recorded with the probe connected to the specimen holder by a 2 cm wire.

FIG. 13: A block diagram illustrating the principle of the operation of the digital timer; see Section 3.3 for more details.

FIG. 14: A block diagram illustrating the functions of the interface circuit.

FIG. 15: Computer program heirarchy showing the EXECUTIVE program, the BASIC language subroutines and the ASSEMBLY language subroutines used to operate the TOF atom-probe FIM.

FIG. 16: A synthetically generated spectrum for a tungsten-25at.% rhenium alloy; see Section 4.4 for a discussion of the program used to generate this data.

FIG. 17: A spectrum for tungsten, between 0 and 100 amu, recorded at a specimen temperature (T_t) of $\simeq$25K in a background vacuum of 6×10^{-10} torr. Note that the spectrum consists solely of W^{+3}, W^{+4} and a small He^{+} peak.

FIG. 18: A blow-up of the W^{+3} portion of the spectrum shown in Fig. 17. Note the clear separation of the five naturally ocurring isotopes of tungsten.

FIG. 19: A blow-up of the W^{+4} portion of the spectrum shown in Fig. 17.

FIG. 20: A blow-up of the He^{+} portion of the spectrum shown in Fig. 17.

FIG. 21: A spectrum for molybdenum; between 0 to 100 amu, recorded at a T_t of $\sim$60K in a background vacuum of $\sim 5 \times 10^{-9}$torr. Note that the spectrum consists of Mo^{+2}, Mo^{+3}, Mo^{+4}, He^{+} and H^{+}.

FIG. 22: A blow-up of the Mo^{+2} portion of the spectrum shown in Fig. 21. Note the clear separation of the seven naturally ocurring isotopes of molybdenum. The Mo^{+2} spectrum pulse-field evaporated at a specimen temperature between 57 and 69K for V_{dc} varied continuously from 11.6 to 15.5 kV. The ions were collected from a region near the (110) pole and the background vacuum in the TOF atom-probe FIM was 5×10^{-9}torr (microscope not baked after the specimen was inserted through the specimen exchange device). The total number of Mo^{+2} events in this histogram is 696. This constitutes 0.322 of the total number (2157) of Mo^{+2}, Mo^{+3} and Mo^{+4} events observed in this run.

FIG. 23: A blow-up of the Mo^{+3} portion of the spectrum shown in Fig. 21.

FIG. 24: A spectrum for a W-25at.% Re alloy, between 0 to 100 amu, recorded at a T_t of $\sim$25K in a background vacuum of $\sim 5 \times 10^{-9}$torr. Note that the spectrum consists of W^{+3}, Re^{+3}, W^{+4}, Re^{+4} and Ne^{+}.

FIG. 25: A blow-up of the W^{+3} and Re^{+3} portion of the spectrum shown in Fig. 24. Note the clear separation of the two rhenium isotopes Re^{185} and Re^{187} from the five tungsten isotopes.

FIG. 26: A composition profile for the Re^{185} isotope in the W-25at.% Re alloy. The integrated number of events in the range 61.6 to 62.0 is plotted as a function of the integrated number of events in the entire W-Re^{+3} peak from 59.9 to 65 amu. Since the integrated number of events is plotted, the slope of a straight line from the origin to the end point gives the overall average concentration of 10.7%.

FIG. 27: A composition profile for the Re^{187} isotope in the W-25at.% Re alloy. The integrated number of events in the range 62.3 to 62.6 are plotted as a function of the integrated number of events in the entire $W\text{-}Re^{+3}$ peak from 59.9 to 65 amu. The average concentration is 14.7%.

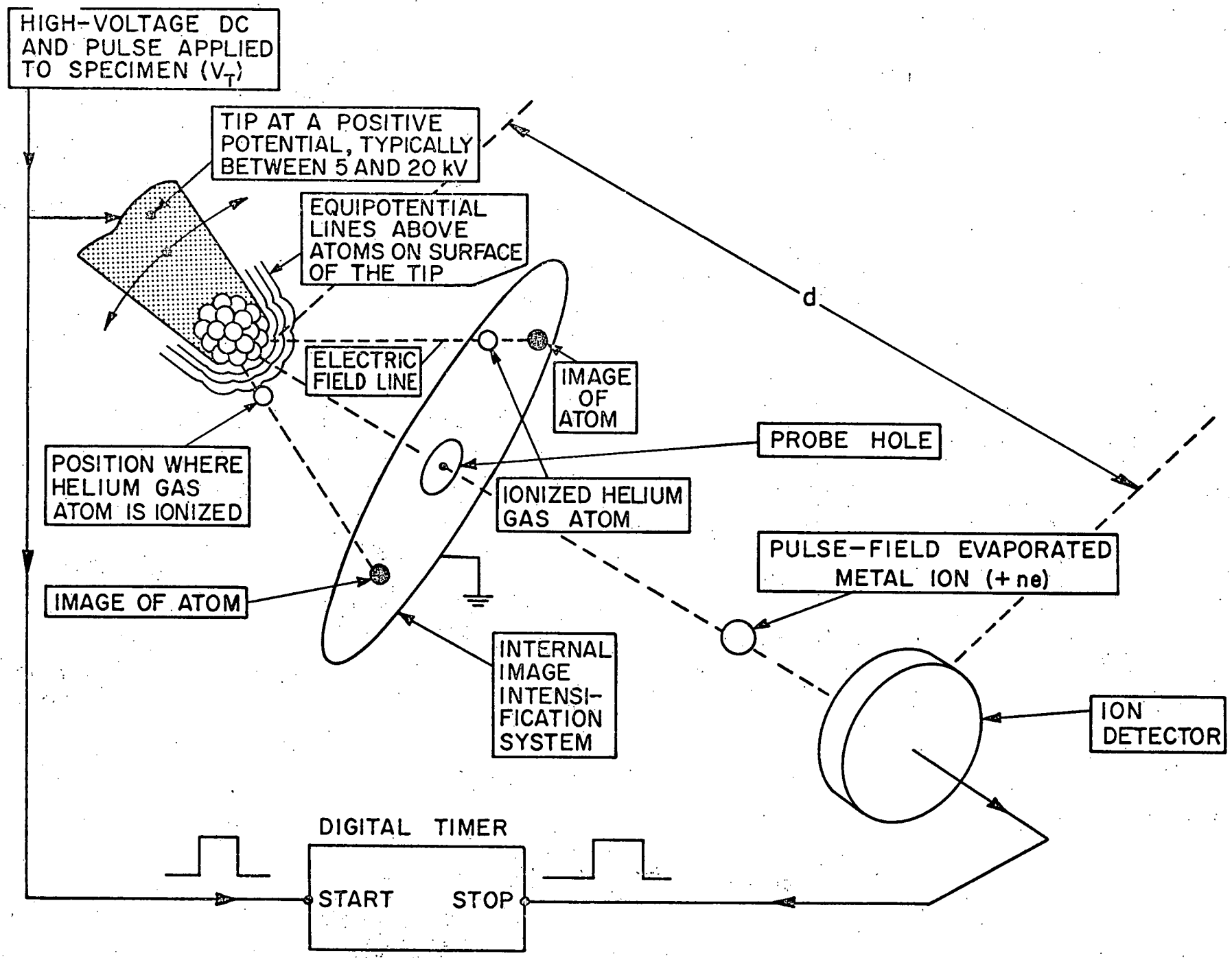

$$\text{mass-to-charge ratio} = \frac{m}{n} = 2eV_T\frac{t^2}{d^2}$$

Figure 1.

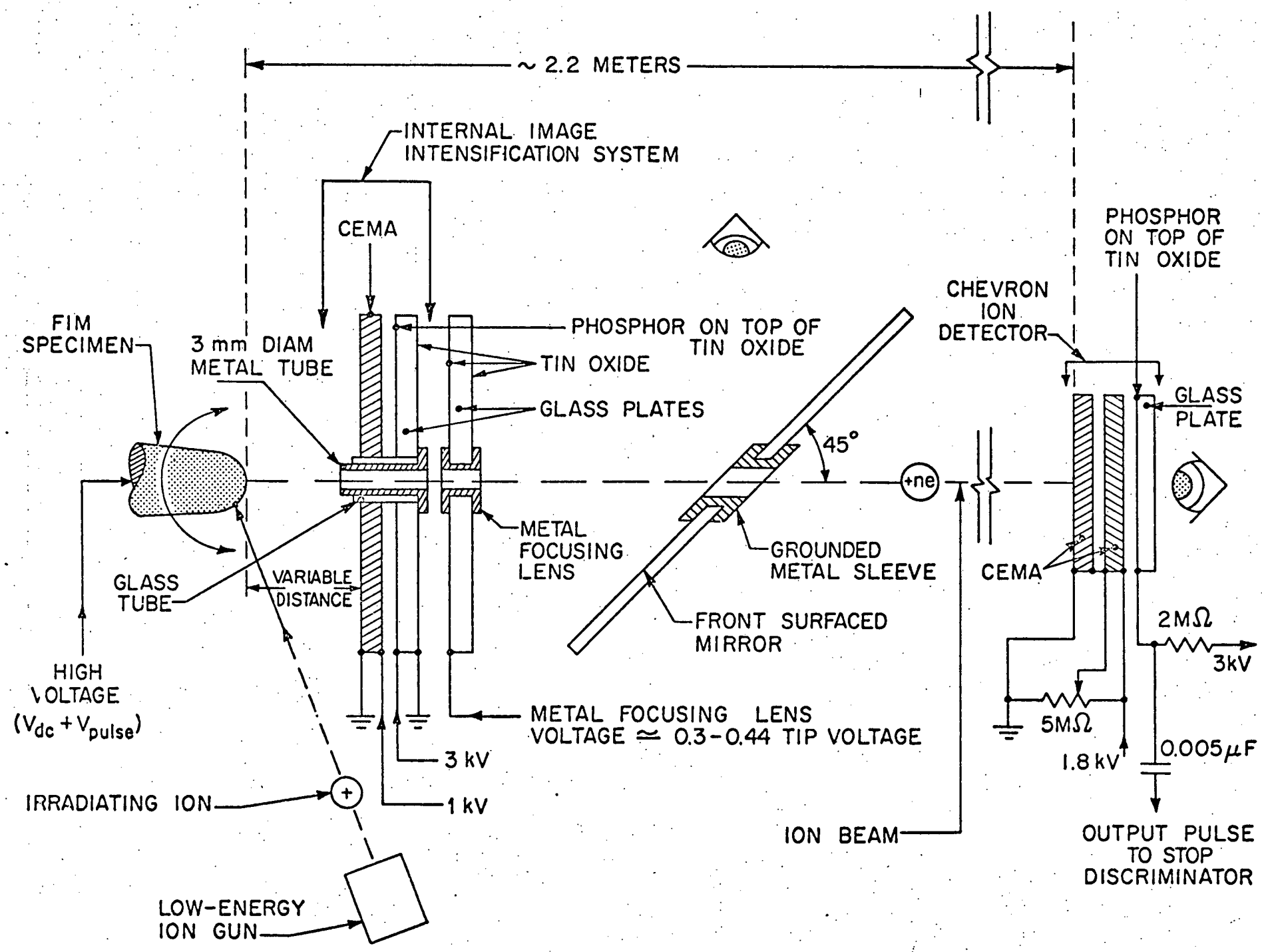
~ 2.2 METERS
INTERNAL IMAGE INTENSIFICATION SYSTEM
CEMA
PHOSPHOR ON TOP OF TIN OXIDE
CHEVRON ION DETECTOR
FIM SPECIMEN
3 mm DIAM METAL TUBE
PHOSPHOR ON TOP OF TIN OXIDE
TIN OXIDE
GLASS PLATES
GLASS PLATE
45°
+ne
METAL FOCUSING LENS
GROUNDED METAL SLEEVE
CEMA
GLASS TUBE
VARIABLE DISTANCE
FRONT SURFACED MIRROR
2MΩ
3kV
HIGH VOLTAGE ($V_{dc} + V_{pulse}$)
5MΩ
1.8 kV
0.005μF
METAL FOCUSING LENS VOLTAGE ≃ 0.3-0.44 TIP VOLTAGE
3 kV
1 kV
IRRADIATING ION
ION BEAM
OUTPUT PULSE TO STOP DISCRIMINATOR
LOW-ENERGY ION GUN

Figure 2.

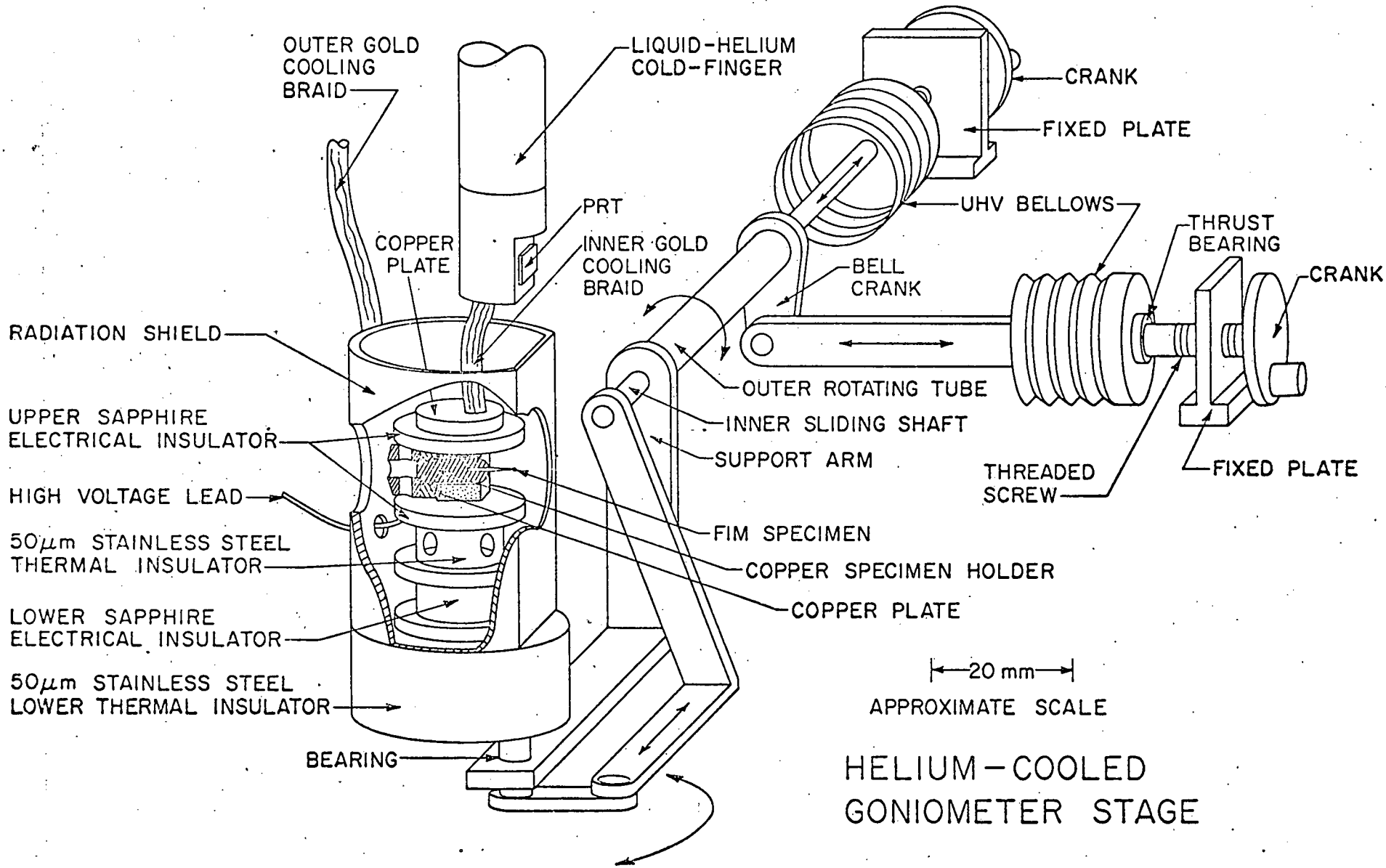
OUTER GOLD COOLING BRAID
LIQUID-HELIUM COLD-FINGER
CRANK
FIXED PLATE
UHV BELLOWS
THRUST BEARING
CRANK
PRT
COPPER PLATE
INNER GOLD COOLING BRAID
BELL CRANK
RADIATION SHIELD
OUTER ROTATING TUBE
INNER SLIDING SHAFT
UPPER SAPPHIRE ELECTRICAL INSULATOR
SUPPORT ARM
THREADED SCREW
FIXED PLATE
HIGH VOLTAGE LEAD
FIM SPECIMEN
50μm STAINLESS STEEL THERMAL INSULATOR
COPPER SPECIMEN HOLDER
COPPER PLATE
LOWER SAPPHIRE ELECTRICAL INSULATOR
20 mm
APPROXIMATE SCALE
50μm STAINLESS STEEL LOWER THERMAL INSULATOR
BEARING
HELIUM-COOLED GONIOMETER STAGE

Figure 3.

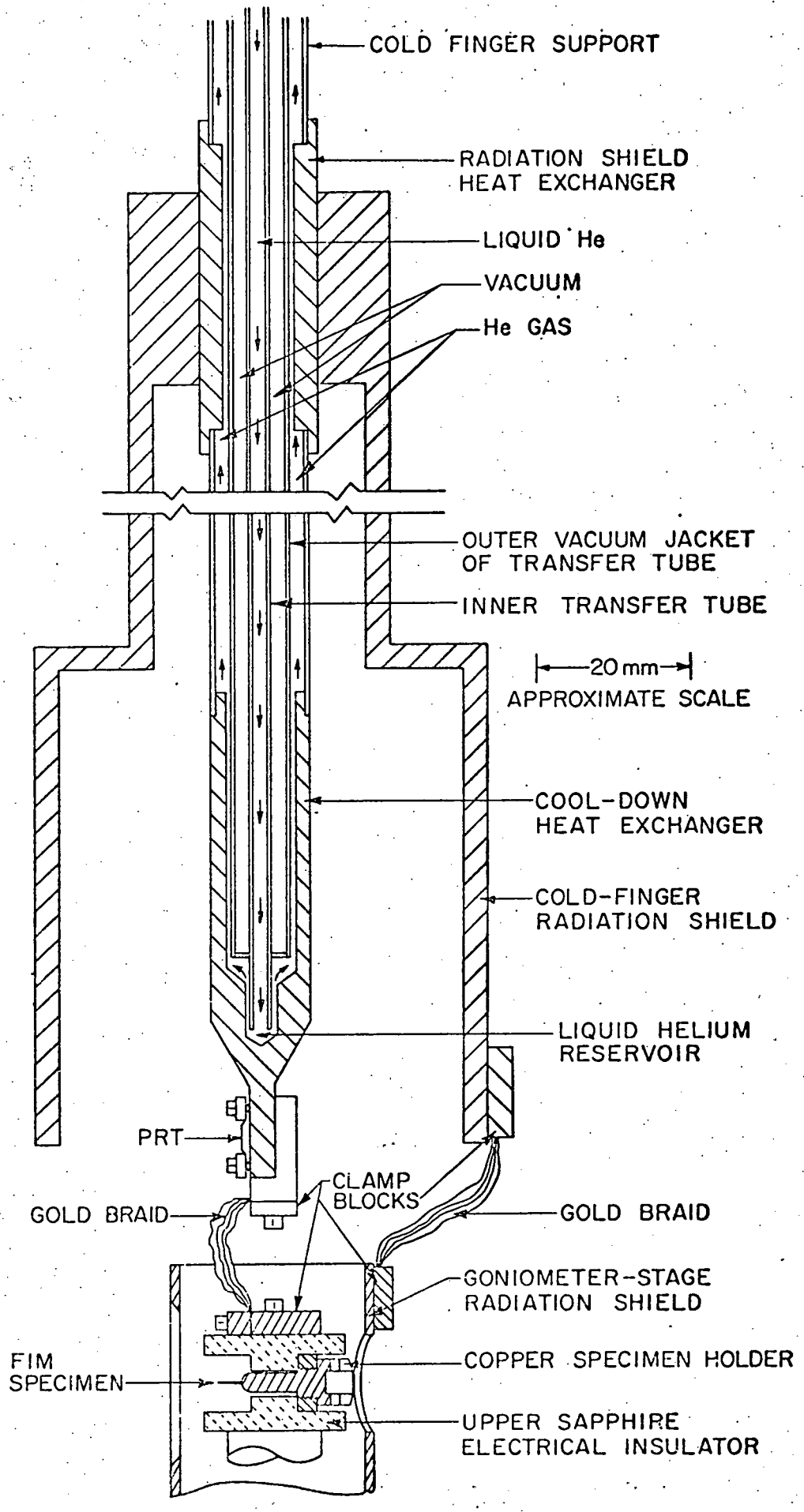
COLD FINGER SUPPORT
RADIATION SHIELD HEAT EXCHANGER
LIQUID He
VACUUM
He GAS
OUTER VACUUM JACKET OF TRANSFER TUBE
INNER TRANSFER TUBE
20 mm
APPROXIMATE SCALE
COOL-DOWN HEAT EXCHANGER
COLD-FINGER RADIATION SHIELD
LIQUID HELIUM RESERVOIR
PRT
CLAMP BLOCKS
GOLD BRAID
GOLD BRAID
GONIOMETER-STAGE RADIATION SHIELD
FIM SPECIMEN
COPPER SPECIMEN HOLDER
UPPER SAPPHIRE ELECTRICAL INSULATOR

Figure 4.

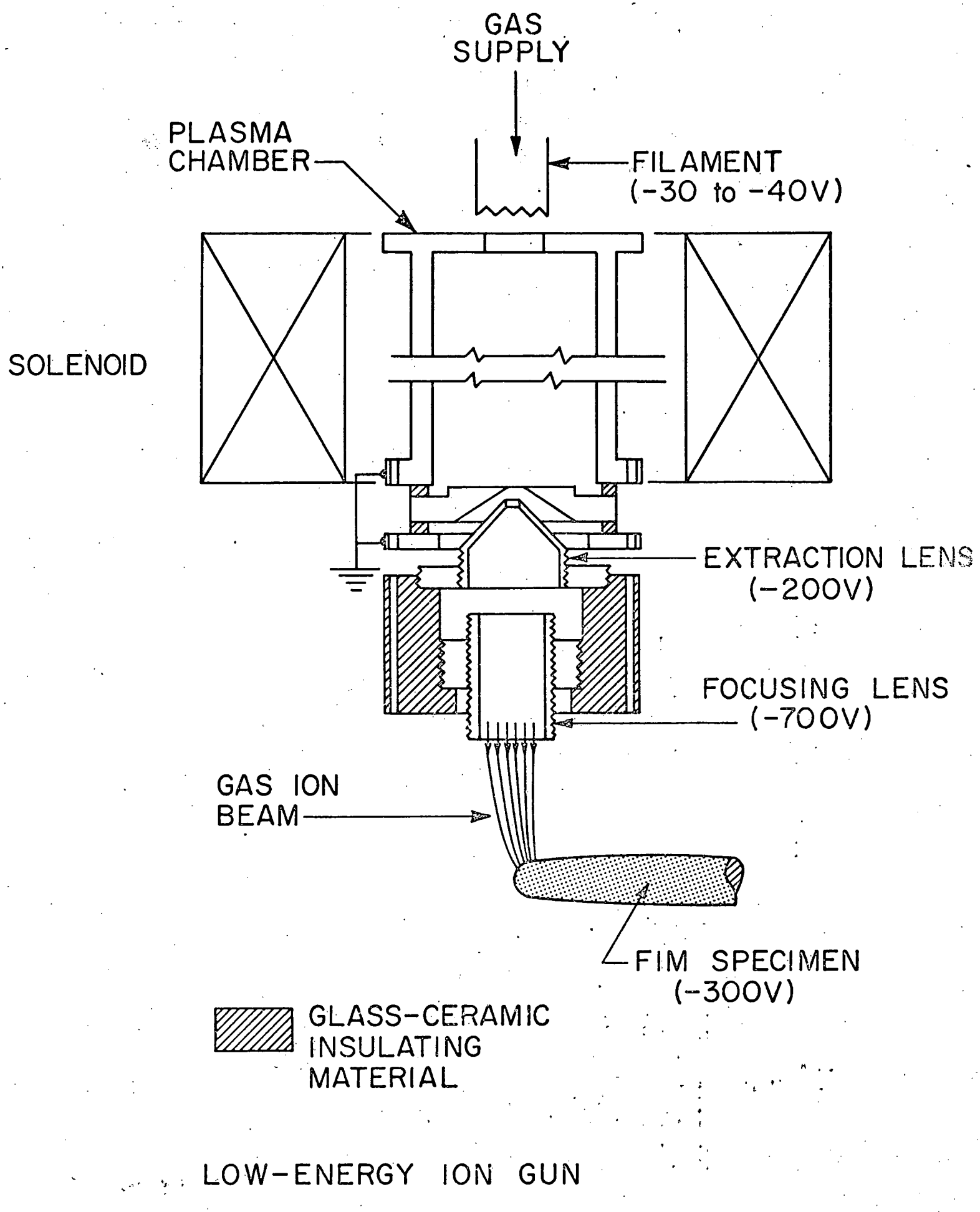
GAS
SUPPLY
PLASMA
CHAMBER
FILAMENT
(-30 to -40V)
SOLENOID
EXTRACTION LENS
(-200V)
FOCUSING LENS
(-700V)
GAS ION
BEAM
FIM SPECIMEN
(-300V)
GLASS-CERAMIC
INSULATING
MATERIAL
LOW-ENERGY ION GUN

Figure 5.

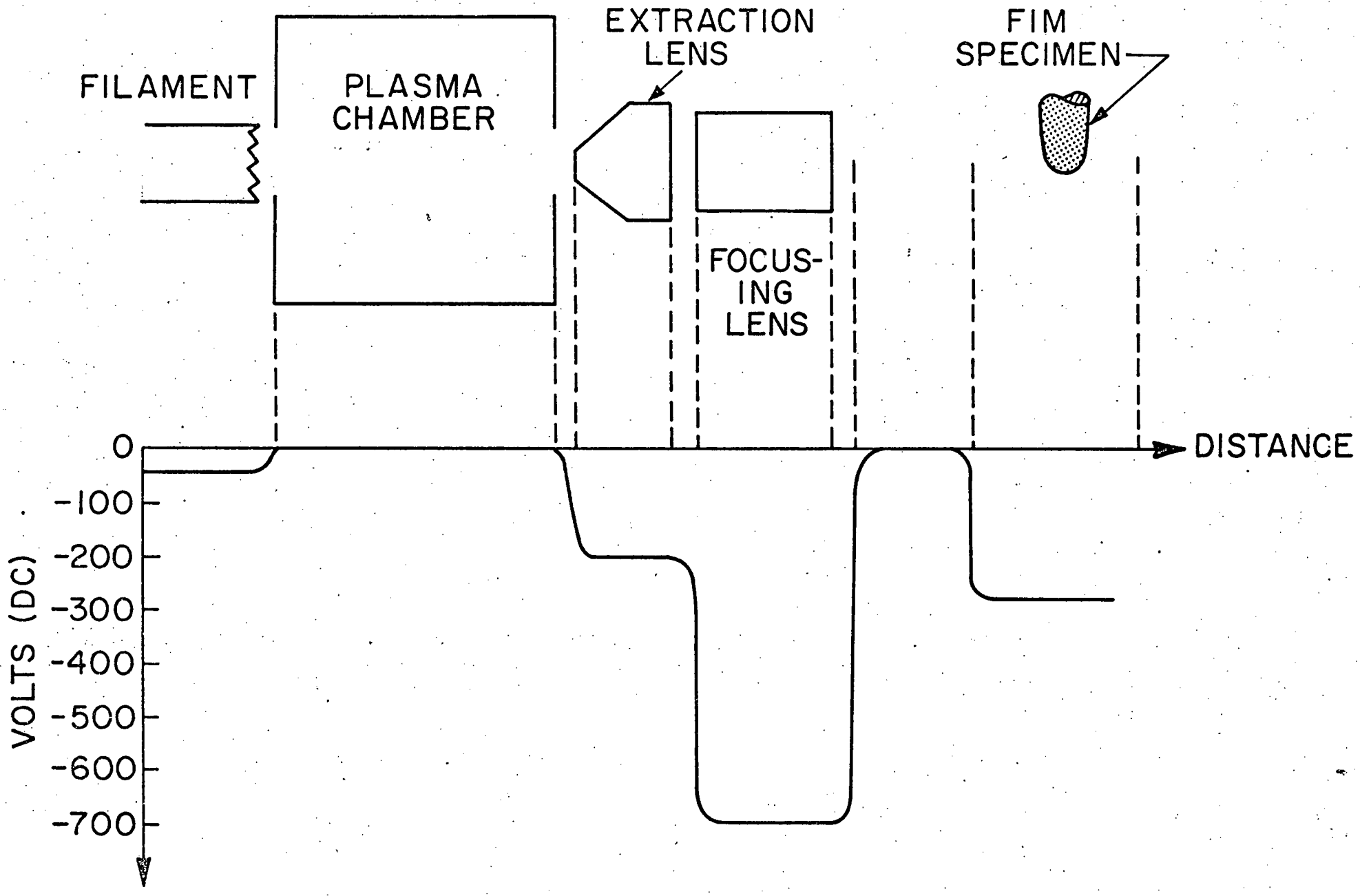

ION-GUN POTENTIALS

Figure 6.

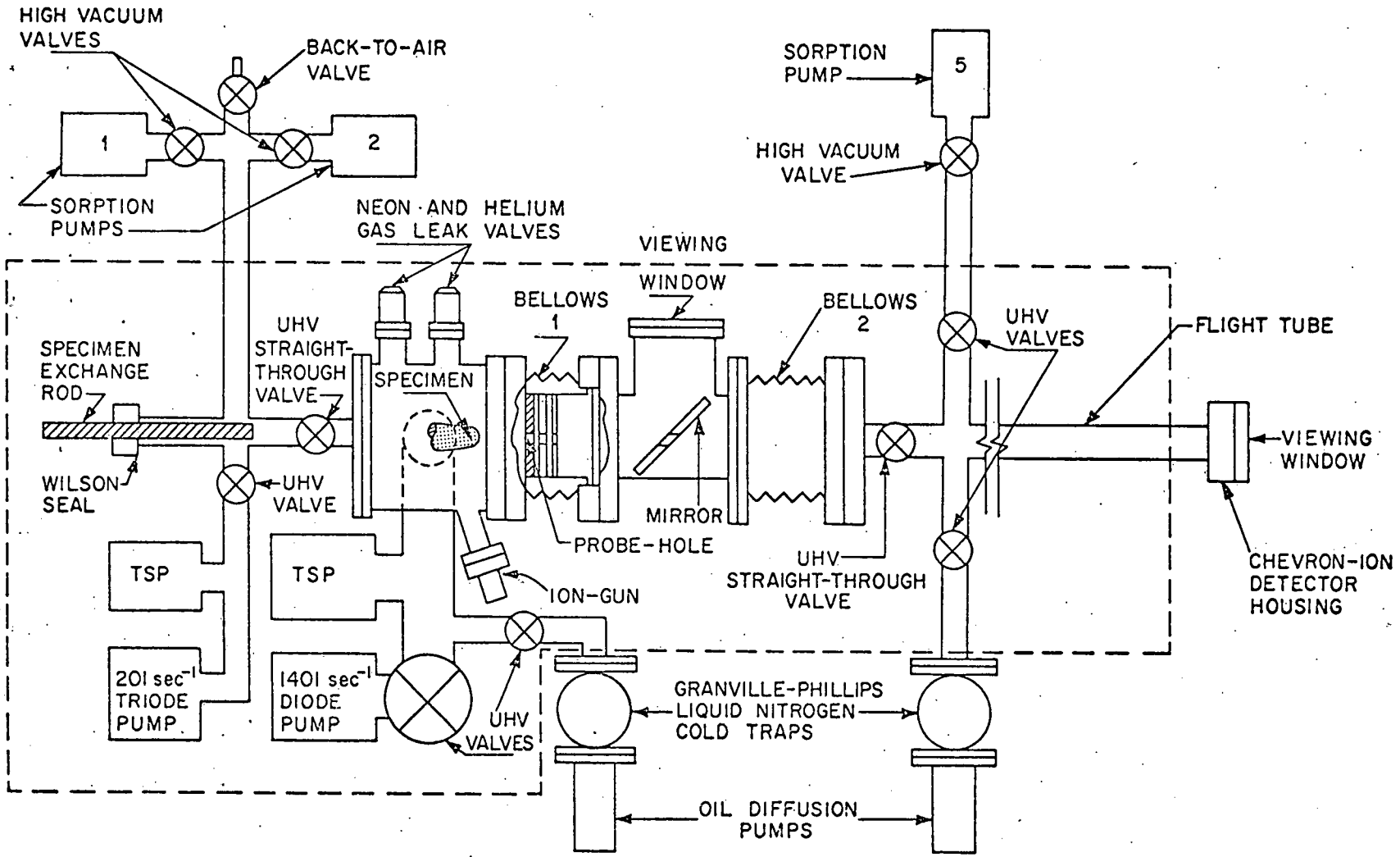
HIGH VACUUM VALVES
BACK-TO-AIR VALVE
1
2
SORPTION PUMPS
NEON AND HELIUM GAS LEAK VALVES
VIEWING WINDOW
BELLOWS 1
BELLOWS 2
SORPTION PUMP
5
HIGH VACUUM VALVE
UHV VALVES
FLIGHT TUBE
SPECIMEN EXCHANGE ROD
UHV STRAIGHT-THROUGH VALVE
SPECIMEN
WILSON SEAL
UHV VALVE
MIRROR
VIEWING WINDOW
PROBE-HOLE
UHV STRAIGHT-THROUGH VALVE
CHEVRON-ION DETECTOR HOUSING
TSP
TSP
ION-GUN
201 sec⁻¹ TRIODE PUMP
1401 sec⁻¹ DIODE PUMP
UHV VALVES
GRANVILLE-PHILLIPS LIQUID NITROGEN COLD TRAPS
OIL DIFFUSION PUMPS

Figure 7.

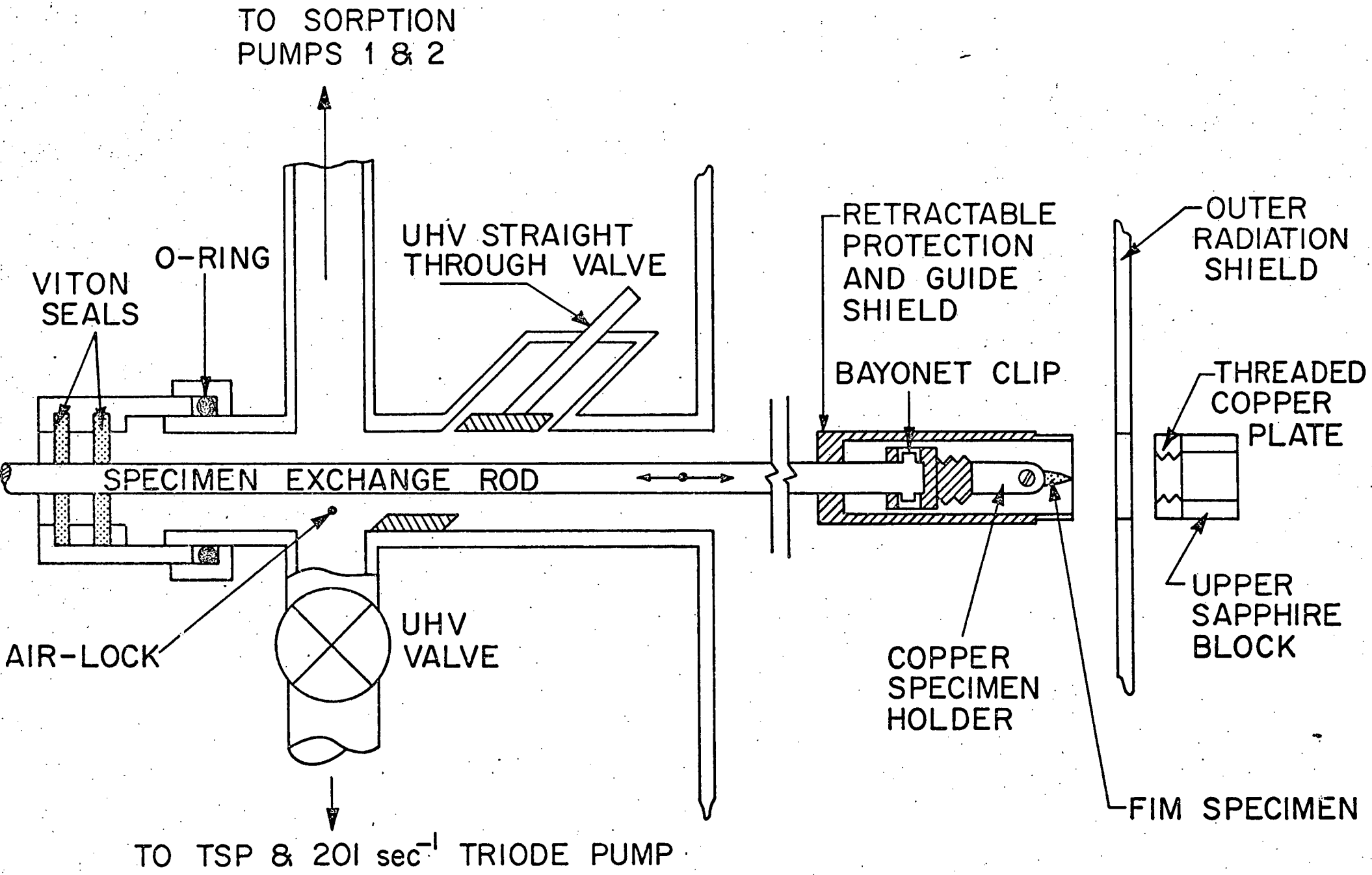

SPECIMEN EXCHANGE DEVICE

Figure 8.

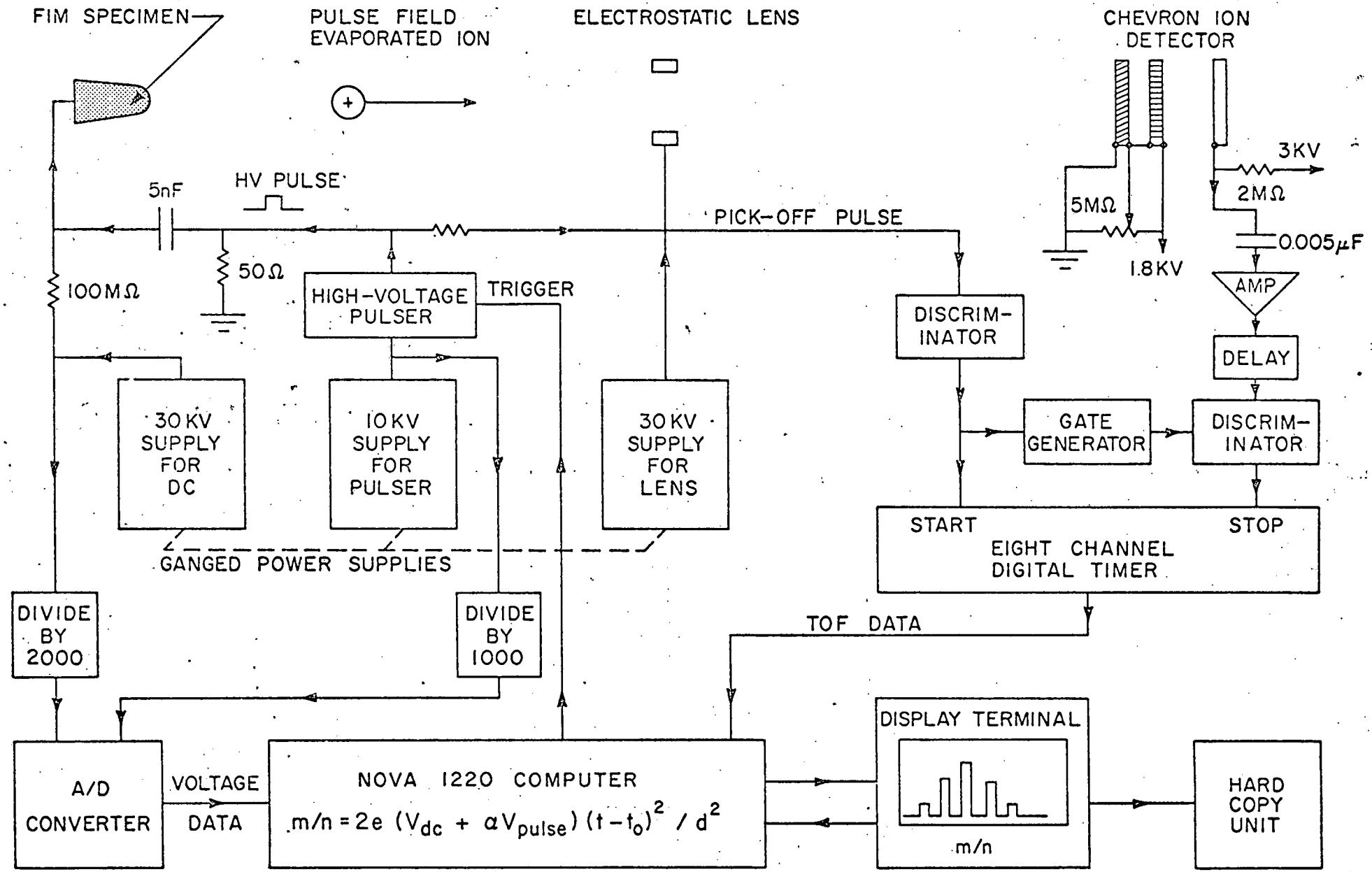
FIM SPECIMEN
PULSE FIELD EVAPORATED ION
ELECTROSTATIC LENS
CHEVRON ION DETECTOR
5nF
HV PULSE
PICK-OFF PULSE
3KV
2MΩ
5MΩ
1.8KV
0.005μF
AMP
100MΩ
50Ω
HIGH-VOLTAGE PULSER
TRIGGER
DISCRIM-INATOR
DELAY
30 KV SUPPLY FOR DC
10 KV SUPPLY FOR PULSER
30 KV SUPPLY FOR LENS
GATE GENERATOR
DISCRIM-INATOR
START
STOP
EIGHT CHANNEL DIGITAL TIMER
GANGED POWER SUPPLIES
DIVIDE BY 2000
DIVIDE BY 1000
TOF DATA
DISPLAY TERMINAL
A/D CONVERTER
VOLTAGE DATA
NOVA 1220 COMPUTER
$m/n = 2e\,(V_{dc} + \alpha V_{pulse})\,(t - t_o)^2 / d^2$
m/n
HARD COPY UNIT

Figure 9.

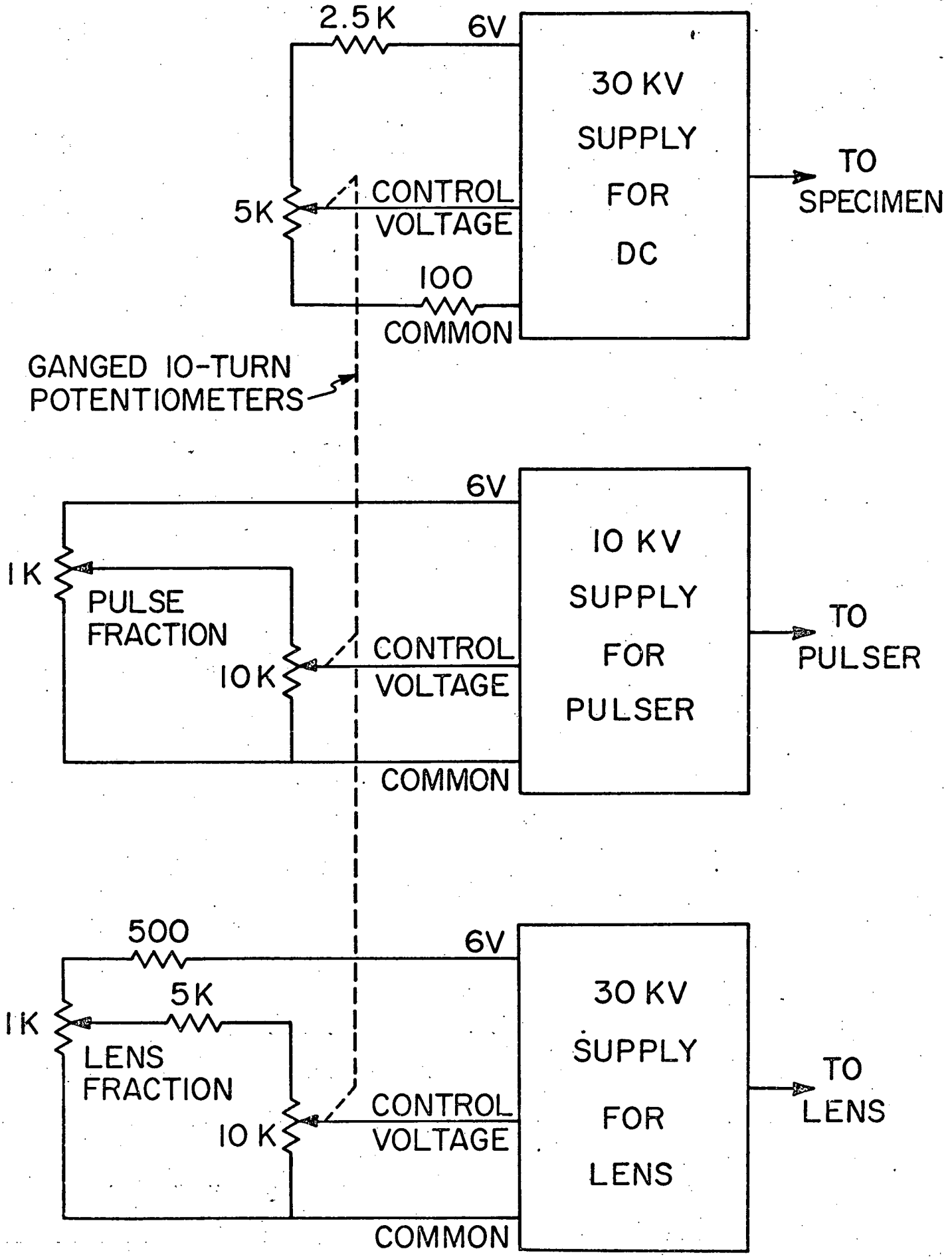
2.5K
6V
30 KV
SUPPLY
FOR
DC
TO
SPECIMEN
5K
CONTROL
VOLTAGE
100
COMMON
GANGED 10-TURN
POTENTIOMETERS
6V
10 KV
SUPPLY
FOR
PULSER
TO
PULSER
1K
PULSE
FRACTION
10K
CONTROL
VOLTAGE
COMMON
500
6V
5K
1K
LENS
FRACTION
10 K
CONTROL
VOLTAGE
30 KV
SUPPLY
FOR
LENS
TO
LENS
COMMON
ALL RESISTORS Ω

Figure 10.

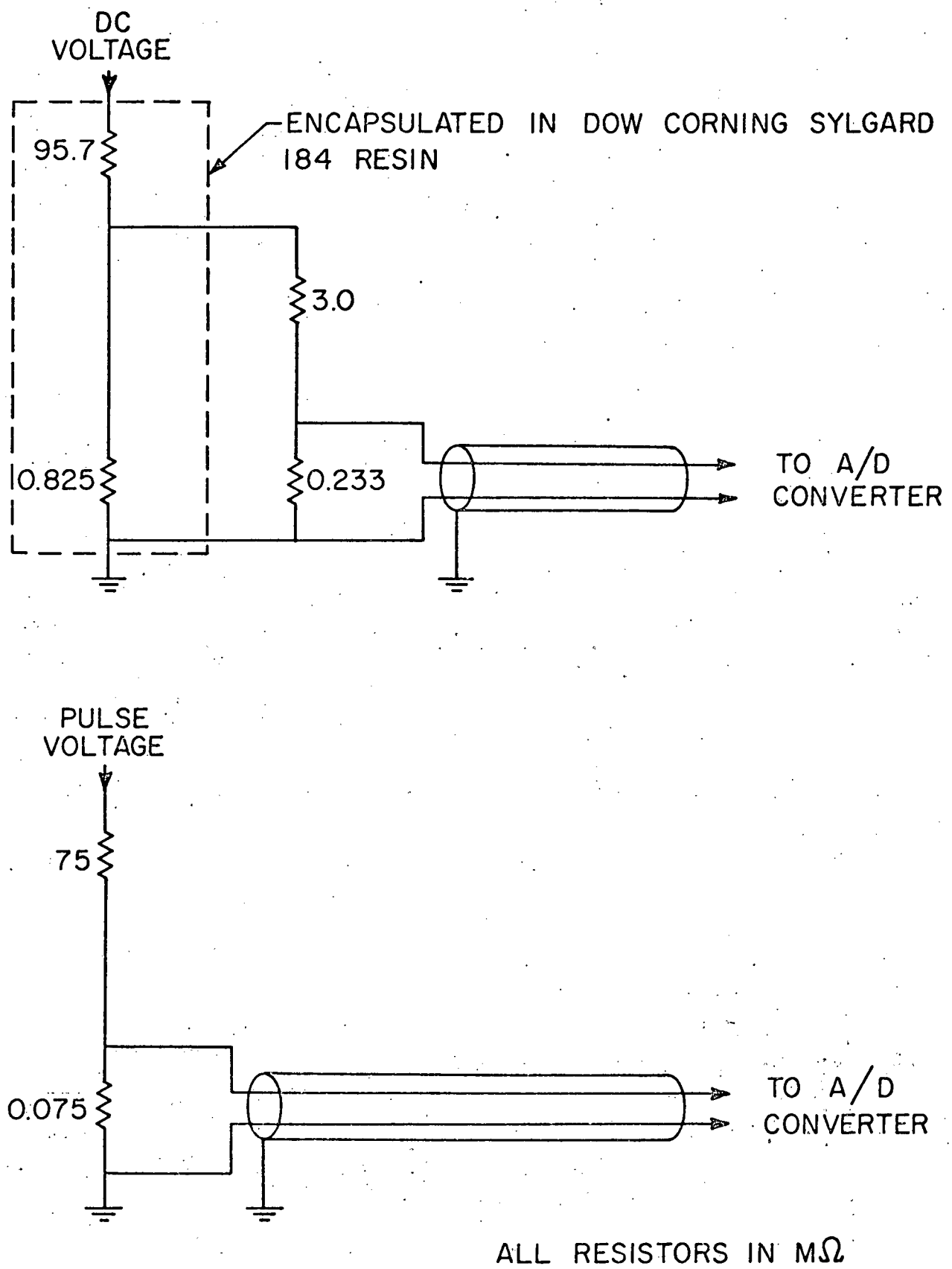
DC
VOLTAGE
ENCAPSULATED IN DOW CORNING SYLGARD
184 RESIN
95.7
3.0
0.825
0.233
TO A/D
CONVERTER
PULSE
VOLTAGE
75
0.075
TO A/D
CONVERTER
ALL RESISTORS IN MΩ

Figure 11.

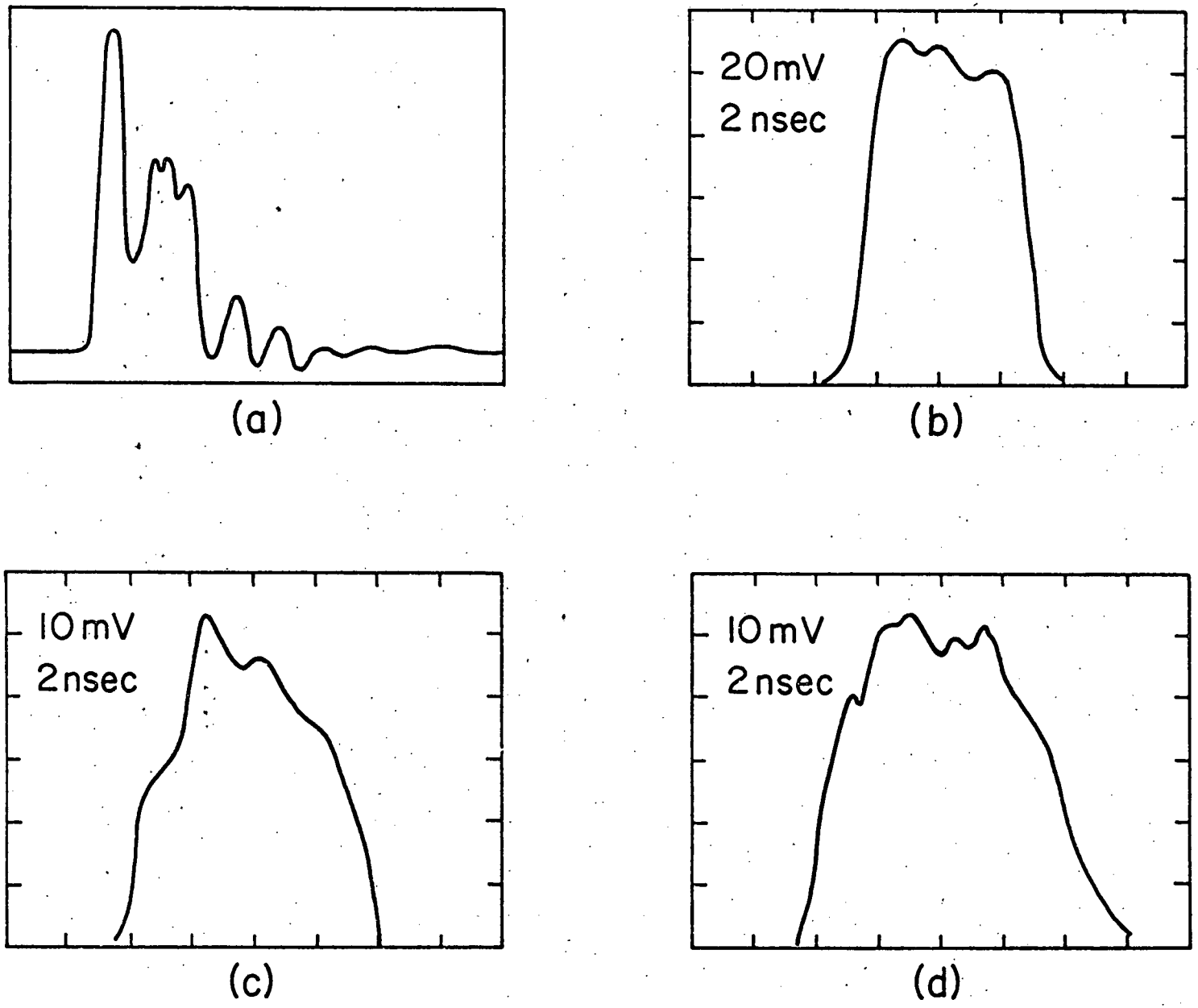

Figure 12.

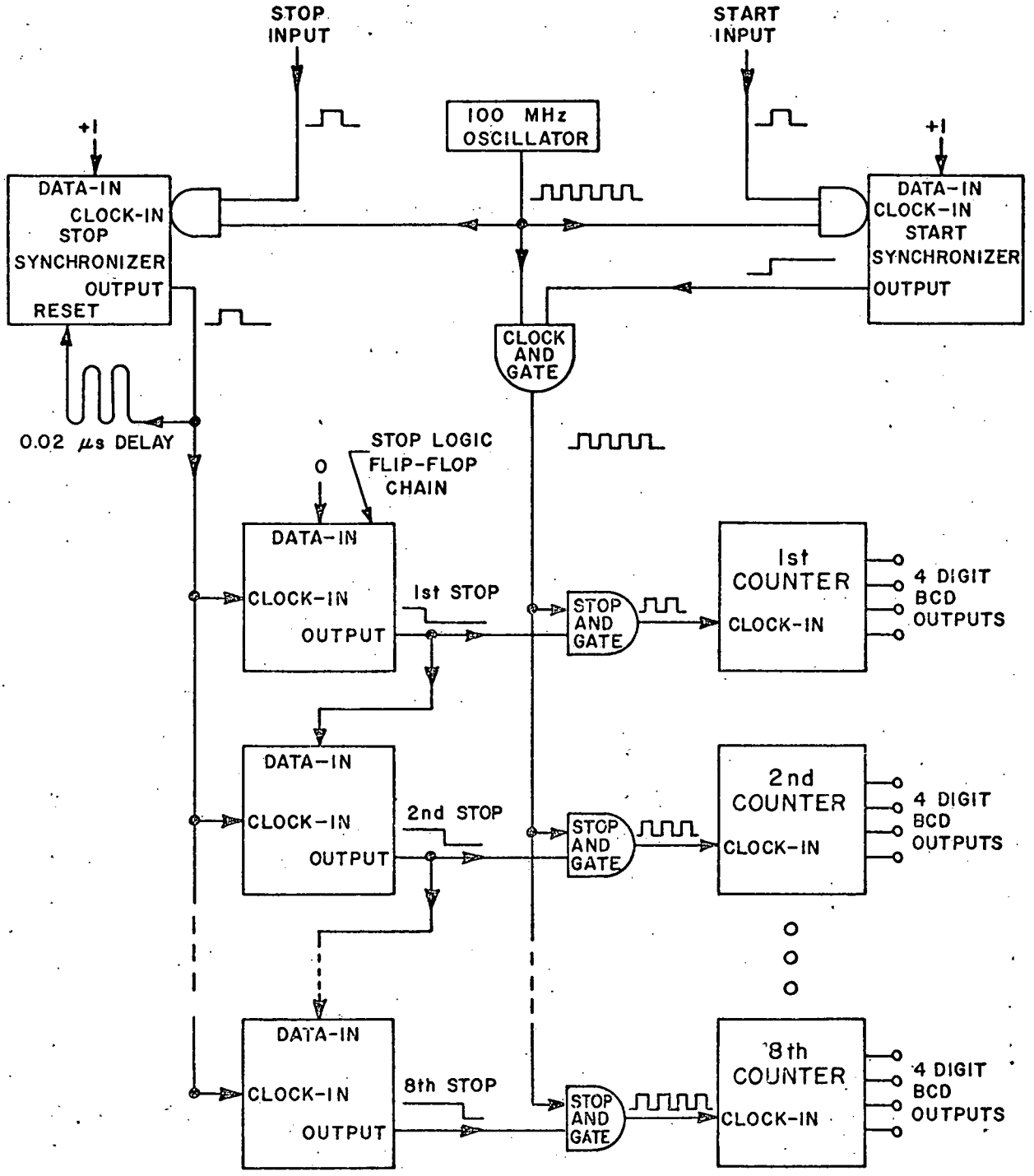

EIGHT-CHANNEL DIGITAL TIMER

Figure 13.

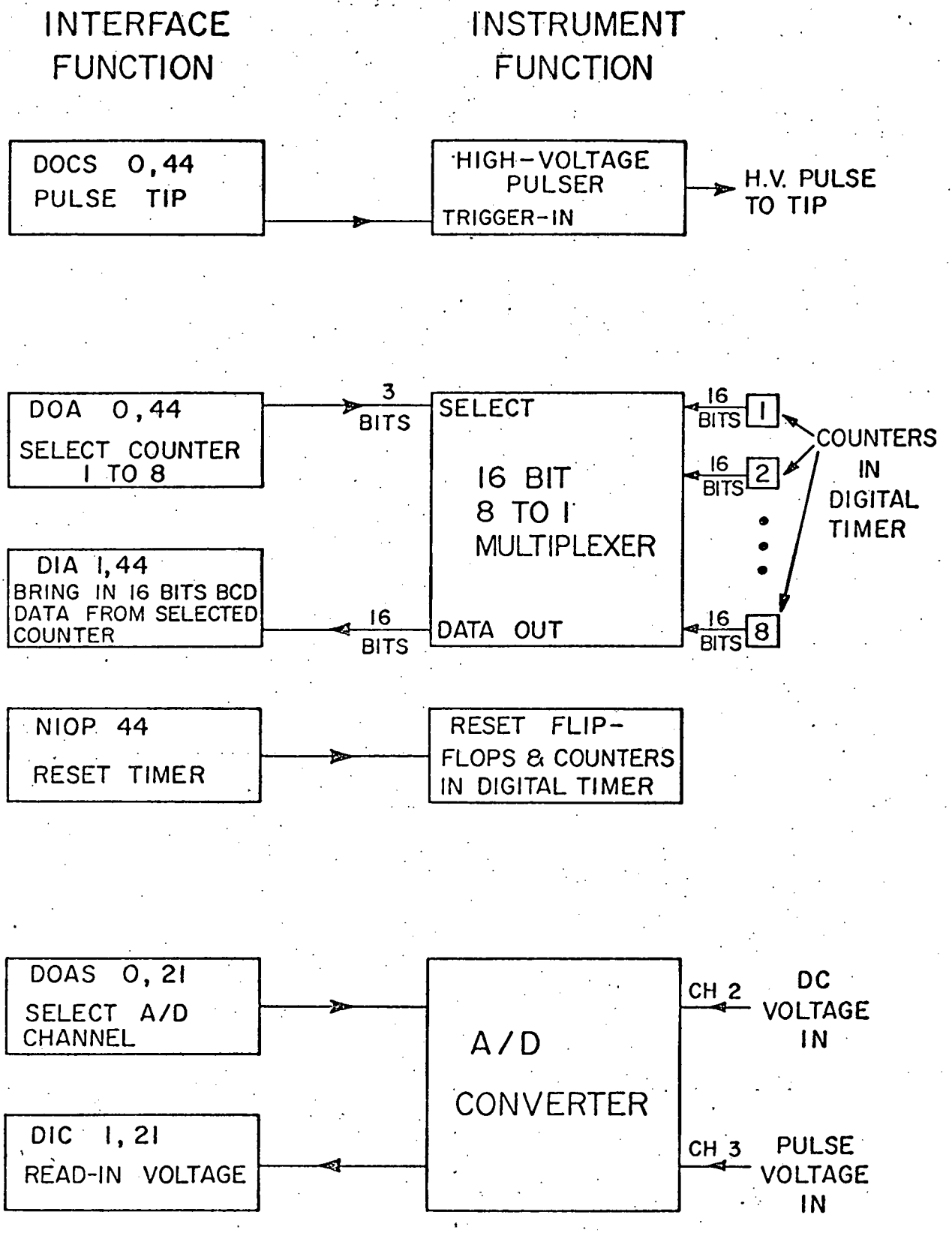

COMPUTER – INSTRUMENT INTERFACE

Figure 14.

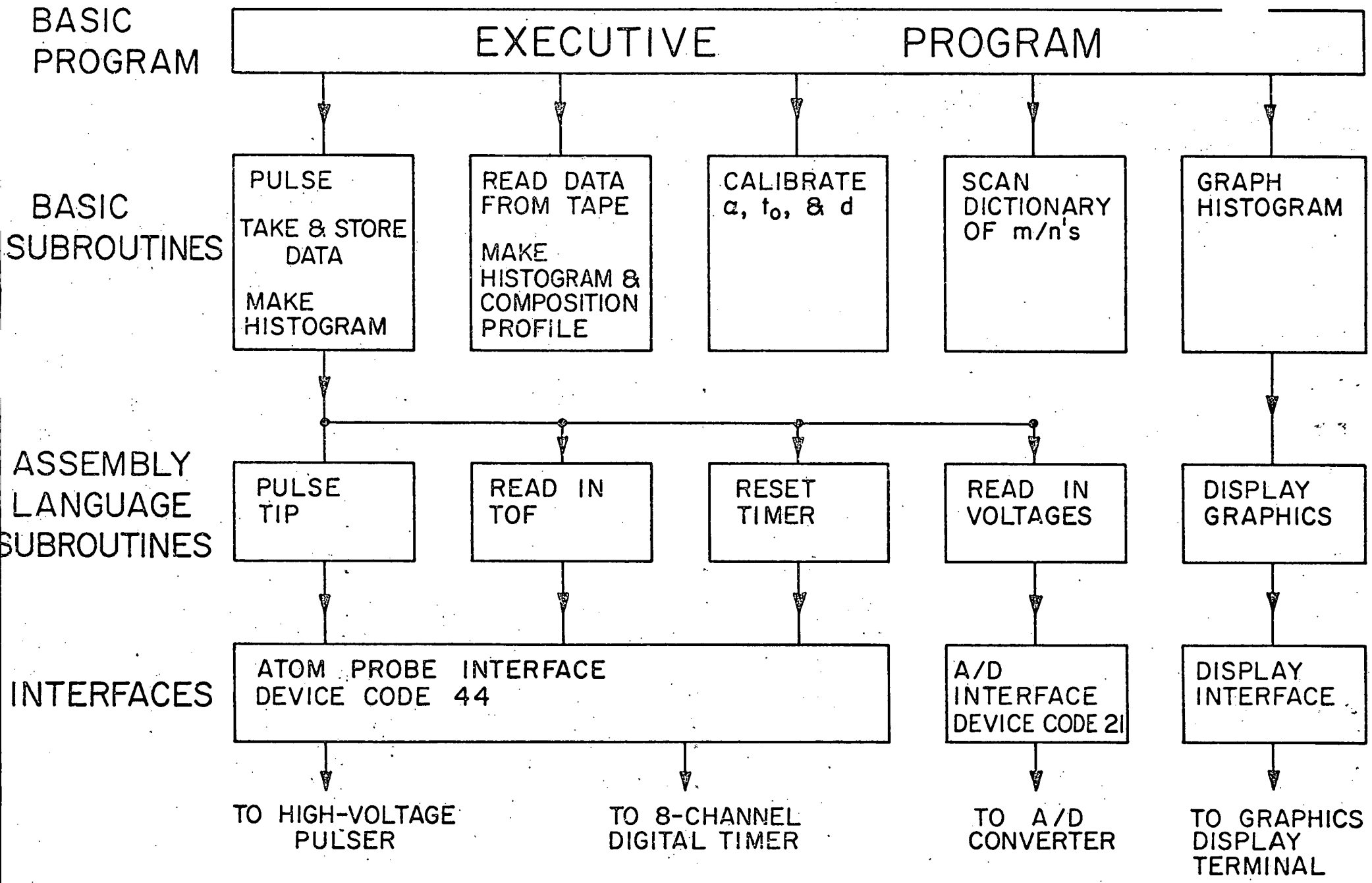

Figure 15.

COMPUTER PROGRAM HIERARCHY

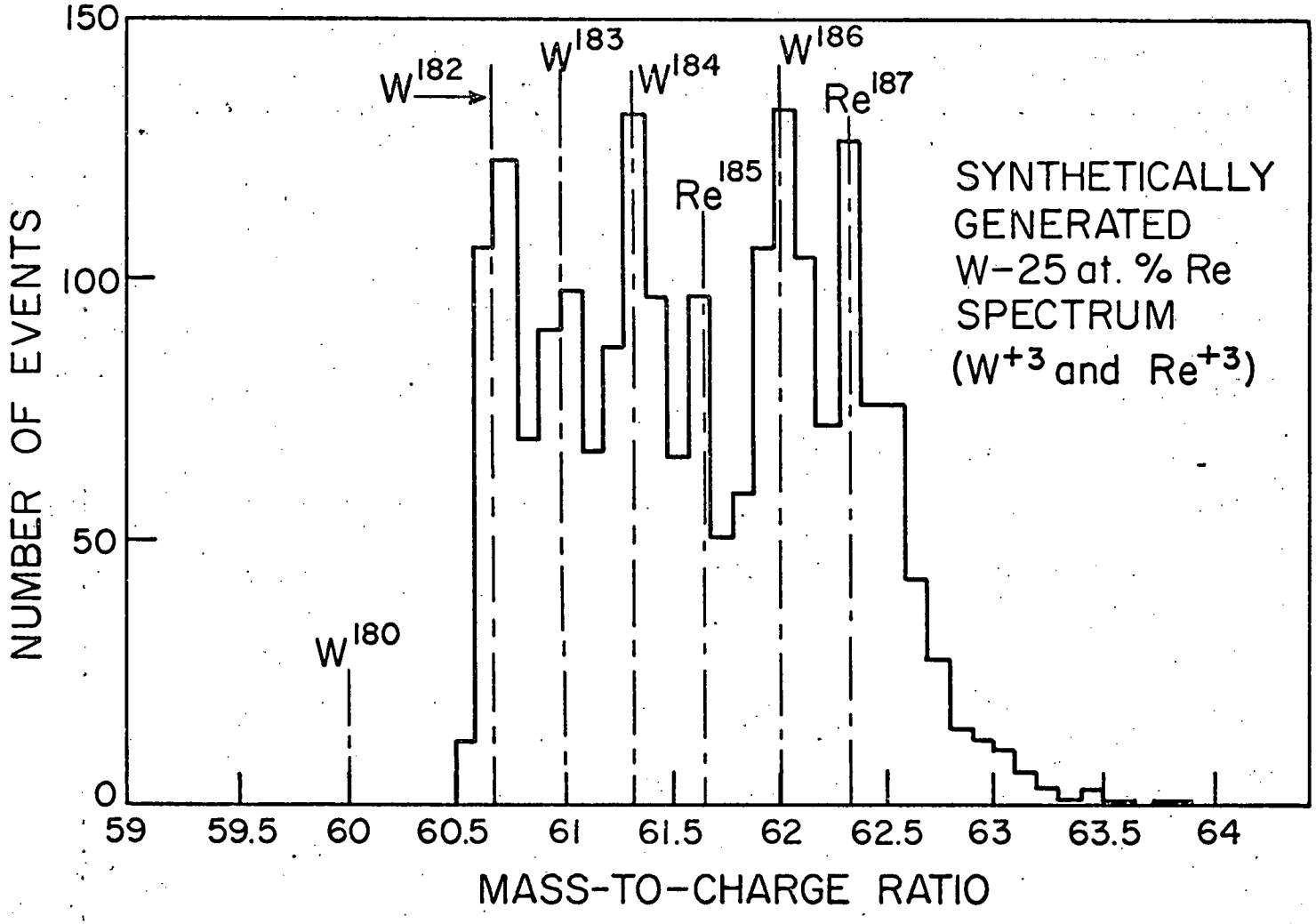
150
100
50
0
NUMBER OF EVENTS
W182
W183
W184
W186
Re187
Re185
W180
SYNTHETICALLY
GENERATED
W-25 at. % Re
SPECTRUM
(W+3 and Re+3)
59
59.5
60
60.5
61
61.5
62
62.5
63
63.5
64
MASS-TO-CHARGE RATIO

Figure 16.

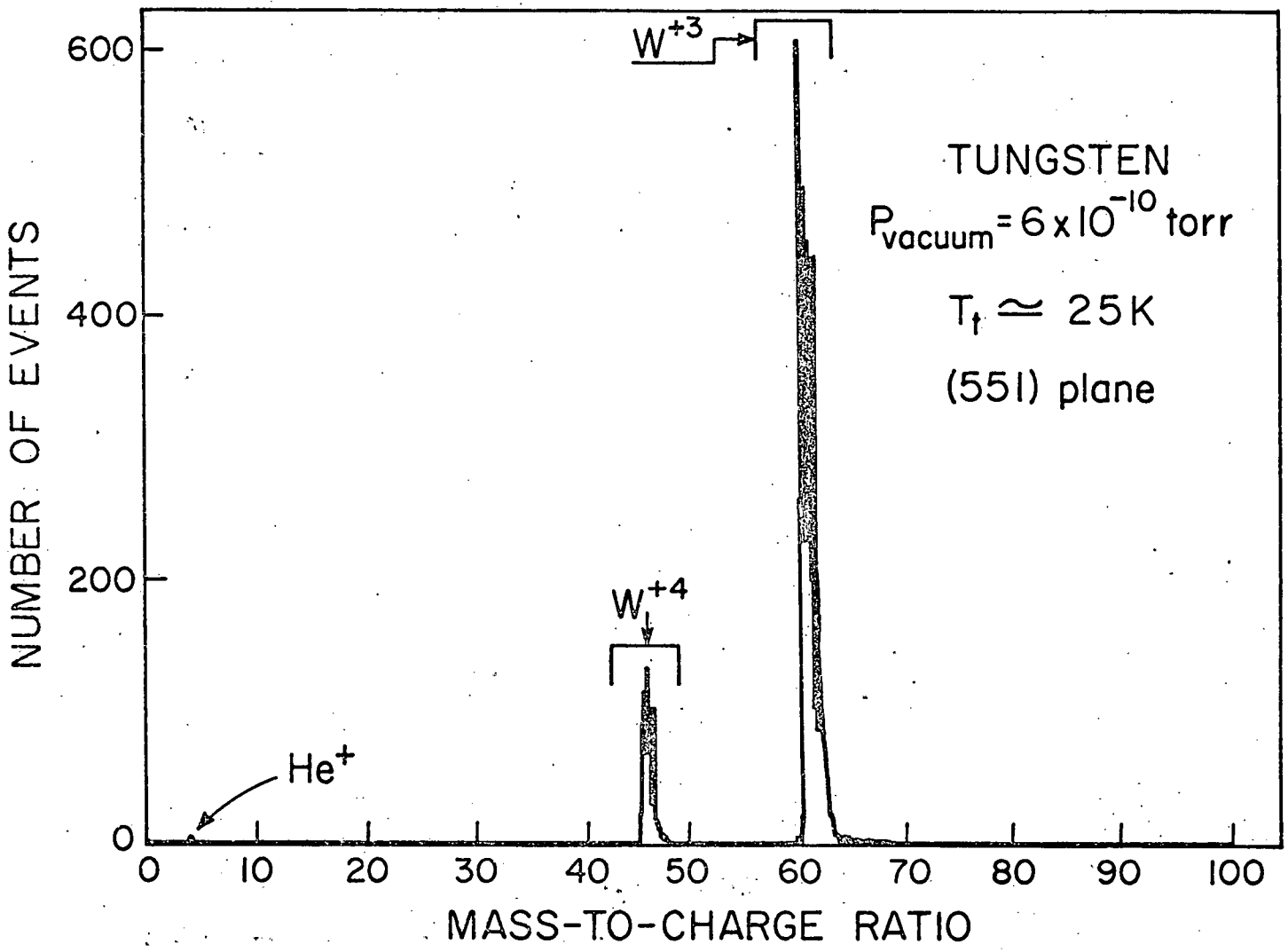
NUMBER OF EVENTS
600
400
200
0
0
10
20
30
40
50
60
70
80
90
100
MASS-TO-CHARGE RATIO
W+3
W+4
He+
TUNGSTEN
Pvacuum = 6 x 10-10 torr
Tf ≃ 25K
(551) plane

Figure 17.

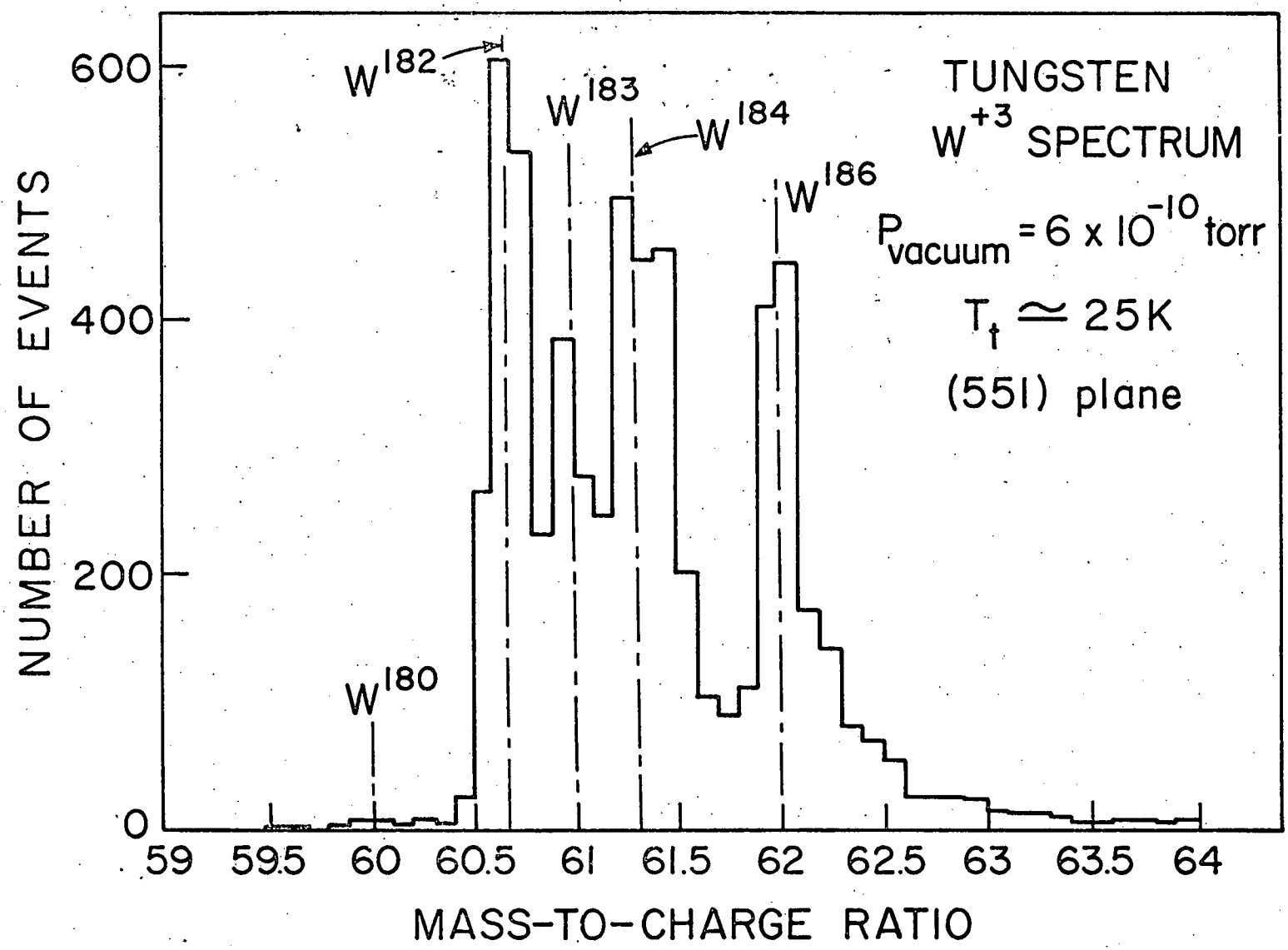
TUNGSTEN
W+3 SPECTRUM
Pvacuum = 6 x 10-10 torr
Tt ≃ 25K
(551) plane
W180
W182
W183
W184
W186
NUMBER OF EVENTS
0
200
400
600
59
59.5
60
60.5
61
61.5
62
62.5
63
63.5
64
MASS-TO-CHARGE RATIO

Figure 18.

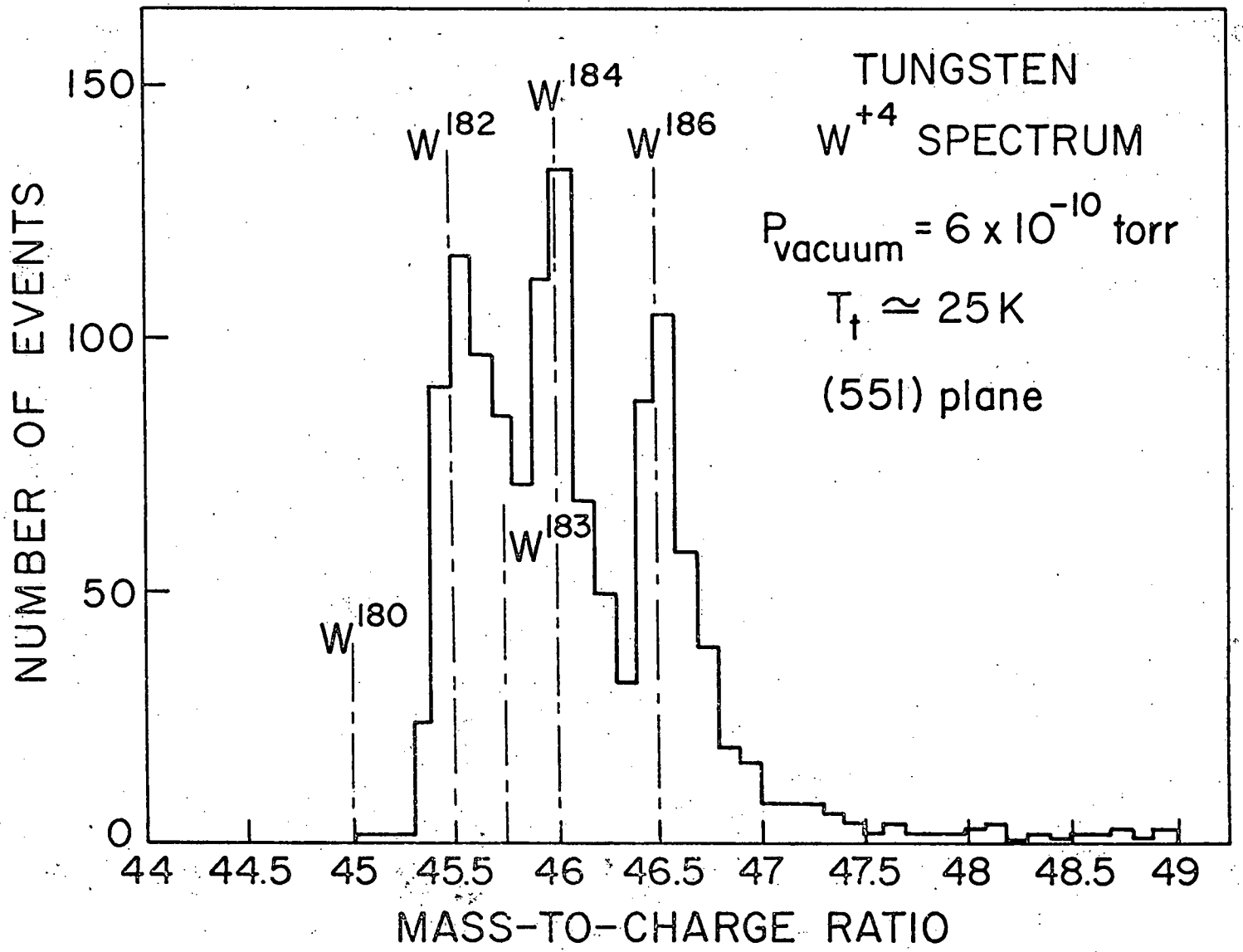
TUNGSTEN
W+4 SPECTRUM
Pvacuum = 6 x 10-10 torr
Tt ≃ 25 K
(551) plane
W180
W182
W183
W184
W186
NUMBER OF EVENTS
MASS-TO-CHARGE RATIO
0
50
100
150
44
44.5
45
45.5
46
46.5
47
47.5
48
48.5
49

Figure 19.

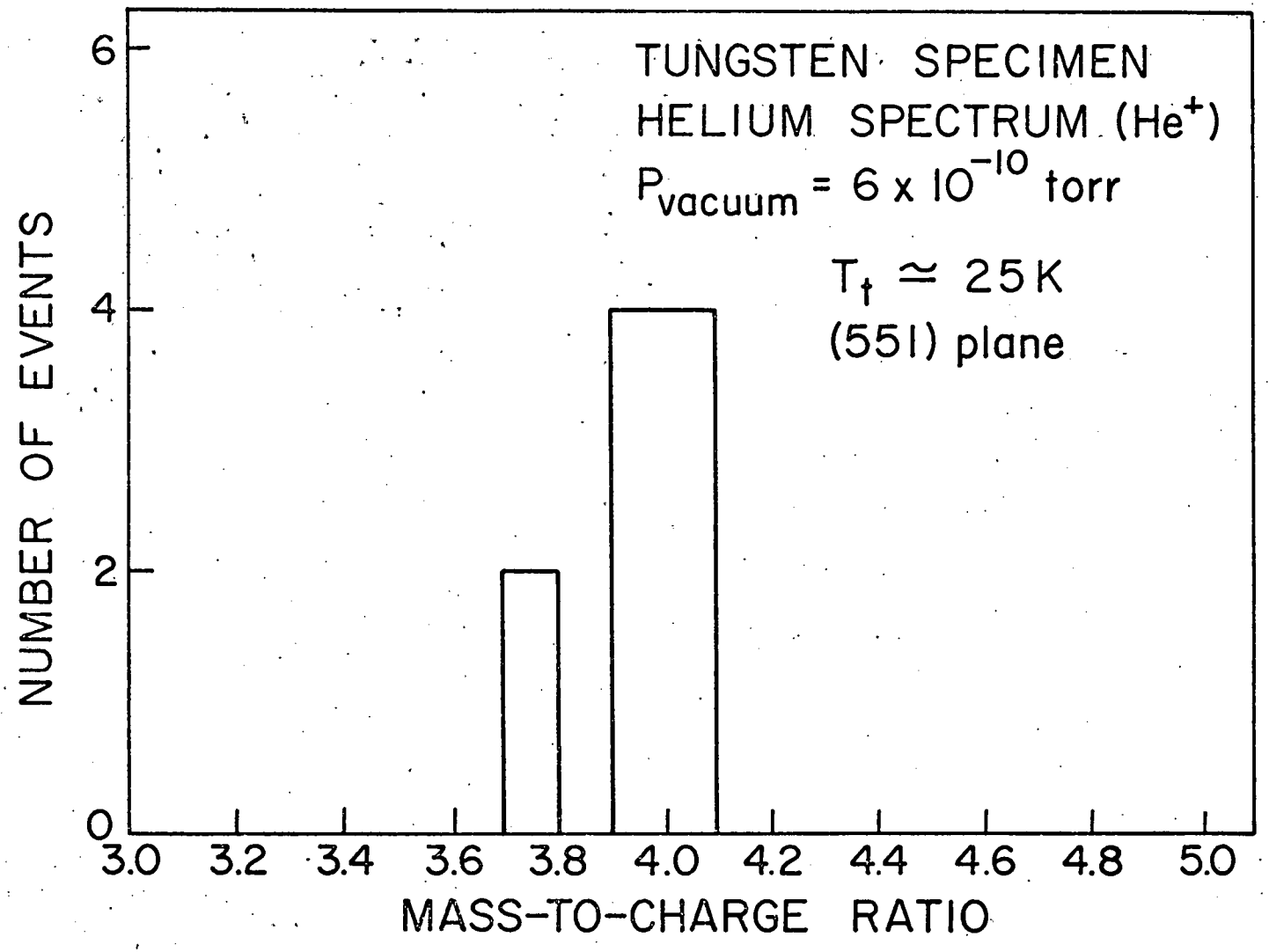
TUNGSTEN SPECIMEN
HELIUM SPECTRUM (He^+)
$P_{vacuum} = 6 \times 10^{-10}$ torr
$T_t \simeq 25$K
(551) plane
NUMBER OF EVENTS
0
2
4
6
3.0
3.2
3.4
3.6
3.8
4.0
4.2
4.4
4.6
4.8
5.0
MASS-TO-CHARGE RATIO

Figure 20.

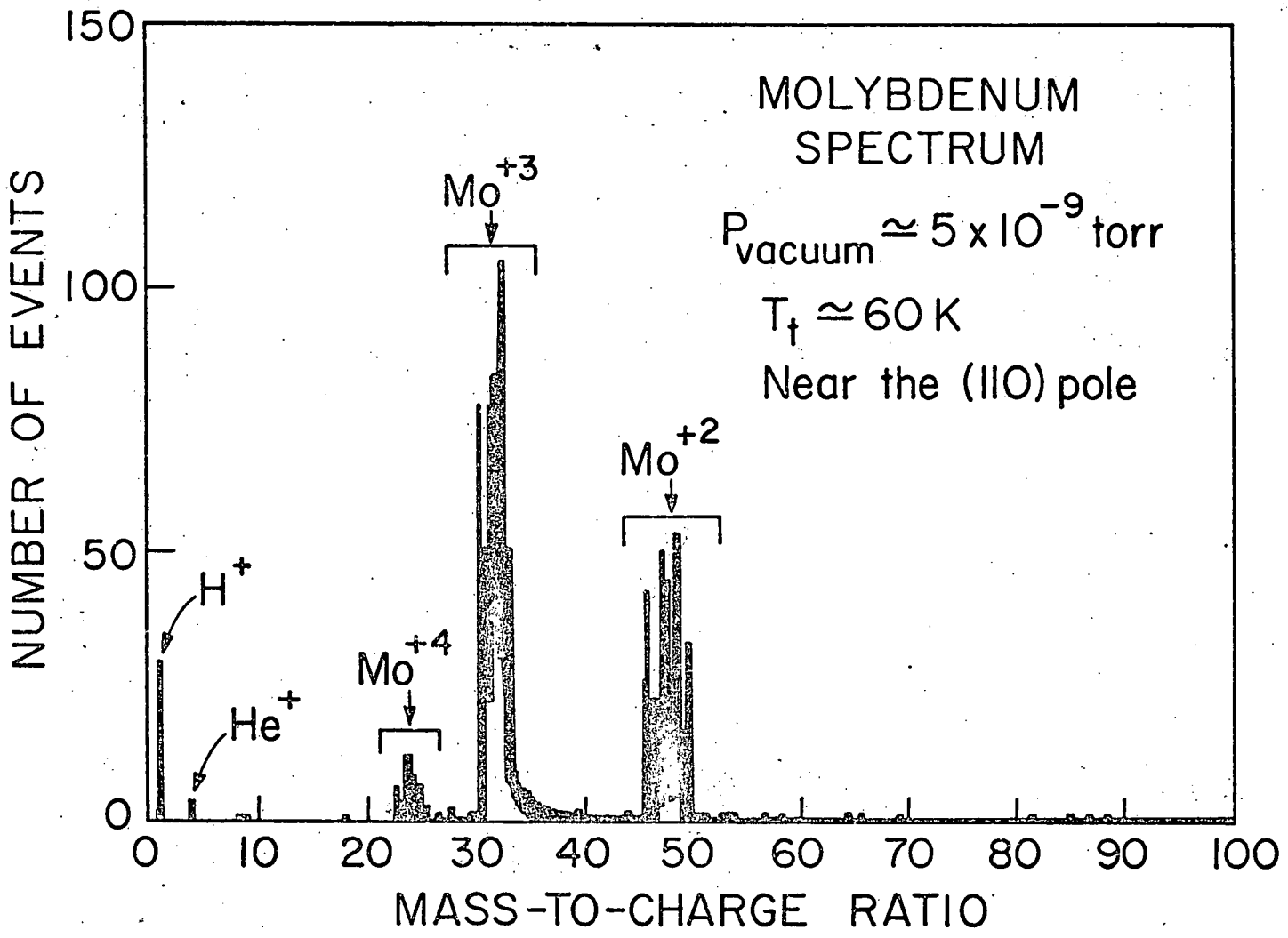
MOLYBDENUM
SPECTRUM
$P_{vacuum} \simeq 5 \times 10^{-9}$ torr
$T_t \simeq 60$ K
Near the (110) pole
NUMBER OF EVENTS
MASS-TO-CHARGE RATIO
H^+
He^+
Mo^{+4}
Mo^{+3}
Mo^{+2}
0
50
100
150
0
10
20
30
40
50
60
70
80
90
100

Figure 21.

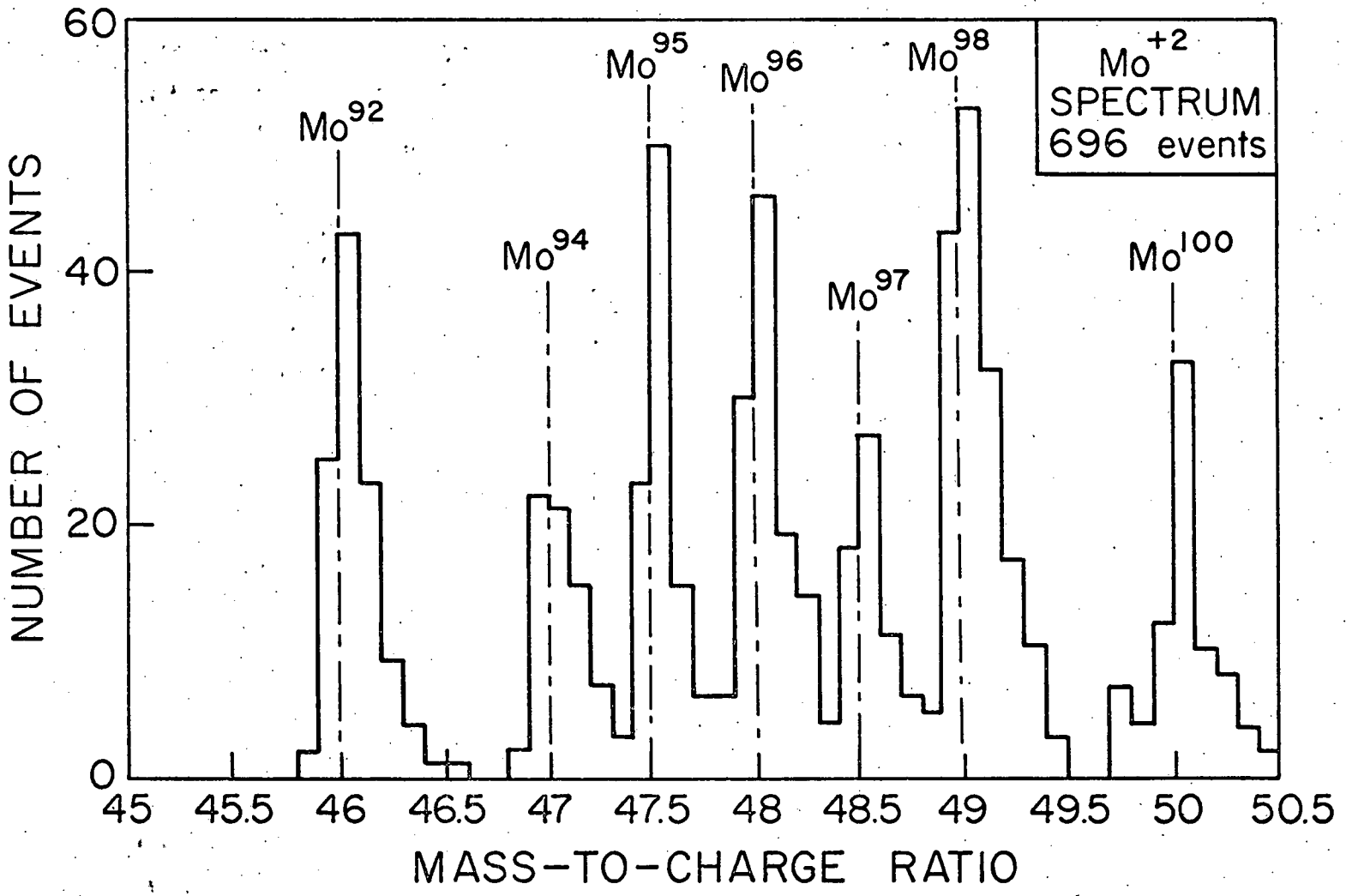
60
40
20
0
NUMBER OF EVENTS
Mo92
Mo94
Mo95
Mo96
Mo97
Mo98
Mo100
Mo+2
SPECTRUM
696 events
45
45.5
46
46.5
47
47.5
48
48.5
49
49.5
50
50.5
MASS-TO-CHARGE RATIO

Figure 22.

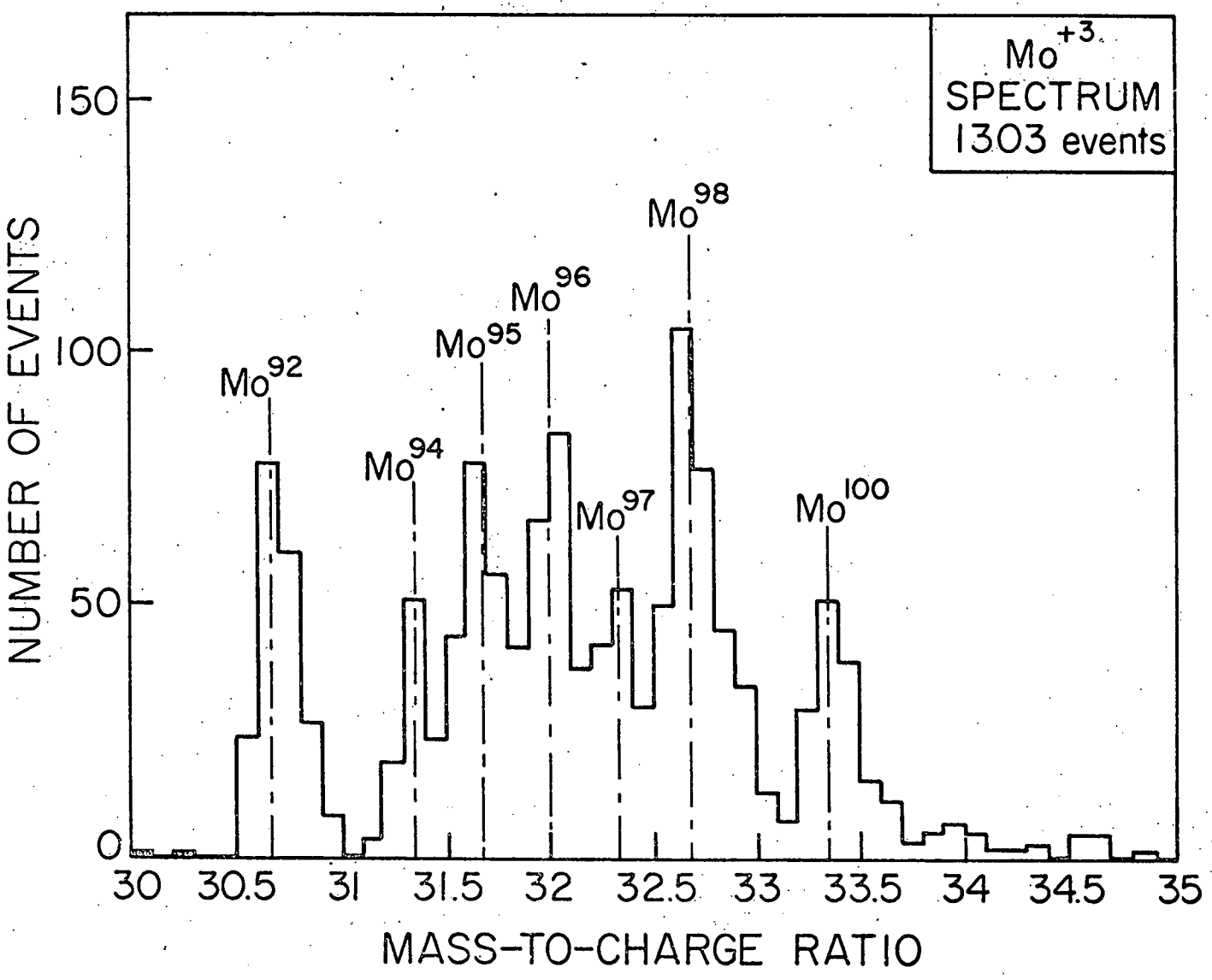
Mo+3
SPECTRUM
1303 events
NUMBER OF EVENTS
150
100
50
0
Mo92
Mo94
Mo95
Mo96
Mo97
Mo98
Mo100
30
30.5
31
31.5
32
32.5
33
33.5
34
34.5
35
MASS-TO-CHARGE RATIO

Figure 23.

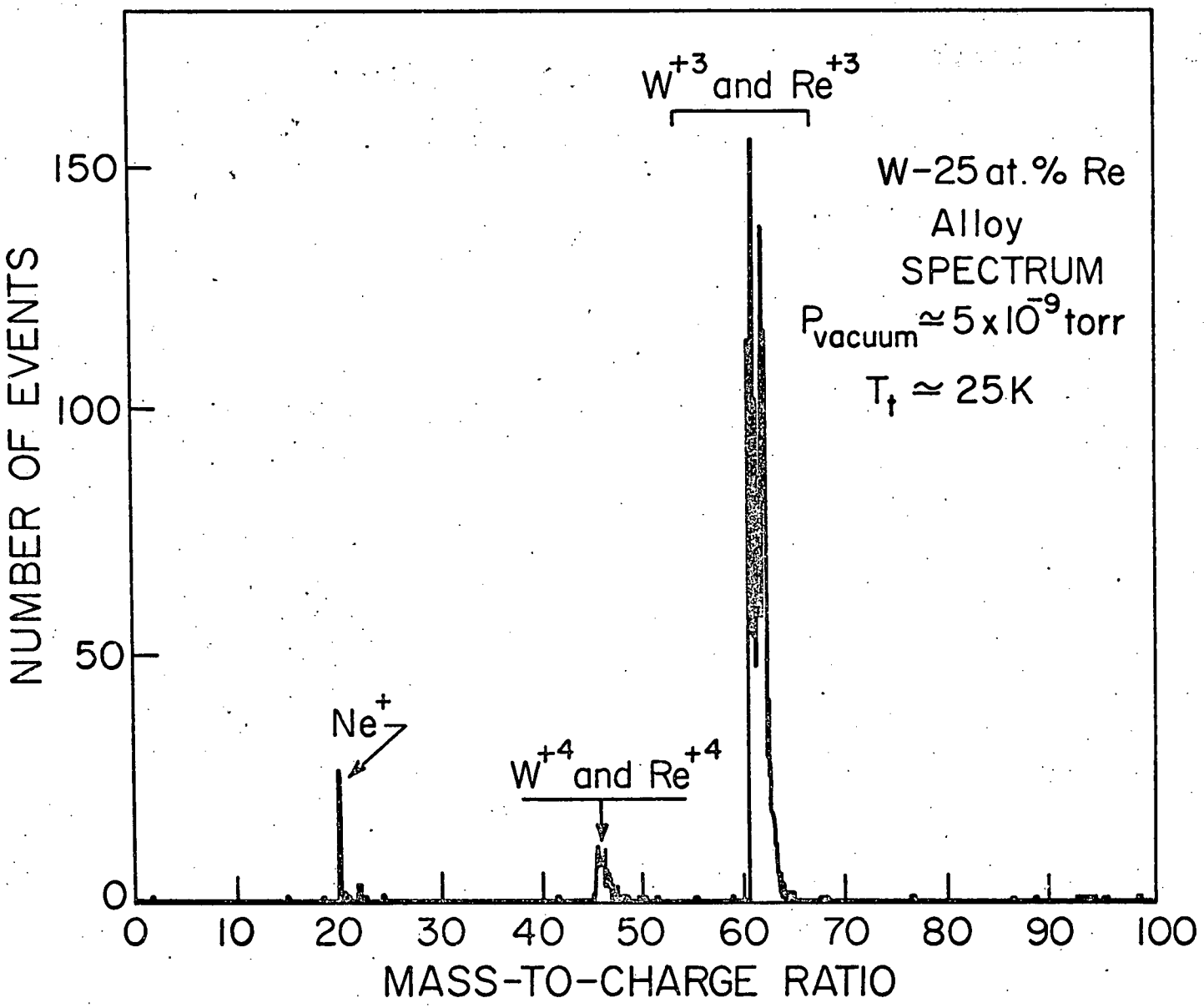
W+3 and Re+3
W-25 at.% Re
Alloy
SPECTRUM
Pvacuum ≃ 5 x 10-9 torr
Tf ≃ 25K
NUMBER OF EVENTS
150
100
50
0
Ne+
W+4 and Re+4
0
10
20
30
40
50
60
70
80
90
100
MASS-TO-CHARGE RATIO

Figure 24.

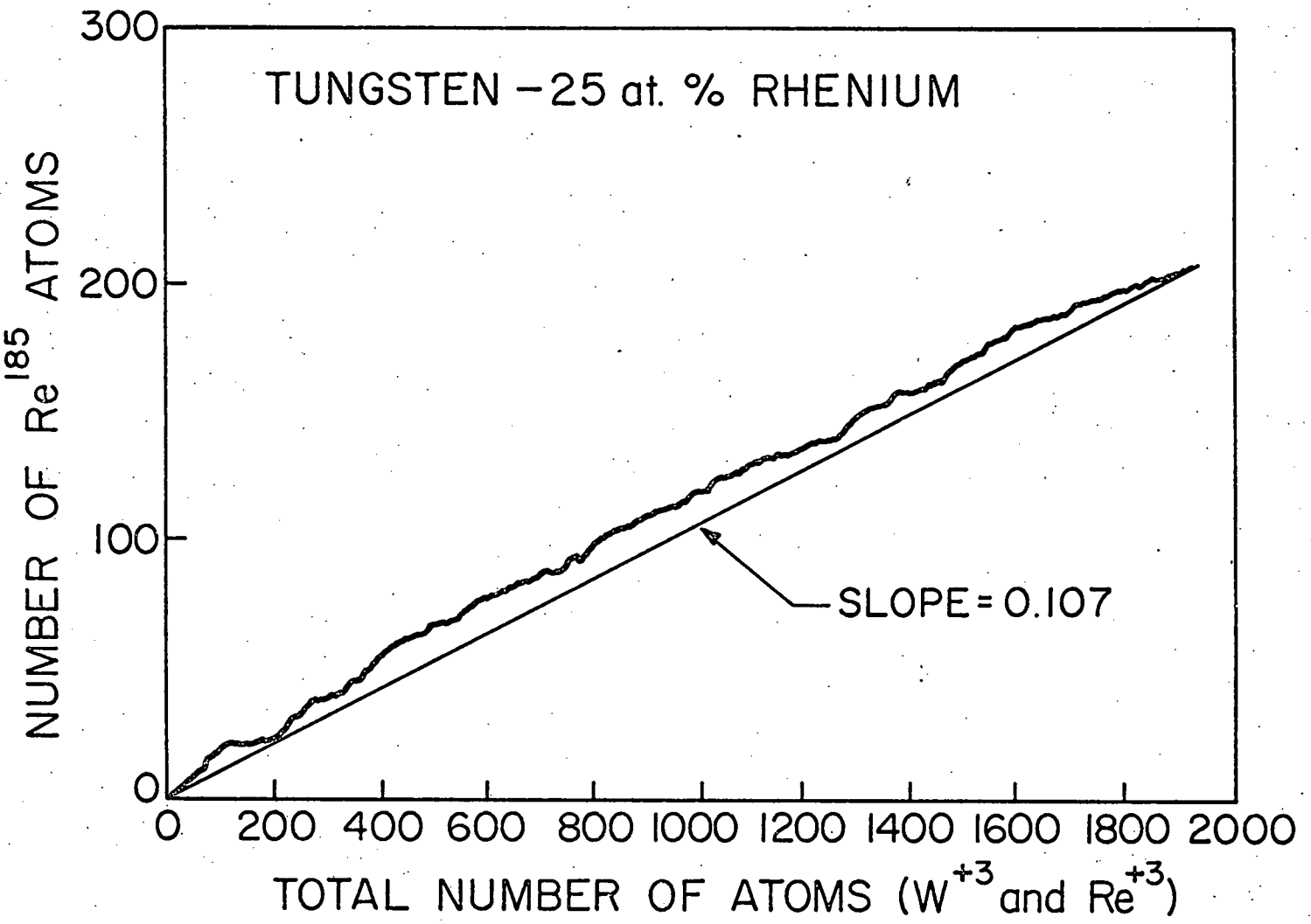
TUNGSTEN – 25 at. % RHENIUM
NUMBER OF Re^{185} ATOMS
TOTAL NUMBER OF ATOMS (W^{+3} and Re^{+3})
SLOPE = 0.107
0
100
200
300
0
200
400
600
800
1000
1200
1400
1600
1800
2000

Figure 26.

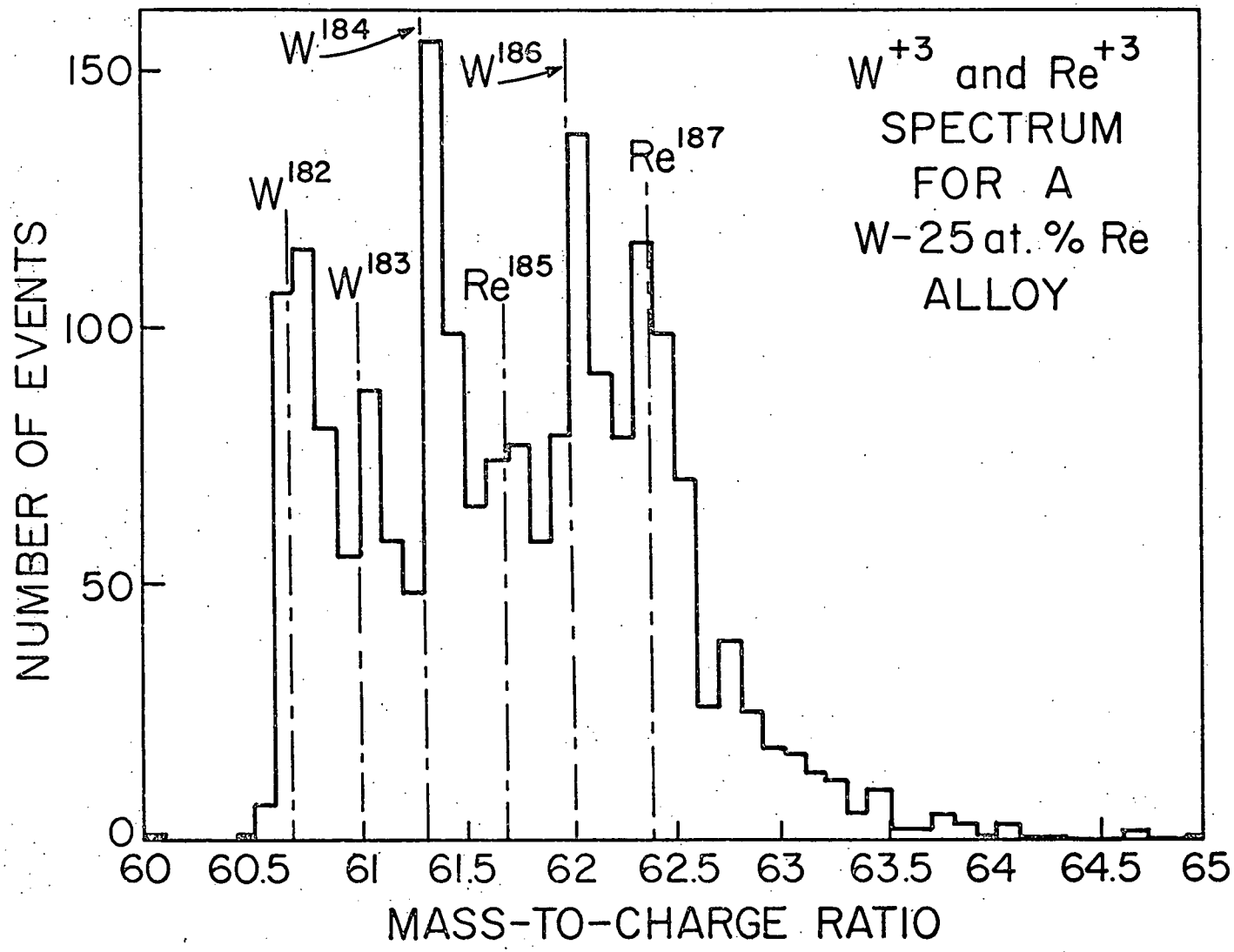
W184
W186
W182
W183
Re185
Re187
W+3 and Re+3
SPECTRUM
FOR A
W-25 at. % Re
ALLOY
NUMBER OF EVENTS
150
100
50
0
60
60.5
61
61.5
62
62.5
63
63.5
64
64.5
65
MASS-TO-CHARGE RATIO

Figure 25.

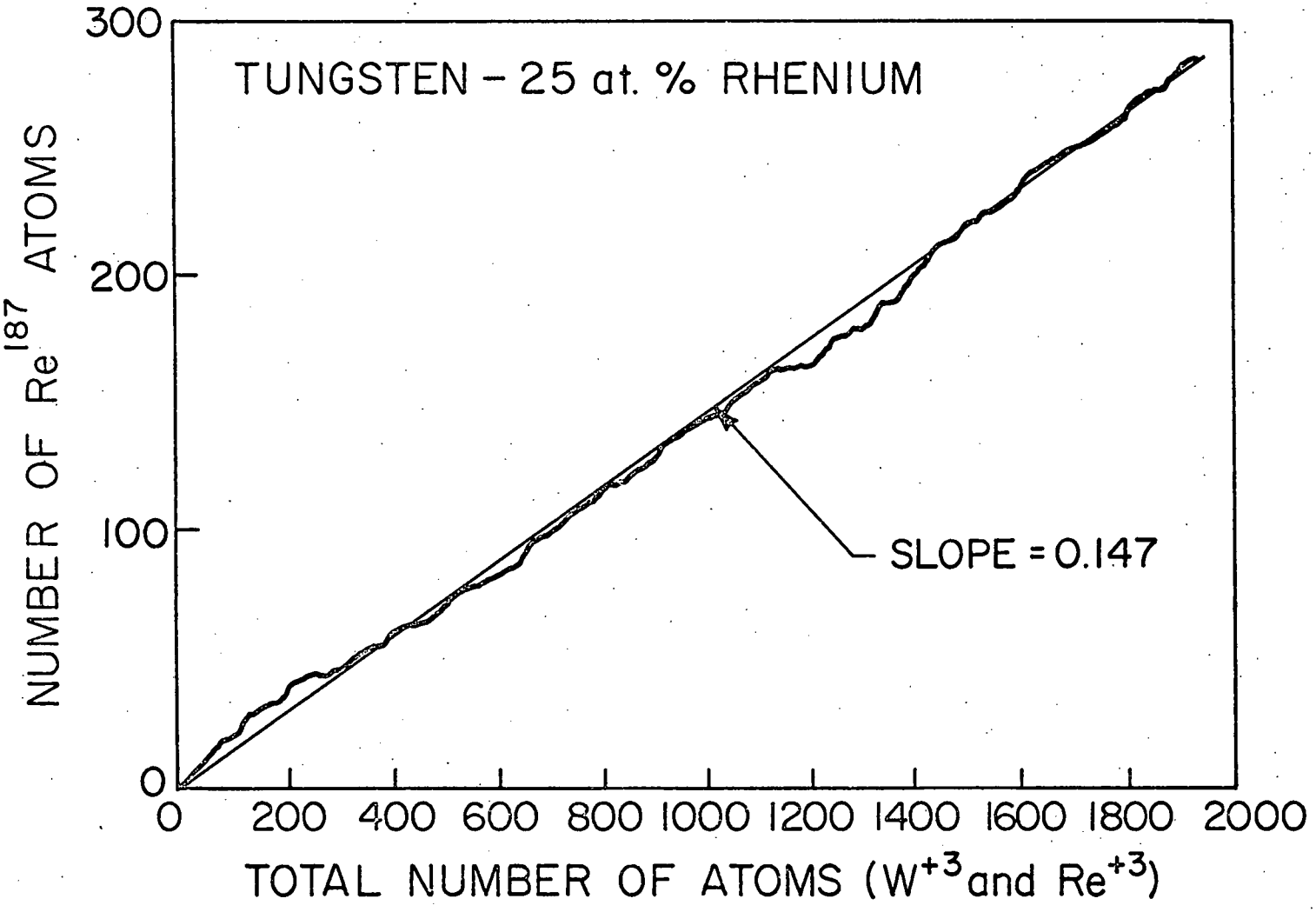
TUNGSTEN – 25 at. % RHENIUM
NUMBER OF Re^{187} ATOMS
300
200
100
0
SLOPE = 0.147
0 200 400 600 800 1000 1200 1400 1600 1800 2000
TOTAL NUMBER OF ATOMS (W^{+3} and Re^{+3})

Figure 27.